AKKUYU NUCLEAR POWER PLANT

TSUNAMI STUDY

Sponsored By

Turkish Electric Authority

ANKARA - TURKEY

Prepared By

INSTITUTE OF MARINE SCIENCES

MIDDLE EAST TECHNICAL UNIVERSITY

March,1979.

Project Code No:77-07-00-06

ACKNOWLEDGEMENTS

This study was sponsored by the Turkish Electric Authority under Project Code No.77-07-00-06.

Special thanks are due to Dr.Erhan Ermutlu for moral assistance while he was at T.E.K. The investigation gained much from discussions with Mr.G.G.Baumgartner, of Basler and Hofman, Prof.T.Norman kindly aided in the acquisition of the earthquake data from England.

The study was carried out under the general supervision of Dr. O.Ünlüata, Assistant Professor in Marine Sciences. Doç.Dr.Mustafa Aral was involved in the numerical modelling,and the project would not be made possible without his endless efforts in difficult times. Dr.Özsoy contributed greatly toward the final phases of the study. Dr.M.A.Latif kindly provided assistance in storm surge evaluation.

The acknowledgements would not be complete without sincere expressions of gratitude to Prof.T.I.Balkaş for continuous propulsion and Ms.Ella Balkaş for her patient, pain-staking and charge-free typing of the final report.

TABLE OF CONTENTS

LIST OF FIGURES

LIST OF TABLES

I. INTRODUCTION

1.1 Purpose of the Study

The Turkish Electric Authority (TEK) is engaged in a program concerning the environmental site assesment of Akkuyu Bay, the site of a proposed nuclear power generating station. The objective of the program is to provide information required for TEK to obtain licences to construct the generating station.

The fluctuations in sea level in Akkuyu Bay and its vicinity, induced by incident seismic sea waves -Tsunami- is among the information needed by TEK. In order to provide this information, the present study was undertaken by the Institute of Marine Sciences (IMS) of the Middle East Technical University.

The present tsunami study involves the numerical investigation of tsunami generation in the Eastern Mediterranean and the propagation of seismic sea wave systems toward the southern coast of Turkey, including their transformation over shallow depths in approach to Akkuyu Bay and its vicinity. The eventual interest is in the tsunami induced run-up and drawdown that may occur in waters surrounding the proposed nuclear power plant site. Scattering of tsunami by Cyprus, topographical variations and sufficient detail of perinent coastlines are included in the study.

1.2 Scope of the Study

The investigation was carried out by solving numerically the governing hydrodynamic equations of motion. Tsunami generating design earthquakes with estimated 10.000 year (or greater) return periods are selected as inputs to the numerial model. The selection of the earthquake sources are based on the available seismo-tectonic information as well as the tsunami history of the Eastern Mediterranean (Chapter II).

The modelling of the geometry of the ground motion is kept as simple as possible (rectangular), with the maximum displacement decaying exponentially along the minor axis of the source area. The ground motions are taken as impulsive. The selection of the model parameters are based on standard graphs (Chapter III).

The selection of the design earthquakes and their parameters were followed by the numerical solutions of the non-linear shallow water equations. A finite difference model is utilized for this purpose (Chapter IV). In addition, a finite element model was developed but kept small in its scope.

Numerical solutions yield surface motions 5.5 - 11 km off-shore of Akkuyu. These results are presented in Chapter V. Using the off-shore motions, the surface displacement on the coastline are evaluated via an analytical model (Chapter VI). Design considerations are then provided in Chapter VII.

1.3 Summary of Results

Table 3.1 summarizes the eight design earthquakes that were considered in this study (see also Fig.5.1). Among these sources, the source R.1 situated southeast of the Cretan Arc proves to be most crucial, giving rise to 1.5 m oscillations off-shore of the target (Akkuyu Bay). All the results shows a resonant coupling of the shelf area to the deeper Cilician Basin. The analytical model that takes into account of the resonance phenomenon detected, gives (as a conservative estimate) an amplification factor of 2.12. Consequently, the expected surface motions at the target corresponds to a ∓3 m tsunami induced drawdown and 3 m run-up.

11.SEISMOTECTONICS OF THE EASTERN MEDITERRANEAN AND SELECTION OF TSUNAMIGENIC DESIGN EARTHQUAKES

2.1 Tsunami History of Eastern Mediterranean

The characteristics of a tsunami obviously depend on the characteristics of the earthquake that generates it. The description of the details of this dependance is delayed to a later section. The present chapter is initially concerned with the history of tsunamis in the Eastern Mediterranean and the seismic features of the region at large. These considerations lead to the identification of a set of regions of the North-Eastern Mediterranean which, in relation to the Akkuyu N.P.P., are potential tsunami source areas. The selection of the design tsunamigenic earthquake magnitudes having approximately 10000 years return periods follow the identification of the various sources.

A list of tsunamis observed in major seas during 479 B.C. to 1947 has been compiled by Heck (1947). Using Heck's data, Van Dorn (1965) provides table 2.1 on the frequency of occurence and distribution of tsunamis in the Pacific Ocean, the Atlantic Ocean and the Mediterranean sea. It can be inferred from table 2.1 that seismic sea waves are most frequently observed in the Pacific Ocean and this fact is attributed to the predominance of trenches and oceanic earthquake zones in the Pacific.

A remarkable compilation of tsunamigenic events in the Eastern Mediterranean(31^{o} - 44^{o}N, 18^{o} - 36^{o}E) has been made, Ambraseys (1962) covering the period II millenium B.C. to 1961. A total of 141 tsunamigenic events are catalogued by Ambraseys and are reproduced in table 2.2. The arrangement of tsunamis in table 2.2 is the same as that given by Ambraseys. The date of the event is followed by the locality where the tsunami was observed. The tsunami intensity follows the regions affected and is given in Sieberg modified intensity scale (see end of table 2.1). The symbols H and L denote the run-up height and length, respectively. In cases where the earthquake epicenter is known its coordinates are given following the information on run-up. Followed by this are the intensity I of the earthquake in the modified Mercalli scale, magnitude M, after Gutenberg, and the focal depth. The symbols used for focal depths are "s" for shallow, "n" for normal and "i" for intermediate. Doubtful events are indicated by a star.

The following conclusions by Ambraseys are worth noting. Tsunamis in the intensity range of i-iv (Mod.Sieberg Scale) are quite often observed in the Eastern Mediterranean. We remark that, even though most of these tsunamis are less severe than those observed in the Pacific, they should be considered historically relevant. In the Eastern Mediterranean, seismic sea waves of intensities greater than iv (which are disasterous to large ships and coastal inhabitants) are indeed rare and localized to a great extent. Among the various seismically active regions in the Eastern Mediterranean, only well-defined and self-contained areas exhibit tsunamigenic events. These areas are i) the Eubean Gulf, ii) the area between Cyprus, Jubeil and Acre, iii) the south of Aegean, iv) the Gulf of Corinth. Ambraseys indicates that the generic cause of the tsunamis that have occured in the various regions of the Eastern Mediterranean can not be attributed to a specific and single mechanism, "No predominant cause is indicated from both old and recent data as well as from tectonics and seismic history of the region" (Ambraseys, 1962).

Using Ambraseys' catalogue we have indicated in Fig.2.1 two regions (shaded areas) where sufficiently intense tsunamis have been frequently observed in the past. These regions have obvious relevance to the present study. In Fig.2.1 the selective locations that have been subjected to tsunamis of intensities greater than or equal to iii (or the Modified Sieberg Scale) are shown by a star. We remark that Fig.2.1 should not be regarded as a summary of Ambraseys' catalogue.

Referring to Ambraseys' catalogue and Fig.2.1, we find that southern Aegean has frequently been subjected to tsunamis. The most disastrous tsunami in recent history (1956) have occurred in this area with run-up of 100 feet at Amargos, of 67 feet at Astipalaea, of 10 feet at Crete (see No.138). In another event in 1948 the Island of Karpathos has been flooded by 3000 feet† evidently as a result of an earthquake in the close proximity of the island, (see No.136). Similarly, there have been intense and frequent tsunamis along the entire coast of Crete and Rhodes. The possible significance of the tsunami generation in this region with regard to the southern coast of Turkey appears at first sight as worthy of examination, though we

† run-up is implied here.

find no evidence to this effect. Indeed, there is a strong evidence that tsunamis occurring in the southern Grecian Archipelago and to the north of the Cretan Arc (formed by the islands of Rhodes, Karpathos and Crete) are dissipated locally as a result of narrow passages and coastline configuration so that their effect on the southern coastal waters of Turkey in general and the Akkuyu N.P.P. site in particular do not seem to be significant. In fact, when the severe tsunamis of 1948 (No.136) and 1956 (no.138) occurred to the north of Cretan arc, no simultaneous tsunamis were observed along the south coast of Asia minor and at Cyprus. Conversely, in three other tsunamis of intensity (iii) listed by Anbraseys (nos. 29,54 and 56), do not seem to be connected with tsunamis emanating from the region lying to the N and NW of the Cretan Arc. However, the seismically equally active region to the south and south-east of the Cretan Arc must be examined for tsunamis originating from this region as this will definetely influence the N.P.P. site.

Moving toward the eastern end of the southern coast of Turkey, it is found that Iskenderun and its vicinity has also been subjected to seismic sea waves (Nos. 36 and 37). The close proximity of Iskenderun to the tsunamigenically active region between Cyprus and Israel (ref.Fig.1) and the simultaneous occurence of other tsunamis in Syria and south Asia Minor (see event No.54) suggest a possible influence of this region on the eastern segment of the southern Turkish coast. On the other hand, we find no specific tsunami observation in Anamur, a historical town near Akkuyu Bay. We do not also find a mention of a tsumamigenic event along the northern coast of Cyprus across Akkuyu even though the southern coastline of this island has been frequently subjected to tsunamis. There is thus a possibility that Cyprus provides some protection against tsunamis generated in seismically active regions to the south of Cyprus. However, an investigation of tsunami generation here on the nuclear power plant site in Akkuyu Bay was considered.

It is also worth mentioning that, even though historical records indicate tsunami generation in self-contained areas of the Eastern Mediterranean, there have been tsunamis that have affected the entire body of water (see No.49). This fact further strengthens the decisions made with regard to the investigation of the tsunamis generated in a set of regions rather than in only one region.

Finally, it can be inferred from Ambraseys catalogue that the region between Cyprus and the Asia Minor south coast is itself a self-contained tsunamigenic area in the sense of Grecian Archipelago as suggested by Ambraseys. This possibility, is investigated in the present study.

2.2 Seismotectonics - General Aspects.

2.2.1 Tectonics.

In the Eastern Mediterranean tsunamigenic earthquakes i.e., the earthquakes with magnitudes greater than 6 are common and are often associated with slips on major faults (Fig.2.2. - 2.5). The seismic activity in the Eastern Mediterranean increases from south to north and is evidently due to the existence of two-small plates that are moving rapidly (McKenzie,1970). One of these plates encompasses the Aegean Sea, part of Greece, Crete and part of Western Turkey, and the other plate contains most of Turkey, Cyprus and the northern waters of the Eastern Mediterranean (Fig.2.6). These plates are referred to as the Aegean and the Turkish plates, respectively. The importance of the southern parts of the Aegean and the Turkish plates to the present study is quite clear. A succint discussion of these segments of the two plates follows.

According to McKenzie (1970), the motion of the southern boundary of the Aegean plate is to the southwest. In doing so the plate is evidently overthrusting the Mediterranean Sea floor. The direction of motion is determined via fault plane solutions and also by the existence of the intermediate earthquakes beneath Greece and the southern part of the Aegean. The features of this plate boundary indicates that it is a trench. McKenzie points out the various evidences showing that the Mediterranean is, being overridden from the north-east, sinking beneath the Aegean Sea. Among the evidences supporting this claim are a) the seismic reflection records of sediment deformation showing thrust features (Ryan,1970 , b) a large negative free-air anomoly detected in gravity surveys (Fleischer,1964 and Rabinowitz,1969) and, c) a deep depression in the sea floor extending from Zakinthos to Rhodes (Emery,et.al.,1966).

It is inferred from the seismic activity and the fault plane solutions that the Turkish plate is moving westwards. The seismic activity does not allow a clear definition of the southern boundary of the Turkish plate, but apparently its junction with the southern boundary of the Aegean plate is south-south-west of Turkey. It continues therefrom in a south-easterly direction toward the western coast of Cyprus and then follows a north-easterly direction toward the south of Iskenderun Bay. In a recent study, Lort and Gray (1974), have found that a zone of deformation exists west of Cyprus coinciding with deep waters. Lort and Gray indicate that this deformation possibly represents a northwest-southeast trending fault described by Giermann (1966) and Wong et.al. (1971) with the north-western tip of the fault lying somewhat west of that proposed by these authors. Wide-spread tectonic activity is evidently associated with this fault. The fault is evident in the light of reflection, seismic and magnetic data. Lort and Gray maintain that the western boundary of the Turkish boundary emanate from the Gulf of Fethiye (rather than the Gulf of Antalya as drawn by McKenzie), passes through Rhodes and proceeds toward the western coast of Cyprus.

It is worth mentioning that, Ritsema (1969 and 1970) has concluded that drift of plates is not the only active agent in the North eastern Mediterranean. Gravity sliding (passive) and flow of mantle material in the low velocity layer of the mantle are likely to play a significant role.

The geophysical features of the regions to the north-east of the eastern tip of Cyprus have been partially investigated by Beltrandi and Biro (Fig.2.7). Two basins of the region, called Adana and Iskenderun basins are identified in this study. These basins have the Misis range as their common boundary, lie within a complex Alpine folded belt and are bounded by the Amanos mountains in the east and Taurus mountains in the north. The geophysical data shows that the Kyrenia range of Cyprus is connected with the Misis uplift's southwesterly extension to define a major fault and/or flexure zones on the eastern and western sides of the range (Beltrandi and Biro, 1974). Parallel to this is the apparent trend of the Amanos mountains toward the Troodes range of Cyprus.

In a recent reiew article Papazachos (1974) concludes that "the tectonics of the Eastern Mediterranean area are too complicated to be fully understood by simple seismotectonic models".

Various points discussed above as well as geophysical features of further interest are summarized in the tectonic sketch in Fig.2.8 (Neev, 1975). We refer the reader to the review article by Papazachos for details of the seismotectonics of the Eastern Mediterranean area.†

2.2.2 Seismic Data Base.

In view of various uncertainties, it is worth to discuss the various data utilized before a consideration of the seismicity of the area is given.

The seismic data employed in the present study can be deliniated into three groups:

A. The first data-set contains descriptive information of earthquakes and possible tsunamigenic events in the eastern Mediterranean region covering the period 1800 to 1900. The main source of this information is the study prepared by V.Karnik (1969,1971). The information extracted from this source for our specific region is presented in Table I-A Appendix A. Various sources utilized in gathering information for this catalogue is presented at the end of Table 2.4. It can be seen in this list that reference is given to Ambraseys Tsunami catalogue. Table I-A therefore contains some of the data presented in section 2.1. Events listed in Table I-A are mainly the selected events to the east of 24^{o}E in the eastern Mediterranean. Some other important events outside of this region are also included for completeness.

B. The second data-set again contains historical data obtained from two sources. The first source is the report prepared by S.Okamoto, A.Tabban and T.Tanuma (1979), which contains 349 catalogued events covering the period 1605 to 1965 for the general area of Turkey and its vicinity. The second source is the report prepared by K.Ergin and his group (1967) and it contains a large number of events covering the period 11 A.D. to 1964 again for the general area of Turkey and its vicinity. From these two sources a catalogue of historical data is prepared and presented in Table II-A covering the period 11 A.D. to 1900 for the eastern Mediterranean region. In Table II-A intensities are taken directly from the above mentioned sources. However, magnitudes M are computed using the formula

$$M = 0.592\ I + 1.63$$

†See also Fleming (1978).

This formula is suggested by the K.Ergin group for the Turkish data and it gives slightly higher values when it is compared with the formulae suggested by V.Karnik for the eastern Mediterranean region. These magnitudes should also be considered as rough estimations since for historical data, intensities themselves are rough estimates and, furthermore, those two sources state that the coordinates of some historical earthquakes are only approximately determined. The epicenters may thus not be as accurate as desirable. Nevertheless, the catalogue gives a general picture of the areas where epicenters are concentrated. The catalogue presented in Table II-A have been used only for informative purposes. When Table II-A is compared with Table I-A it is seen that they agree in general. There exist definite differences in the longitudes and latitudes ($\pm 0.5^{o}$ to 1.0^{o}) of shocks appearing in both catalogues and for the same shocks data presented in Table I-A gives much higher intensities. This is why these two information sets of historical data are seperated.

C. The third data set contains recorded data covering the period 1900 to 1974. The area covered in this data set is the whole eastern Mediterranean (to the east of 24^{o}E longitude) excluding the region covered by a circle of radius 300 km with its center at Akkuyu. Although the data base for the excluded region is presently available from the sources described below, it is not presented here in order to avoid duplication.

The first source in this data set is the report prepared by E.Alsan, L.Tezuçan and M.Bath (1975). The report contains 2698 catalogued earthquake events covering the period 1913 to 1970 for Turkey and its vicinity. The study is a very recent recompilation of Turkish data prepared by the seismological department of Kandilli Observatory.

The second source is a most recent computer listing of earthquakes obtained from the International Seismological Center, England, (1977), which contains earthquake epicenters as well as other information only for the eastern Mediterranean area. This source is the period 1900 to 1974.

The third source is the catalogue prepared by V.Karnik (1969,1971).

From the three sources above an earthquake catalogue is presented in Table III-A. The catalogue in table III-A contains earthquakes of $M \geq 5.0$ in 1900 to .974.

The information given in the three sources utilized to construct table III-A may show significant differences within the context of another seismic investigation. In conjunction with the present study, however, it is found (in an attempt to construct return periods etc. from the information in table III-A) that the results agree quite well with Karnik's (1971). Since Karnik's data forms one of the sources leading to table III-A, we can conclude that, the data base from Kandilli Observatory and the International Seismic Center does not significantly change (in the context of the present study) what has been provided in Karnik, including frequency, magnitude relations, return period computations etc. The information provided by Karnik thus forms the primary basis utilized in the selection of the sources for relevant tsunamis.

2.2.3 Two Primary Source Regions.

Fig.2.2 shows the epicenters and magnitudes of earthquakes (1901-1955) observed within the region of interest. Fig.2.3 shows the distribution of the epicenters of shallow earthquakes occurring in the region during 1901-1972 (Papazachos,1974). The distribution maps by Toksöz (1977) and McKenzie (1970) are shown in Figs.2.4 and 2.5. An attempt to construct a distribution map via table III-A was aborted for it did not produce any features that were not readily available in Figs. 2.2 - 2-5.

It can be seen in Figs.2.2 - 2.5 that, in relation to the N.P.P. site, the earthquakes of primary interest can be defined to lie within two regions called PR1 and PR2. The region PR1 is bounded by 30^{o}E longitude to the east 34^{o}N latitude to the south and by the Cretan Arc (formed by Rhodes, Karpathos and Crete) to the NW (Fig.2.1). PR1 is essentially a subregion of the region 26 in Karnik (Fig.2.11). The region PR2 lies to the east of 30^{o}E and between the south coast of Turkey and 34^{o}N (Fig.2.1). PR2 is contained within both of Karmik's regions 26c and 31 (Fig.2.11). The regions PR1 and PR2 essentially form the southern-most border areas of the Aegean and the Turkish plates, respectively (Fig.2.6).

In view of the similarity between the distribution of the earthquakes in general (Fig.2.2) and the shallow shocks in particular (Fig.2.3), the two regions are defined here by virtue of the differences in the magnitude of strong shocks, density of shocks having magnitudes greater than 6.0 and by the known tectonic features. The first two sets of differences will become apparent in the following sections. The matters concerning tectonics are already discussed in section 2.2.1.

It should be pointed out that, because of the protective positioning of Cyprus, the shallow earthquakes aligned along 32°N (Fig.2.3) do not make the identification of another source region to the south of 34° necessary.

The seismicity of the two regions identified are discussed next.

2.3 Seismicity of PR1 and Selection of the Source R.1.

2.3.1 General Considerations.

The average annual seismic activity in the region bounded by 34-42°N and 19-29°E is two percent of the seismic activity observed throughout the world (Galanopoulos,1963). The domain under consideration is actually larger than the area defined as the Aegean Plate (APL) though we will refer to it as APL. If an annual seismic energy release of the order of 10^{25} Ergs is assumed for the entire earth (Gutenberg and Richter,1954), then the seismic energy relased in APL is of the order of 2×10^{23} Ergs. This amount of seismic energy release is evidently constant as shown in Fig.2.9 and constitutes a significant portion of the seismic activity observed in Europe (4×10^{23} Ergs). In fact, more than 800 potential earthquake foci have been detected in APL, with 620 of these becoming active during 1951 to 1963 (Galanopoulos,1971).

2.3.2 Determination of PR1

The large conjugate fault system shown in Fig.2.10 is largely responsible for the earthquake activity in APL, defining its southern segment. It is seen in Fig.2.10 (and also from 1700-1960 data) that seismic epicenters are mostly shallow. The seismic activity increases further in the regions defined by the two edges of the fault zone, that is, in the shallow parts of the Ionian Sea (called APL-SW) and in the region to the east of Crete (APL-SE).

In the region APL-SW of the southern boundary of the Aegean Plate steep slopes are encountered and this end of the fault zone terminates at the maximum observed depth (5015m) of the eastern Mediterranean.

The strongest shallow shocks in APL-SW were on Oct.6,1957, M = 6.9 (Messini), April 30, 1954, M - 6.8 (Thessalia), August 12, 1953, M = 6.7

(Kefallinia). Intermediate-depth shocks with M 7.4 (h.100 km) and M-7.3 (h-120 km) occurred in Kithira on August 30,1926 and July 1,1927, respectively (Karnik,1971). The seismic activity in deep waters to the west of APL-SW is minimal.

The earthquake epicenters in the APL-SW lie in the shallow waters, with very small amounts of seismic activity occurring in deep waters to the further west of this region. The orientation of a potential tsunami source area is thus expected to be in the close proximity of Western Grecean, Albanian and the Yugoslavian coasts, with the major axis being parallel to the coastline. Since the major water wave energy radiation is in a direction perpendicular to the major axis of the tsunami source region (Houston and Garcia,1974), the tsunami generated in ALL-SW will preferentially radiate into the western Mediterranean and the Adriatic, the easterly wave propagation being partially blocked by Greece. Only the diffracted waves will penetrate into the eastern Mediterranean. Noting that the earthquake magnitudes observed in both APL-SW and APL-SE are of the same order, it is expected that the N.P.P. site will be less affected by the tsunamis generated in APL-SW in comparison to those emanating from APL-SE.

In APL-SE, the strongest intermediate-depth earthquake occurred on June 26,1926 (M = 7.7, h=100 km) and the strongest shallow depth earthquake on July 9,1956 (M = 7.4).

It is seen in Fig.2.10 that we can divide the eastern edge of the southern boundary of APL, i.e., APL-SE, into two regions. One of these regions is to the north and the other to the south (and SE) of the arc formed by Crete, Karpathos and Rhodes. The latter region is defined as PR1. Severe tsunamis and earthquakes have been observed in the region north of the arc, but the tsunami data clearly shows that the tsunamis observed in this region is contained within the area (Ambraseys,1962). The reason for this is attributed to the presence of narrow passages and the complex coastal geometry of the region causing dissipation and wave trapping due to multiple reflections. In addition, long waves incident to Cretan arc from the north will suffer significant reflections due to sudden increase in depth. Consequently, it is anticipated that the design earthquakes for the tsunamis that could severely affect the N.P.P. must be sought in PR1, i.e., to the south of the arc, emanating near the Gulf of Fethiye and terminating at the western tip of Crete.

2.3.3. Selection of the Tsunamigenic Earthquake source R.1. in PR1.

The statistical information concerning earthquakes in the southern Aegean Plate is provided by Karnik (1971), who utilizes the seismic data during the period 1901-1955. For details in various statistical computations the reader is referred to the text by Karnik. Only the salient matters of interest are summarized here.

Figure 2.11 shows the seismic regions specified by Karmik. The relevance of the region 26b and 26c to the region PR1 is clear. Fig. 2.12, a,b gives the frequency of occurance of earthquakes of magnitude M for the regions 26b and 26c. From these figures a possible upper bound M_{max} can be estimated. For the region 26b M_{max} is estimated to be 7.25 while for the region 26c , $M_{max} = 7.5$.These values are close to the observed maximum values(7.4 and 7.7 respectively).

Using Gumbel's theory of largest values, Karnik (1971).also provides for shallow-depth earthquakes the return periods T for earthquakes of given magnitude. These are given in Table 2.3a.

Further useful information given by Karnik involves, the earthquakes of magnitude $\hat{M}$ having return period of $\hat{T} = 100$ years with earthquakes of magnitude M greater than $\hat{M}$ occuring with a probability of one percent. This information is provided in Table 2.3b. The differences found for the calculated and the observed values of $\hat{M}$ for the region 26c indicates the possibility of occurance of yet stronger shocks.

It can be inferred from the information above that an earthquake of magnitude M 8.0 should be considered as an upper bound on the design tsunami earthquake. According to Karnik's data such an earthquake has not yet occured in this region but falls into the catogory of earthquakes that can occur every 100-800 years which time period is probably sufficient for the manifestation of seismitectonic forces in this area. However, it is felt that this estimate is on the conservative side. Indeed, seperate analysis by Basler and Hofmann (1978) indicates that an earthquake of this magnitude in PR1 has a return period of approximately 10,000 years. The source thus chosen is indicated in Fig.5.1 as RUN-1†.

2.4 Region PR2 and the Selection of the Sources R.2-R.8.

The region PR2 contains a part of Karnik's region 26c and most of the region 31 (Fig.2.11). The frequency versus magnitude relations for Karnik's regions 26c and 31 are given in Fig.2.12.

2.4.1 Southern PR2 Area: Sources R2 and R6.

The increased seismic activity along the southern and the south eastern coast of Cyprus is quite consistent with the tsunamis observed in this region (Ref.table 2.2). The statistics based on old sources (Ambraseys, 1965) indicate a frequency of about 180 years for earthquakes with intensity IX, the maximum intensity exceptionally reached on the island being X. Historical records show an apparent increase of seismic activity in Paphos, Limassol, Famagusta and Salamis. On September 29,1918 a shock of $M = 6.5$ and on September 10,1953 another shock of $M = 6.3$ have been observed as the strongest shocks, both occuring on the southern coast of the island.

Fig.31, viz., strictly applicable to this part of PR2, indicates a maximum observed magnitude of $M = 6.5$. Basler and Hofmann (1978) estimates once in a 10,000 year event in this area as an earthquake with magnitude of $m = 7.1$.

Cyprus should provide protection against tsunamis emanating from this part of PR2. In order to be on the safe side however, two earthquakes R.2 and R.6 were selected from this region. The source R.6 has a magnitude M - 7.5 and is located off the eastern tip of the island (Fig.5.1). It was felt that the tsunami originating from this source may suffer multiple reflections from the Syrian and the Turkish coastline and consequently amplify in spite of the partial blockage of Cyprus.

† In what follows, the source Rj corresponds to RUN-J; $J = 1,2,\ldots,8$ in Fig.5.1.

The source R.2 was chosen to have a magnitude $M = 6.75$ and is situated on the western end of Cyprus (Fig.5.1). Because of another nearby source having a larger magnitude and more critical positioning than R.2, this source was considered essentially for comparison purposes.

2.4.2 Western PR2 Area: Sources R.3 and R.7.

This area is essentially a transition region between the southern tips of the Aegean and the Turkish Plates and the distribution of seismic activity therefore differs from the southern PR2 and PR1. Consequently, frequency-magnitude relations (Fig.2.12) for Karnik's regions 31 and 26c will respectively provide under and over estimates for a design tsunamigenic earthquake. However this fact itself indicates that the magnitude of the tsunamigenic earthquake event should lie between $M = 7.0$ and M 8.0, Basler and Hormann (1978), estimates indicate that in this region once in a 10,000 year design event should have a magnitude between $M = 6.6$ and 7.1.

Therefore, an earthquake of a magnitude $M = 7.5$ (called source R.7) lying to the NNW of the western end of Cyprus seems to be appropriate for a conservative choice (Fig.5.1).

In view of the existence of earthquakes with $6.0 \leq M \leq 7$ in Antalya bay and to its south, another earthquake (called S.3) having magnitude 7.0 was selected to lie in Antalya Bay (Fig.5.1).

2.4.3 Northern PR2 Area: Sources R.4, R.5 and R.8.

This part of PR2 is the canal-like region extending from the southern coast of Turkey to the arc formed by connecting the Kyrenia Range to the Bay of Iskenderun (Fig.2.7). The area shows very little seismic activity, though the Bay of Iskenderun and its vicinity have experienced tsunamis of unknown source origin in the past (Event 36 and 37 in Table 2.2). In any event, the critical importance of a tsunami occuring in the northern PR2 to the N.P.P. site is clear.

Three possibly hypothetical sources R.4, R.5 and R.8 are selected in the northern part of PR2 by extrapolating the information available for the other parts of PR2 and recent surveys (unpublished).

R.4 is located on the northern coast of Cyprus across the N.P.P. site. The source R.8 is located midway between R.4 and the N.P.P. site. R.5 is situated in Iskenderun Bay. All the three sources have magnitudes of $M = 7.0$ (Fig.5.1). Basler and Hofmann (1978) estimates the magnitude $M = 6.6$ in this region to correspond once in a 10,000 year event.

III. SOURCE PARAMETERS

Once the design tsunamigenic earthquake magnitudes and source locations are selected, the next task is to evaluate the parameters of the design events. These parameters are needed in the modelling of the ground motion for numerical computations and involve the geometric characteristics of the earthquake, the maximum displacement expected and the time history of the ground motion.

3.1 Modelling the Form of Ground Motion.

In modelling the ground motions we will closely follow NARCO-NP-1 study (Appendix 4B,1975). Some aspects of the modelling of ground motions that are relevant to the present study are discussed briefly below.

The boundary of large earthquakes are elliptical in shape. Vertical displacement has a maximum at the center of the ellipse and diminishes at the boundary of the source region. Seismic sea waves emanate from a source region in such a fashion that wave energy is radiated along the minor axis of the ellipse (Momoi 1962, Houston and Garcia,1974).

In the present study the shape of boundary of source regions is modelled by a rectangle of width b_0 and length l_0 (Fig.3.1). The maximum ground displacement Δ_0 occurs uniformly along the entire major axis of the motion. This model of probable earthquake is conservative, for in reality displacement decays to zero at the two tips of the major axis. Referring to the Cartesian co-ordinate system shown in Fig.3.1 the assumed form ground displacement is

$$\Delta = \Delta_0 \, e^{-Bx} \qquad (3.1)$$

viz., in accordance with the elastic rebound theory of Reid (1910). This type of ground displacement has attained wide acceptance among seismologists and has also been verified in field (Benioff,1964). In Eqn.(3.1), B is a suitably chosen coefficient. It should be noted that aside its maxima Δ_0 , the displacement itself is also uniform along the direction parallel to the major axis.

The above model of ground motions requires that given an earthquake of magnitude M, the source parameters Δ_o, l_o, b_o, B and a source orientation be presceibed. The ways in which these source parameters are determined are discussed in this section.

3.1.1 Maximum Displacement: Δ_o.

There exist some seismic data indicating a possible functional relationship between the magnitude M (in Richter scale) of an earthquake and the maximum displacement Δ_o (Wilson,1974). This functional relationship is shown in Fig.3.2.

The maximum displacement Δ_o is in general composed of both the horizontal (strike-slip) component, ξ_o, and the vertical (dip-slip) component, ζ_o, of the motion, i.e.,

$$\Delta_o = (\xi_o^2 + \zeta_o^2)^{1/2} . \qquad (3.2)$$

An examination of various earthquake data indicates that earthquakes displaying strike-slip motions are not potential large tsunami generators (Wiegel,1970). Therefore, in utilizing the data presented in Fig.3.2, the horizontal motion ξ_o will be taken to be zero.

3.1.2 Length of Major Axis: l_o.

Wilson (1969) presents a summary, in functional form, of data on the lengths of shallow focus earthquakes v.s. earthquake magnitude M. The functional relationship $l_o = l_o$ (M) is depicted in Fig.3.3 and is utilized in the present study.

3.1.3 Width of Source Area: b_o.

Iida (1963) provides the following relationship between M and an equivalent source diameter D (in Km).

$$\log_{10} D = 0.5 M - 1.7, \qquad (3.3)$$

with the understanding that the source area is given by $\pi D^2/4$ (see also Hatori,1969).

An alternate empirical relation is provided by Wilson and Torum (1968):

$$\log_{10} D = 0.67\ M - 3.0. \qquad (3.4)$$

If b_{01} denotes the width of a rectangular earthquake estimated through Eq. (3.3) and b_{02} the width estimated through Eq.(3.4), then it is easy to show that

$$\frac{b_{01}}{b_{02}} = 13.47\ e^{-0.34\ M}. \qquad (3.5)$$

Earthquakes capable of generating significant tsunami have been known to have magnitudes greater than 6.5. For $6.5 < M < 7.65$ Eqn. (3.5) yields $b_{01}/b_{02} > 1$, while for $M > 7.65$ this ratio is less than unity. Consequently, when $M < 7.65$ Eqn.(3.3) is used for a conservative estimate of width and when $M > 7.65$ Eqn.(3.4) is appropriate.

3.1.4 Decay Constant: B.

The constant B in Eq.(3.1) is chosen, for a given earthquake of magnitude M, in such a way that a reasonable decay in displacement is attained. In NARCO-NP-1 study B is chosen in such a way that over a distance of one-half . width 95 percent decay occurs in Δ_0

3.1.5 Source Orientation.

In the present investigation essentially all the sources are oriented in such a way that the most of the wave energy emanating from a source area will radiate toward the target, i.e., the N.P.P. site (see Fif.5.1). The source R.2 forms an exception in that it is chosen to lie parallel to the fault to the south east of the Cretan Arc. This orientation is very close to a N-S orientation which will perhaps provide slightly larger radiation toward the target. By virtue of the known seismic characteristics of the region, the orientation selected here is felt to be more appropriate for this highly conservative choice of a tsunamigenic source, especially in view of its relatively small deviation from a N-S hypothetical orientation.

3.1.6 Summary.

The geometric parameters of the various sources are summarized in Table 3.1.

3.2 Modelling the Time Dependence.

A parameter that is useful in defining ground motions has been found by Hammack (1972). The parameter is called the time-size ratio and is defined by

$$T = t_c \, (gh)^{1/2}/b$$

wherein t_c is the time scale of the bed deformation, h the depth, b the length scale of the bed movement and g the gravitational constant. Note that the quantity $t_c \, (gh)^{1/2}$ is the distance travelled by long wave during the ground motion. Consequently, for $T << 1$ a significant amount of ground motion occurs before the disturbance have an opportunity to leave the source area. This type of motion is called "Inpulsive". On the other hand when $T >> 1$, the disturbance have ample enough time to leave the generation area and motions of this type are called "Creeping". Motions for which T is of order unity are reffered to as "Intermediate".

Hammack's results indicate that for impulsive type of motions ($T<<1$) the actual time-history of the ground motion is not expected to be of critical importance. Most large tsunamis have this feature (Wang and Divoky 1970, Wilson and Torum,1968),i.e. they are impulsive.

All the ground motions in this study are impulsive and chosen to occur in 5-10 seconds as a uniform upward motion of the sea floor (Table 3.1).

IV NUMERICAL MODELLING

Numerical models employed in the present study are discussed in this chapter.

The purpose of the numerical modelling is to simulate the generation of the tsunami design events and the propagation of the seismic sea waves generated towards the southern coast of Turkey, including their transformation over topography, scattering by Cyprus and the coastline configurations at large. This is achieved by the numerical solution of the shallow-water wave equations. A succint discussion of the two numerical models utilized follows:

4.1. The Finite Difference Model (FDM)

4.1.1 Equations of Motion

The main part of the computations involved the employment of a FDM for the non-linear, non-dispersive shallow-water equations in which the otation of the earth is accounted for through the Coriolis force and the bottom friction is modelled by a non-linear resistance term in the momentum equation (Dronkers,1964 Sec.3.4)

$$\vec{u}_t + (\vec{u}.\nabla)\vec{u} + g\nabla\eta + f\hat{k}\times\vec{u} + g\vec{u}|\vec{u}|/C^2(\eta+h) = 0 \quad (4.1)$$

where $\vec{u} = (u,v)$ is the horizontal velocity, the subscript implies partial derivative with respect to time t, ∇ is the horizontal gradient operator, g the gravitational acceleration, η the surface displacement from the still water level, f the Coriolis parameter, $\hat{k}$ the unit vector along the vertical, C the Chezy coefficient and h the water depth from bottom to the still water level.

The ground motion ξ is taken into account in the continuity equation (Tuck and Hwang,1971)

$$\eta_t + \nabla\cdot(\eta + h) = \xi_t \qquad (4.2)$$

which follows directly from the vertical integration of the three dimensional continuity equation by making use of the kinematic free-surface and the bottom boundary conditions.

The boundary conditions of the problem are that the velocity normal to a coastline must vanish and that at an open boundary surface displacement must be in the form of an out going wave (radiation condition).

The FDM used to achieve the numerical solution of the partial differential Eqns. (4.1) and 4.2) is the model developed by Leendertse (1967), modification being introduced to account for the time-dependent ground motion ξ (x,y,t): :

$$\xi = \bar{h}(x,y) - h(x,y,t) \qquad (4.3)$$

where $\bar{h}(x,y)$ refer to the depth of water under still-water conditions, and (x,y) to the horizontal Cartesian coordinates on the still-water plane. Leendertse's model is well documented (Leendertse, 1967, Section 3) and utilized in other tsunami studies (e.g. Hwang and Divoky, 1971). Therefore, only the salient features of the model are summarized here.

4.1.2 Computational Aspects.

Upon descretizing the space as $(x,y) = (j\Delta x, k\Delta y)$ and time as $t = n\Delta t$, a space-staggered scheme is employed where η is described at integer values of j and k, u at integer-and-one-half values of j and integer values of k, v at integer values of j and integer-and-one-half values of k, and h at integer-and-one-half values of j and k (Fig.4.1). The scheme is advantageous in that for the linear terms operated in time, there is a centrally located spatial derivative.

Computations are carried out in two cycles. In advancing from time $n\Delta t$ to $(n+1/2)\Delta t$ during the first cycle v is computed explicitly while u and η are computed implicitly. In the second cycle from $t = (n+1/2)\Delta t$ to $(n+1)\Delta t$ v and η are computed implicitly and u explicitly.

Computation of convective accelerations and bottom stress terms require special but straightforward techniques to be employed. Very little purpose will be served here to document these techniques and the reader is refferred to Leendertse (1967), section 3.2.

Computational aspects concerning the open-boundary (radiation) condition will be discussed in the next section.

4.1.3 STABILITY AND VERIFICATION OF FDM.

The FDM discussed in the preceeding sections is esentially the algorithm generated by Leendertse with some modification due to the earthquake generation terms. These terms, which can be considered as forcing-terms, are given as initial data operating in a restricted region and in a restricted time interval. The presence of forcing do not affect the amplification matrix in the stability analysis. Thus the propagation of errors in the time direction is independent of these terms. The effect of such terms should only be investigated in relation to the accuracy of generation of the initial wave pattern. Therefore, the stability question is concerned with the stability of the general FDM and this has been investigated and tested in detail in Leendertse (1967). Briefly, it is shown that, ommiting the nonlinear terms, the model is an unconditionally stable algorithm. This has been established through a von Neumann stability analysis. The stability characteristics of individual terms such as, effects of convective inertia terms, the nonlinear terms, the bottom stress terms have also been investigated separately by Leendertse. The combined influence and analysis of such terms has not been given but it is stated that if a stability investigation of all such individual factors does show numerical stability of the procedure, which is the case in the algorithm generated, then the combined effect of these factors would also lead to a stable numerical procedure. Since this statement is not necessarily true as shown by Kasahara (1955) and others, the computational model is extensively tested both by Leendertse and the present study by comparing results with other numerical studies and field data. It is found that the propagation of long-waves in coastal waters can be studied successfully by the use of the implicit-explicit algorithm developed and that there is no upper limit on the time step for stability reasons implying an unconditionally stable algorithm.

The test problems performed in this study to further control the model can be summarised as follows:

Problem one: The first problem for which computations are made is the "Haringvliet" model. This area is in the estuary of the Rhine River in the Netherlands. The input data for the problem is taken exactly as given in Leendertse (1967). In this problem the mathematical model is used to compare the measurements of tidal waves with the computational data. Our interest in this problem is to see whether the model duplicated performs as described in Leendertse and does not contain errors which might originate due to the misprints of the document programs and due to the changes introduced. In addition to the modelling of the ground motion terms, the variable time stepping changes were introduced to the model since in the earthquake tsunami solutions the duration of earthquake, Δt_Z , and the time step if the numerical algorithm, Δt, is of different orders. For a characteristic problem $\Delta t_Z = 5$ secs and $\Delta t = 100$ secs so in an earthquake-tsunami problem, the solution starts initially with $\Delta t_Z = \Delta t$, generating the initial wave pattern, then for time $t > \Delta t_Z$, the time step Δt is changed to a larger prescribed time interval. This operation is necessary to use the computer time efficiently. In this test problem the earthquake ground motion is not existing and the forcing wave pattern is introduced as boundary data at the entrance of the estuary. So this problem is mainly used tod ebug the computer code. After some corrections it is found out that the computer program is in operating condition and the variable time stepping changes introduced are operating properly. During the solution sequence, the half time step, Δt, is changed from 90 secs to 270 secs after ten steps of computation. The results as given in Figure 4.2, agree well with the numerical results of Leendertse.

Problem two: The performance of the terms introduced to simulate the gound motion is controlled by running several test problems following the main lines of the theoretical and experimental studies performed by Hammack (1972). In Hammack's study, experimental and theoretical studies for two dimensional and three dimensional models were made analyzing the relation between the maximum wave amplitudes and the maximum bed displacement as a function of the time size ratio., $t_c \sqrt{gh}/b$, for two dimensional model ($t_c \sqrt{gh}/r_0$ for three dimensional model) in the generati[illegible] region The numerical simulation of two and three dimensional models can be seen in Figures 4.3 and 4.4. In the three dimensional model the circular generation region used by Hammack is represented by a square generation region as an approximation, keeping the surface areas the same. Solid boundaries represent regions of perfect wave reflection and the open boundaries are considered as transmission boundaries. Computational procedures for such transmission boundaries are described in Figure 4.5. In this process the water depth is averaged between the last two cells approaching a sea boundary and η η δ at the last cell is set equal to the previous cell value of η taking into account the time it takes for the wave to propagate between the cells. Although this standard procedure works perfectly only for waves approaching the boundaries normally, the reflection effects are minimised in all the problems analyzed in this study for oblique wave approaches by keeping the sea boundaries away from the area of interest.

Several numerical results obtained which closely agree with the results presented by Hammack as seen in Figures 4.6 and 4.7. These test runs are considered sufficient to safely use the computer code generated in the analysis of tsunami wave propagation problem in the Eastern Mediterranean. Analysis of several runs made can by seen in the following chapter.

4.2 The Finite Element Model (FEM).

A finite element model was also developed partially for checking at least one of the FDM computations and partially for an assesment of dispersive effects. FEM model check is rather limited in its extent to provide a greater number of runs through FDM formulation.

4.2.1 On Dispersion.

Equations of motion (4.1) and (4.2) adopted for FDM do not account for dispersion (Carrier,1971). It is known however that dispersive effects play a crucial role in the propagation of a long-wave with an Ursell number $U = aL^2/h^3$ of order unity, with h, L and a denoting the scales of depth, horizontal motion and surface displacement, respectively (Hammack, 1972 and Hammack and Segur, 1978). When the Ursell number is of order unity the leading edge of the wave train in general contains a (sequence of) solitary wave(s) followed by an oscillatory tail. In addition, a wave train with $U=0(1)$ disintegrates upon interacting with bottom topography in such a fashion that can not be predicted by Eqs. (4.1) and (4.2) (Madsen and Mei,1969).

In the present study an attempt is made only to check a possible disintegration of the incident tsunami when,in approach to the N.P.P. site, it encounters the continental shelf. It is worth mentioning in any event that, in view of the distances involved between the source regions and the target, the criteria given by Hammack and Segur (1978) implies the applicability of the non-linear, non-dispersive equations to the problems considered in the present study.

4.2.2 Features of the FEM.

Dispersive effects are accounted by the addition of the term

$$\vec{F} = \frac{1}{3} h\nabla(\nabla.(h\vec{u})_t) - \frac{1}{6} h^2\nabla(\nabla.\vec{u}_t) \qquad (4.4)$$

to the right hand side of Eqn. (4.1). The term thus added accounts for weak dispersion when $U=0(1)$ (Peregrine 1972).

The FEM utilized here follows in essence Connor and Wang (1973). Very little purpose will be served in spelling out the lengthy details which are readily available in Connor and Wang (1973). Only the salient aspects are summarized here.

The model equations of Connor and Wang do not contain dispersive terms expressed in Eqn. (4.1), but involve lateral diffusion and wind-stress forcing which are not relevant here and hence are set equal to zero. A Galerkin formulation is then made leading to the weak solutions of the equations. The equation of continuity is weighted with respect to δy and the momentum equation $(4.1 = \vec{F})$ with respect to $\delta\vec{u}$, with δy and $\delta\vec{u}$ being weighting functions. Forming the residual equations leads, after employing Gauss' theorem:

$$\iint_A \{\eta_t + \nabla.\ (\hat{h}+\eta)\ \vec{u} - q\}\ \delta\eta dA = 0$$

$$\iint_A \{(\vec{u}_t - \vec{B}).\ \ \delta\vec{u} - \underset{\sim}{F}.\ \Delta\} dA - \oint_{S_o} \underset{\sim}{F}.\hat{n} dS = 0 \qquad (4.5a,b)$$

Where A denotes the domain, S_o the open boundary, $\hat{n}$ the unit normal vector to S_o, q the ground motion ξ_t and where

$$\Delta = \{(\delta u)_x,\ (\ \delta v)_y\} \qquad (4.6)$$

$$\underset{\sim}{F} = \frac{1}{3}\ \bar{h}^2 \begin{Bmatrix} \langle u_t \rangle x & \langle v_t \rangle x \\ \langle u_t \rangle y & \langle v_t \rangle y \end{Bmatrix} \qquad (4.7)$$

with $\bar{h}$ being defined through Eq. (4.3), and subscripts implying differentiation. In the 2x2 matrix defined by Eq.(4.7) $\langle\ \rangle$ implies (dispersive) terms evaluated by central differences from time level computations t_{n+1} and t_n at the t_{n+1} time computation level by means of an iteration to be discussed shortly. The forms expressed in Eqs. (4.5a) and (4.5b) are similar to those in Connor and Wang (1973, Eqs. (24) and (27)) with F matrix being defined here by (4.7) while implying the turbulent stress tenser in Connor and Wang. (This similarity is due to the fact that the dyadic operation $\nabla.\underset{\sim}{F}$ on $\underset{\sim}{F}$ leads, to a good degree of numerical approximation, to F defined by (4.4), assuming slow variations in depth h). The FEM computational aspects starting from (4.5) are thus essentially the same as that given in Wang and Connor (1973, Chapters 4 and 5) and therefore are not discussed here.

It is worth pointing out however that, in the present work three model triangular elements are also choosen with linear variation of the unknown parameters in each element. The trapezoidal rule is employed in the time integration scheme. An iteration is required since the forcing terms in the final matrix equations obtained are non-linear. A relaxation factor was used to accelerate the convergence of this computation. The mass matrix are fractured initially and time stepping consists of successive forward and backward substitutions and convergence is defined by the percentage change in the Euclidean norms for the surface elevations and mass flux vectors.

4.2.3 Testing FEM.

In order to check the computer code generated tests similar to those carried out for FDM were made. Results obtained using FEM also show close agreement with the theoretical and experimental studies of Hammack and these results are also shown in Figs.4.6. and 4.7. In addition, the problem given in Connor and Wang (1973) is duplicated to debug the computer code. Results obtained (not presented here) follows perfectly the numerical results of Connor and Wang (1973). It is felt however that the FEM scheme adopted could introduce serious errors as far as the boundary conditions on S_0 are concerned. Considering the fact that FEM is a minor aspect of the present study these matters are not pursued further.

V. NUMERICAL RESULTS

A total of eleven computer runs were made. Eight of the runs made correspond to the tsunamis emanating from the source regions R.1-R.8, and the computations are carried out by using the FDM. The run R.3 was repeated to investigate the sensitivity of the results to the magnitude of the source area selected. Run R.8 was repeated twice, firstly for an assesment of the sensitivity of the results to friction, and, secondly, for investigating, through FEM, the possibility of the disintegration of the incident wave while shoaling over the shelf.

The idealization of the regional characteristics, the data used and the numerical results are summarized in this chapter.

5.1 Finite Difference Model Results

5.1.1 Basic Input-Output

The finite difference meshes used in the FDM runs are of size (11 x11 km^2) and (5.5 x 5.5 km^2). The depths and the coastal configuration were read from the Admiralty maps of scale 1:1100000. These maps have been updated by the Hydrographic Office of the Turkish Navy, with corrections up to 1976. Additional bathymetric data giving the details of the region between Turkey and Cyprus was obtained from a 1:300000 map prepared by M.T.A. Institute.

Approximate locations of the various source regions are provided in Fig.5.1. The locations of the meshes referred below are shown in Fig.5.2. The source parameters of each run are given in Table 3.1.

Figures (5.3) to (5.10) give, for each Source R.1 through R.8, the surface displacement as a function of time in the close proximity of Akkuyu Bay with the mesh point ($M = 42$, $N = 18$) corresponding to the entrance of Akkuyu Bay. The mesh points ($M = 40$, $N = 18$) and ($M = 44$, $N = 18$) are located, respectively, to the east and west of the bay (Fig.5.2).

5.1.2 Sensitivity to Source Area and Friction.

In order to check the sensitivity of results to the source area selected, the run R.3 (Antalya Bay) was repeated as run R.9 by enlarging the source area by a factor of 1.5. The results are presented in Fig.5.11. The main difference found is that the waves emanating from the source with larger area (:R.9) arrive at an earlier time. The differences in the time history of two runs are otherwise insignificant. This is comforting because it shows that the available magnitude-area relations (ref. Chapter III) can be used though they are deduced mostly from data obtained in other seismically active regions of the world.

Another sensitivity run made involves the effect of friction. The run R.8 is repeated as run R.10 using a constant Chezy coefficient of 100. The R.10 output is presented in Fig. 5.12. It can be inferred by comparing Figs. 5.10 and 5.12 that effect of friction is insignificant. The frictional terms in the equations of motion were thus set equal to zero in runs R.1 - R.8.

5.1.3 Supplementary Output

In order to discuss the salient aspects of the preceeding results, supplementary information is provided along selected traverses and at pertinent locations that are shown in Fig.5.13. This is done for runs R.1, R.4 and R.7 which are found to be more critical than the others.

Starting shortly after the ground motion, Fig.5.14 gives the surface displacement along section 1-1'. Section 1-1' extends from Rhodes to the south of Iskenderun Bay along a line essentially parallel to the southern coast of Turkey. The profile of the surface motion along 1-1' at successive times provides, in particular, a picture of the penetration of the incident tsunami into the Cilician Basin (for runs R.1 and R.7) or spreading from there (run R.4).

Figs. 5.15 - 5.17 shows for R.1 the profile of the surface motions along transverse sections 2-2', 3-3' and 4-4' at successive times. The sections 3-3' and 4-4' are essentially input-output control sections for the canal-like region between the south coast of Turkey and Cyprus. The section 2-2' extends from Akkuyu to Cyprus.

Fig.5.18 gives for R.1 the time histories of the free surface motion at a point directly opposite to Akkuyu (point 4) on the Cyprus coast, at Anamur (point 5) located on the Turkish coast and at the north-eastern Antalya Bay (point 6) also on the Turkish coast.

The contours of constant height of the water surface in the Cilician basin is provided in Fig.5.19 for initial times after the generation of Run R.1 tsunami. At subsequent times, the motion becomes too complex, therefore not allowing the extraction of relevant information with ease.

Figures 5.20 - 5.29 provides, for runs R.4 and R.7, the same information discussed above in conjuction with run R.1.

5.2 Finite Element Run.

The region considered in the finite element run is the region between Turkey and Cyprus. In the idealization of this region 235 elements with 154 nodes are used. The bathymetry data and the coastal configuration for this idealization are obtained from the 1:3000,000 scale map by M.T.A. Institute. Run R.8 is repeated using this idealization. The results are presented in Fig.5.31.

VI. DISCUSSION OF RESULTS

The preceeding results are discussed in the present chapter which is organized as follows.

The magnitude of the tsunamis 5 - 11 km off-shore of the target are discussed first and a resonant tuning is pointed out. Space-time characteristics of the motions are then examined in detail. The results indicate a resonant coupling of the deep waters of the Cilician Basin to the shallower waters along the Turkish coast. The tsunamis at the target are then examined in the light of the resonant-coupling using both the numerical results and the analytical methods.

6.1 Magnitude of Off-shore Surface Motions.

A cursory examination of Figs. 5.3 - 5.10 reveals that the largest surface displacements are induced by source R.1, situated to the south-east of the Cretan Arc (Fig.5.1). R.1 is the severest of all the tsunami sources under consideration because the associated earthquake magnitude is $M = 8.0$, yielding a ground displacement of eight meters (Table 3.1). The remoteness of R.1 to the target (:Akkuyu Bay) in comparison to the other sources in only deceptive. This is because the tsunami emanating from R.1 propagates in deep waters (4000 - 1000 m) and therefore arrives at the target area in a relatively short time ($\simeq$ 43 min), the measure of its speed of propagation being $\sqrt{gh}$, where h is the water depth and g the gravitational acceleration. Indeed, the tsunami originating from R.7 located less than half way between R.1 and the target arrives approximately 26 minutes earlier than that emanating from R.1 (Figs.5.3 and 5.9). The rapid propagation of R.1 tsunami because of the deep waters on its path also implies that the initial disturbance reaches to the target region (i.e. waters separating Turkey from Cyprus) before the radiation of the energy into the Eastern Mediterranean at large becoming significant (following multiple reflections from the coastal features). This implies a delivery of significant amount of the incident energy into the target region.

Another, and perhaps more important, reason for significant amount of energy radiation from R.1 into the target region lies in the fact that the source R.1 is blocked by the island arc to its north-west. The initial disturbance generated is thus reflected and partially radiated back toward the target. The reflection of the initial disturbance can be inferred easily in Fig. 5.14 by examining the motion at 820 and 2820 seconds after the commencing of the motion. This is not the case for the tsunami originating from source R.7, because the initial disturbance is radiated more or less the same amount toward and away from the target region (Fig.5.20). Consequently, the differences in source parameters of R.1 and R.7 are enhanced further to make R.1 a more important source than R.7 in spite of its deceptive remoteness.

Moving on these lines, it is worth noting next that the source R.6 located to the north-east of Cyprus (Fig.5.1) with source parameters equal to that of R.7 yields oscillations comparable to that due to R.7 and hence is not as crucial as source R.1. The relative unimportance of R.6 is consistent with the historical data, for no evidence of a simultaneous occurance of tsunamis at the Syrian coasts and the target area can be found. However, simultaneous tsunamis along the Syrian coast and the Bay of Iskenderun have been observed in the past (see events 36 and 37 in Ambraseys catalogue). Consequently, both the numerical results and historical evidence shows that the tsunamis generated near or at the source R.6 area are preferentially tadiated towards south. Therefore, the possibility of the tsunami originating from R.6 amplifying within the Cilician Basin as a result of multiple reflections from the Turkish and Cyprus coasts is small.

In relation to the target region, the blockage provided by Cyprus makes R.2 an unimportant source (Fig.5.4). This is as expected and historical evidence points out the same (ref.sec.2.1).

The source R.3, located in Antalya bay, is also not as important as the source R.1, mostly because of the differences in the parameters of these two sources (Figs.5.3 and 5.5 and Table 3.1). This run was made due to the presence of the tsunamigenic earthquakes observed in the bay (see, e.g.Fig. 2.4).

The tsunami source R.5 in Iskenderun bay yields small surface motions (Fig.5.7) in the target area, indicating perhaps, partial radiation to the south through the opening between the eastern tip of Cyprus and the Syrian coast.

Next to the source R.1, the sources R.4 and R.8 are found to be crucial with regard to the surface motions they generat at the target in spite of their small (with respect to R.1) source parameters. In view of the absence of past tsunamis and seismic activity in the area, the sources R.4 and R.8 are both highly hypothetical. The source R.4 lies along the Cyprus coast and opposite to the target and the source R.8 is located mid-way between Cyprus and the Turkish coastline. A comparison of Figs.5.6 and 5.10 shows that the tsunami height due to R.4 is greater in magnitude by about 40 cm. This can be attributed to the unidirectional spreading (toward the target) of the initial disturbance in case of R.4.

In summarizing the above discussion, it can be said that the source R.1 generates the largest surface motions at the target area. The tsunami originating from R.1 rapidly propagates into the target region, arriving approximately 43 minutes after the initiation of the ground motion.

For R.1, the magnitude of the initial motion at the target is 2 meters (peak to peak) almost evenly splitted as 1 m. rise and 1 m. fall in the still-water level. More significantly, an examination of the motion at times subsequent to the initial oscillations shows that the surface motions are amplified further, leading to ±1.5 m. rise and fall in the still water level. Before proceeding to the examination of this amplification, certain details of the motions must be considered.

6.2 Details of the Motions.

Attention is fixed in this section to the space-time characteristics of the motion in the Cilician Basin (target region) and its shallower easterly extension.

6.2.1 Evolution of the Spatial Characteristics

Figs.5.14 and 5.20 shows for runs R.1 and R.7 the establishment of the motion along the longitudinal axis of the Cilician Basin. Figs (5.18 -

5.17) and (5.21 - 5.23) show that initially the incident tsunami propagates essentially with uniform crests along the transverse axis of this canal-like region. The contours of the surface displacement shown in Figs 5.19 exemplifies further this one dimensional wave propagation with wave speed being reduced along the shallower northern bank of the target region (Figs.5.19 a). It should be noted that the incident wave is diffracted from the eastern tip of Cyprus (Fig.5.19 b), indicating partial radiation of energy into the Eastern Mediterranean through the opening between Cyprus and the Syrian coast.

With increasing time, the incident wave is reflected partially from the step-like decrease in depth at the eastern end of the Cilician basin and partially from Iskenderun area. In addition, transverse oscillations are set up (Figs.5.15 - 5.17 and 5.21 - 5.23) so that the motion in the target region becomes a complex combination of transverse and longitudinal oscillations. For Run R.4 the transverse oscillations are set up immediately after the activation of the source (Figs.5.25 - 5.26) and this is as expected because of the source locations.

In view of the complex geometry it is only natural that transverse motions are excited in the region. However, the amplification of the transverse oscillations with time points out a resonant growth. This is pursued further in the subsequent section.

6.2.2 Frequency Selectivity and Temperal Characteristics near the Target Region.

The most striking temporal characteristics of the time history of all surface motions off-shore of the target (Figs.5.3 - 5.10), resulting from tsunamis generated by quite different sources, is that the motions following the initial disturbance shows an approximate period of 900 seconds $\simeq$ 15 minutes. This feature is most pronounced in Run R.1 (Fig.5.3). Another period somewhat greater than 1.4 hours is also evident, especially at the mesh point $M = 40$, $N = 18$ in Run R.1 (Fig.5.3), where it is also clearly seen that the motion with 900 sec. period amplitude modulates over an oscillation with a larger period. This frequency selectivity of the target region is further demonstrated in Figs. 5.18, 5.24 and 5.29, where we have shown the surface motions due to three different sources, at a location opposite to the target, at a point located at the western entrance to target region, and at a point situated outside the target region in Antalya Bay.

The tsunamis generated by any one of the sources contain an infinite set of frequencies (or a spectrum of waves). The selection of a definite set of frequencies in the target region shows a resonant response. But what further appears to be involved here requires additional examination of data.

In order to examine the frequency selectivity of the target region further, the time history of the surface motions off-shore of the target and at point No.4 opposite to the target is low passed by averaging the oscillations over 1000 second segments. The results are shown in Fig.5.30. It is clearly evident in Fig.5.30 that the motion is composed (for large time) of two basic oscillations, one of which has a 900 sec.period modulating amplitude and the other with 5000 seconds period. There exist phase differences between the amplitude envelopes of the oscillations near the target and at the point located opposite to it. This shows an energy exchange between the shallower waters near the target and the deeper waters it faces. The energy exchange between the two water masses is reminiscent of that observed in coupled oscillators whose resonant periods are nearly coincident (Morse and Ingard,1968). In fact, in the absence dispersion, the observed modulation could only be resulting from resonant coupling. The amplification of the off-shore tsunami in Akkuyu Bay must therefore be investigated in the light of not only the frequency selectivity, i.e. resonant tuning, alone but also in light of the coupled resonant oscillations. This is done next.

6.3 Near-Shore Modifications and Response at the Target.

It has been noted that for large time, the wave motions at the target area evolve into a series of oscillations with selected set of frequencies. The same frequencies seem to persist in all runs, and other components of the initial tsunami spectra have been selectively filtered out. This fact points out to the presence of a resonant response, mainly due to the local bottom topography at the target area and the general geometry of the Cilician Basin at large.

6.3.1 Effects of the Shelf and the Cilician Basin Geometry on Resonant Response.

One of the dominent influences on the observed resonant response is the specific shelf bathymetry. The sourthern Turkish coast joins into a relatively marrow and steep continental shelf area. The shelf break is at an offshore distance of $l_1 = 15$ km and has a depth of $H_1 = 400$ m. Analyses of motions on a shelf with linear depth variation can be found in Appendix B, the n'th mode resonant periods T_n of the shelf can be calculated from

$$T_n \quad \frac{4\pi l_1}{j_n \sqrt{gH_1}}$$

as $T_1 = 20.7$ min., $T_2 = 9.0$ min., $T_3 = 5.7$ min., ...etc. The first mode resonant period $T_1 = 20.7$min. is seen to be close to the observed 15 min. oscillations.

Furthermore, the Cilician Basin covers the area between Turkey and Cyprus and is bounded on the Eastern end by a shallow area (depth dropping from 1000 m. to 600 m.) with sill features joining Iskenderun Bay to Cape Andreas. In view of its approximately parallel banks along the coasts of Turkey and Cyprus and the topographic features towards Iskenderun, the Cilician Basin and its easterly extension can be isolated as an essentially rectangular body of water. Its width and length can be estimated as $W =$ 90 km and $L = 250$ km, respectively. This rectangular basin opens into the rest of the Eastern Mediterranean waters through openings at the Eastern and Western extremities, near which there are also sharp changes in depth. Mainly due to the latter fact, the natural periods of this system can probably be calculated using Merian's formula for a closed rectangular basin (see Ippen,1966):

$$T_{nm} = \frac{2}{\sqrt{gH}\,\sqrt{(\frac{n}{L})^2 + (\frac{m}{W})^2}}$$

where H is the basin depth, and n,m are integers. Taking the depth to be $H = 1000$ m, periods of the pure transverse ($n = 0$) modes are $T_{01} = 30.3$min, $T_{02} = 15.1$ min, $T_{03} = 10.1$ min, etc. and of the pure longitudinal ($m = 0$) modes are $T_{10} = 1.4$ hrs., $T_{20} = 42.1$ min.etc. Of these natural periods, the second mode transverse oscillation of 15 minutes (900 sec.) and the first mode longitudinal oscillation of 1.4 hrs (5000 sec.) are present in the high and low passed time series respectively of Fig.5.30 , Run R.1.

The 1.4 hr. oscillation is present during the initial arrival of the tsunami, but it persists throughout the rest of the time probably because of resonant oscillations in the longitudinal direction of the Cilician Basin. In this case only the first mode is picked up, since in the presence of radiation damping, the first mode is usually the most significant of all modes.

For the transverse oscillations the same argument does not appear to be valid, since it has to be noted that the observed 15 min (900 sec) oscillation is only the second mode of the large canal section between Turkey and Cyprus. However, the 15 min period is also close to the 20 min natural period of the narrow Turkish continental shelf. Therefore it is not unreasonable to expect coupled transverse oscillations of the shelf and the canal regions. In fact, it may be only because of this coupling that not the 30 min first mode of the canal, but the 15 min second mode coupled oscillation has been selected from the initial spectrum. The coupling or quasi-resonance of the shelf and canal modes is evidenced further-more by the observed surging of wave energy from one section to the other as in Fig. 5.30. Beats in the oscillations calculated at Akkuyu and across from Akkuyu at Cyprus are noticably out-of-phase, due to the exchange of energy taking place between the two sections. The energy is stored temporarily in one part of the coupled system, then fed into the other, and the oscillations seem to persist even at the absence of continuous energy supply required by other (uncoupled) systems.

It is also possible that the persistence of the oscillations in Fig. 5.20 is further strengthened by trapping of the waves in the longitudinal direction. The depth steadily decreases as one moves from the Western end of the canal towards Iskenderun. Infact, the bathymetry reveals sudden changes in depth with a decrease from 2000 m to 1000 m. at the Western end and from 1000 m. to 600 m. near the Eastern tip of Cyprus. This can cause trapping of energy at certain frequencies due to multiple reflections at these depth discontinuities.

Whatever the cause for its persistence may be, the beats formed at the two sides of the Cilician basin signify a type of resonant condition which is known as mode coupling that is frequently observed in acoustic, optical or electronic wave guides, or transmission lines. In this type of resonant-tuning of coupled systems, perfect tuning can never occur, therefore the coupled natural frequencies are always slightly mismatched. In the present case, the first mode of the shelf region is seen to be coupled to the second mode of the canal region. This phenomenon is called mode-coupling or mode-jumping in the context of other propagation problems. (see for example,Scott, 1970, Tolstoy,1973, and Tolstoy and Clay,1966).

In Appendix B a simplified treatment of the resonance conditions over the shelf is given. The actual coupling phenomenon is more complicated than the description presented. In the analysis the decoupled modes of the shelf have been found for a motion specified at the shelf break. It is shown that if the forcing frequency is close to one of the natural frequencies of the shelf, only this frequency will be selected and it will be modulated due to resonant tuning. For example taking $H_1 = 400$ m., $l_1 = 15$ km., and $\omega_o = 2\pi/900 \text{ sec}^{-1}$, the beat period T_B and the maximum modulation amplitude A_B at $x = 0$ are obtained as

$$T_B = \frac{4\pi}{\omega_0 - \omega_1} = 110 \text{ min.}$$

$$A_B = \frac{\sqrt{gH_1}\ \eta_o}{2l_1 \ (\omega_0 - \omega_1)\ J_1\ (j_1)} = 2.12\ \eta_o$$

where $\omega_1 = j_1\sqrt{gH_1}/2l_1$ and $j_1 = 2.40$. The calculated period is in agreement with the observed beat period in Fig. 5.30. The beat amplitude is roughly twice the amplitude of the oscillations at the shelf break.

The numerical modelling efforts always use a finite grid size in the calculation procedures and therefore the nearshore modification of the tsunami waves on the part immediately seaward of the coastline cannot easily be resolved by the model simulations. This area actually extends to a considerable offshore distance on the shelf. For example, in the critical run of R.1 the grid size is 11 km. and the grid depth at which the calculations are carried out near Akkuyu is taken as 200 m. This depth corresponds to an offshore distance of about 10 km. The above analytical approach is taken in order to account for the modification in this narrow region on the shelf. Conservatively, the calculated wave heights in this last grid may be taken to be at the shelf break. Then the maximum amplitude of $\eta_0 = 1.5$ m found by numerical modelling is increased to a beat amplitude of the coast of $A_B \approx 3.2$ m. by the analytical extention explained above. Trial runs of the numerical model have indicated the same order of magnitude, even though the assumptions used in modelling nearshore regions of the Akkuyu Bay are considered simplified. Therefore the maximum tsunami amplitude found by this study will be taken as 3.2 m.

VII. DESIGN CONSIDERATIONS

The spatial and temporal characteristics of the design tsunami modelling results have been discussed in the previous chapters of this report. In the present section, sea level changes due to other additional effects such as tides, storm surges, wave runup and their design magnitudes are discussed.

7.1 Design Storm Surge and Storm Wave Runup.

The storm surge and storm wave runup have been calculated for statistically representative storm magnitudes following standard procedures and lined in the Shore Protection Manual (1973), (SPM) prepared by the U.S. Army Corps of Engineers. The wind statistics and design storm parameters were provided by both TEK (1977) and Basler and Hofmann (1978) in separate analyses. A data base of 10 years was used to estimate the 100 year design events and the 10000 year (extreme nonoccurrence probability) events. Both analyses have yielded similar results for the storm wind magnitudes.

Analyses have been made by TEK (1977) for both hourly average winds and gusts. It has been concluded that (Table 7, TEK Akkuyu Meteorology. Report,1977) the gust speeds are roughly twice the hourly average wind speeds, for all frequencies of occurrence.

For storm surge calculations the sustained wind speeds are more important than the gust speeds since the gusts are ineffective due to their shorter duration, and since the empirical methods utilizing sustained wind data statistically include the effects of gusts. The gust speeds for 10^{-2} and 10^{-4} probabilities of occurrence have been estimated as 45-50 m/s and 60 - 65 m/s, respectively, in the previous analyses. The corresponding hourly average values representing sustained winds are therefore roughly 25 m/s (50 knots) and 35 m/s (70 knots) (1/2 the gust speeds) respectively, for 10^{-2} and 10^{-4} probabilities of occurrence. An additional calculation has been carried out for a sustained wind speed of 50 m/sec. (100 knots), mainly for comparison purposes. In the corresponding wave setup calculations, a maximum storm duration of 9 hrs is assumed to be typical. The storm surge and storm wave setup results are summarized in Table 7.1.

7.2. Combined Design Events

Sea level rise due to combined design events are of interest in evaluating the design alternatives. For this purpose two possible statistically independent events are considered: 1) the combined occurrence of storm surge, storm wave setup and tides, 2) the combined occurrence of tsunami runup and tides. The runup of storm generated waves on the beach section has been excluded, since it can be the subject of a separate investigation.

The maximum measured tidal amplitude at Akkuyu is found to be 0.7 m. above mean sea level (ref.TEK-Akkuyu 2nd Progress Report in Physical Oceanography 1978). The maximum tsunami wave runup is found to be about 3.2 m. by the present study, and roughly corresponds to a 10^{-4} probability of occurrence, as noted in earlier chapters. The summary of combined events can be found in Table 7.2. The combined occurrence of the two independent events of the previous paragraph have also been included as an event of 10^{-8} probability.

REFERENCES

1. Ambraseys, N.N., "Data for the Investigation of the Seismic Sea-waves in the Eastern Mediterranean", Bull.Seismol.Soc.Amer., 52,4, pp.895-911,1962.

2. Ambraseys, N.N., "The Seismic History of Cyprus", Revue pour l'etude des calamites, No.40,1965.

3. Aslan,E., Tezuçen,L. and Bath,M., "An Earthquake Catalogue for Turkey for the Interval 1913-1970", Kandilli Observatory Seismological Dept., Istanbul,1975.

4. Bassler and Hoffman, Consultants, "NPP Akkuyu, Stormwind Evaluation Based on Anamur Wind Data", Bassler and Hoffman, Reference Filing No: 1-N. 24-B-D, April 1978.

5. Benioff,H., "Earthquake Source Mechanisms", Science,Vol.143, pp.1399-1406,1964.

6. Beltrandi,M.D., and Biro,P.H., "The Geology and Geophysics of the Iskenderun Basin, offshore Southern Turkey", Rapp.Comm.Int.Mer.Meditt, Vol.23,42,1975.

7. Carrier,G.F., "The Dynamics of Tsunami", Math.Probs.in Geophysical Sciences, Lectures in App.Math., Vol.13,pp.157-187, Am.Math.Soc.,1971.

8. Connor,J.J., and Wang,J.D., Mathematical Models of the Mass.Bay, R.M.Parsons Lab., Tech.Rep.172, M.I.T.,1973.

9. Dronkers,J.J., Tidal Computations, North-Holland Pub.Co., Amsterdam, 1964.

10. Emery,K.O., Heezen,B.C., and Allan,T.R., Deep Sea Res., V.13,pp.173, 1966.

11. Ergin,K., Göçlü,U. and Uz,Z., A catalogue of Earthquakes for Turkey and Surrounding Area, Technical Univ.of Istanbul. Fac.of Mining Eng.,1967.

12. Fleischer,V.U., Deutsche Hydro.Zeit., V.17,pp.152,1964.

13. Fleming,N.C., "Helocene Eustatic Changes and Costal Tectonics in the Northeast Mediterranean", Phil.Trans., Roy.Soc.London,1978. Vol.289, No.1362,1978.

14. Galanopoulos,A., Annali di Geofisica, Rome, V.16,No.1.,1963.

15. Galanopoulos,A., Elements of Seismology, Athens,1971.

16. Gairmann,G., Bull.Inst.Oceanog., Monaco, V.66,pp.1362,1966.

17. Gutenberg,B., and Richter,C., Seismicity of Earth and Associated Phenomena, Princeton Univ.Press,1954.

18. Hammack,J.L., "Tsuanamis-A Model of Their Generation and Propagation", W.M.Keck Lab. of Hyd.and Water Res., Tech.Rep. KH-R-28, Cal.Tech.,1972.

19. Hammack,J.L., and Segur, H., JFM., Vol.84,Part 2,359-373, 1978.

20. Hatori,T., "Dimensions and Geographic Distribution of Tsunami Sources Near Japan", Proc.Int.Symp. on Tsunamis, Hawaii - 1969, East-West Center Press.Honolulu,1970.

21. Heck,N.H.,"List of Seismic Sea Waves", Bull.Seismol.Soc.Am. 37, pp.269-286,1947.

22. Houston,J.R., and Garcia,A.W., "Type 16 Flood Insurance Study: Tsunami Predictions for Pacific Coastal Communities", Tech.R.H.-74-3,U.S.A.E. Waterways Exp.sta.,1974.

23. Hwang,L.S., and Divoky,D., "Tsunami Generation", J.G.R. Vol.75,p.6802, 1970.

24. Iida,K., "Magnitude, Energy and Generation Mechanism of Tsunamis and Calalogue of Earthquakes Associated with Tsunamis", I.U.G.G.Mono., No.24, pp.7-18,1963.

25. Ippen,A.T., (Ed.) Estuary and Coastline Hydrodynamics, McGraw-Hill,1966.

26. Karnik,V., Seismicity of the European Area, Part I, D.Reidel Publ.Co. 1969.

27. Karnik,V., Seismicity of the European Area, Part 2, D.Reidel Publ.Co. 1971.

28. Leendertse,J.J., Aspects of a Computational Model for Long Period Water Wave Propagation, Rand.Corp.Mem., RM-5494-PR,1967.

29. Lort,J.M., and Gray,F., Nature, V.248,pp.745-747,1974.

30. Madsen,O.S., and Mei,C.C., "Dispersive Long Waves of Finite Maplitude Over an Uneven Bottom", T.R.117,Hydrodynamics Lab., M.I.T.,1969.

31. McKenzie,D.P., Ceophys.J.Roy.Astron.Soc., Vol. 18, p.1,1969.

32. McKenzie,D.P., "Plate Tectonics of the Mediterranean Region", Nature, v.226,pp.239-243,1970.

33. McKenzie,D.P., Geophys.J.R.Astr.Soc. V.30,p.109,1972.

34. Momoi,T., "Directivity of Water Waves Generated by Elliptic Bottom Source Movement", Bull.Earthquake Res.Inst., Vol.40,1962.

35. Morse,P.M., and Ingard,U., Theoretical Acoustics, McGraw Hill,1968.

36. Neev,D., Geology,.Vol.3.pp.683-686 1975.

37. Okamoto,S., Tabban,A., and Tanuma,T., Turkiye Deprem Şiddetleri Kataloğu, Deprem Araştırma Enstitüsü, Avıcara, 1970.

38. Papazachos,B.C., Eng.Seis.and Earthquake Eng., Nato Adv.Stud. Inst., Ser.E.App.Sciences, No.3,1974.

39. Peregrine,D.H., "Equations for Water Waves and the Approximations Behind Them", Waves on Beaches, pp.95-121,1972.

40. Rabinowitz,P.D., and Ryan,W.D.F., Trans.Amer.Geophys.Un., Vol.50,pp. 208,1969.

41. Reid,H.P., "The Mechanics of the Earthquake. The California Earthquake of April 18,1906, Report of the State Investigation Commission", Vol. 2, Carnigie Inst.Washington, Washington,D.C.,1910.

42. Ritsema,A.R., Geologische Rundschau,59,36,1969.

43. Ryan,W.B.F., Thesis,Lamont-Doherty Geological Observatory, 1970.

44. Scott,A., "Active and Non-Linear Wave Propagation in Electronics", Wiley-Interscience, 1970.

45. Swakon,Jr.E.A., and Wang,J.D., Modelling of Tide and Wind Induced Flow in South Biscane Bay and Card Sound, Univ.of Miami Tech.Bull.No.37, 1977.

46. Tamer,A., Preliminary Report on Storm Wind Calculations of Akkuyu Nuclear Power Plant, TEK Nuclear Energy Division, Filing No.H-05-T, Sept.,1977.

47. Tolstoy,I., Wave Propagation, McGraw-Hill,1973,

48. Tolstoy,I., and Clay,C.S., Ocean Acoustics, McGraw-Hill,1966.

49. Toksöy,N.M., Arpat,E., and Şaroğlu,F., Nature, V.270,1,pp.423,1977.

50. Tuck,E.O., and Hwang,L.S., "Long Wave Generation on a Sloping Beach" J.F.M., Vol.51,part 3,1972.

51. Van Dorn,W.G.,"Tsunamis", Advances in Hydroscience, Vol.2,pp.1-48, Academic Press,1965.

52. Wiegel,R.L., "Earthquake Engineering" , Prentice Hall Inc., Hemel, Hampstead, Ch.11,p.18,1970.

53. Wilson,B.W. and Torum,A., "Tsunami of the Alaskan Earthquake,1964: Engineering Evaluation", C.E.R.C. Tech.Memo.No.25,1968.

54. Wilson,B.W., "Earthquake Occurance and Effects in Ocean Areas",U.S.Naval Civil Eng.Lab.,T.R. CR 69-027,1969.

55. Wilson,B.W.,"Estimate of Tsunami Effect at Islote site for Nuclear Generating Station",Appendix 2.4 A, NARCO-NP-1,PSAR, Rugro,Inc.,1974.

56. Coastal Engineering Protection Manual U.S.Coastal Engineering Research Center, Virginia, U.S.A.

57. Anonymous, PSAR, NARCO-NP-1, Appendix 4 B, 1975.

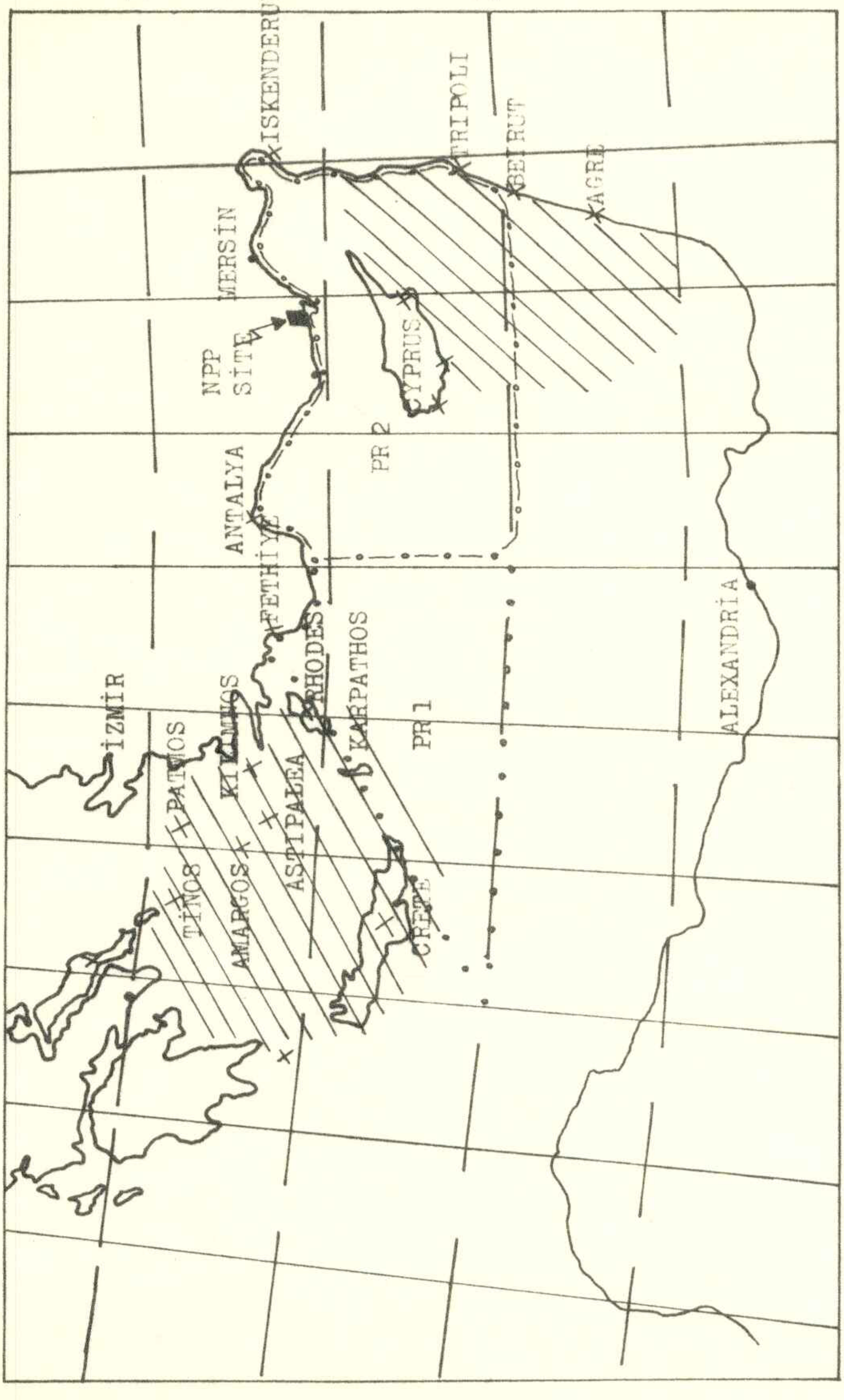
38
34
ISKENDERUN
TRIPOLI
BEIRUT
AGRE
MERSİN
NPP
SİTE
CYPRUS
PR 2
ANTALYA
FETHİYE
RHODES
KARPATHOS
İZMİR
PATMOS
PR 1
ALEXANDRİA
ASTIPALEA
AMARGOS
TİNOS
CRETE

Figure 2.1

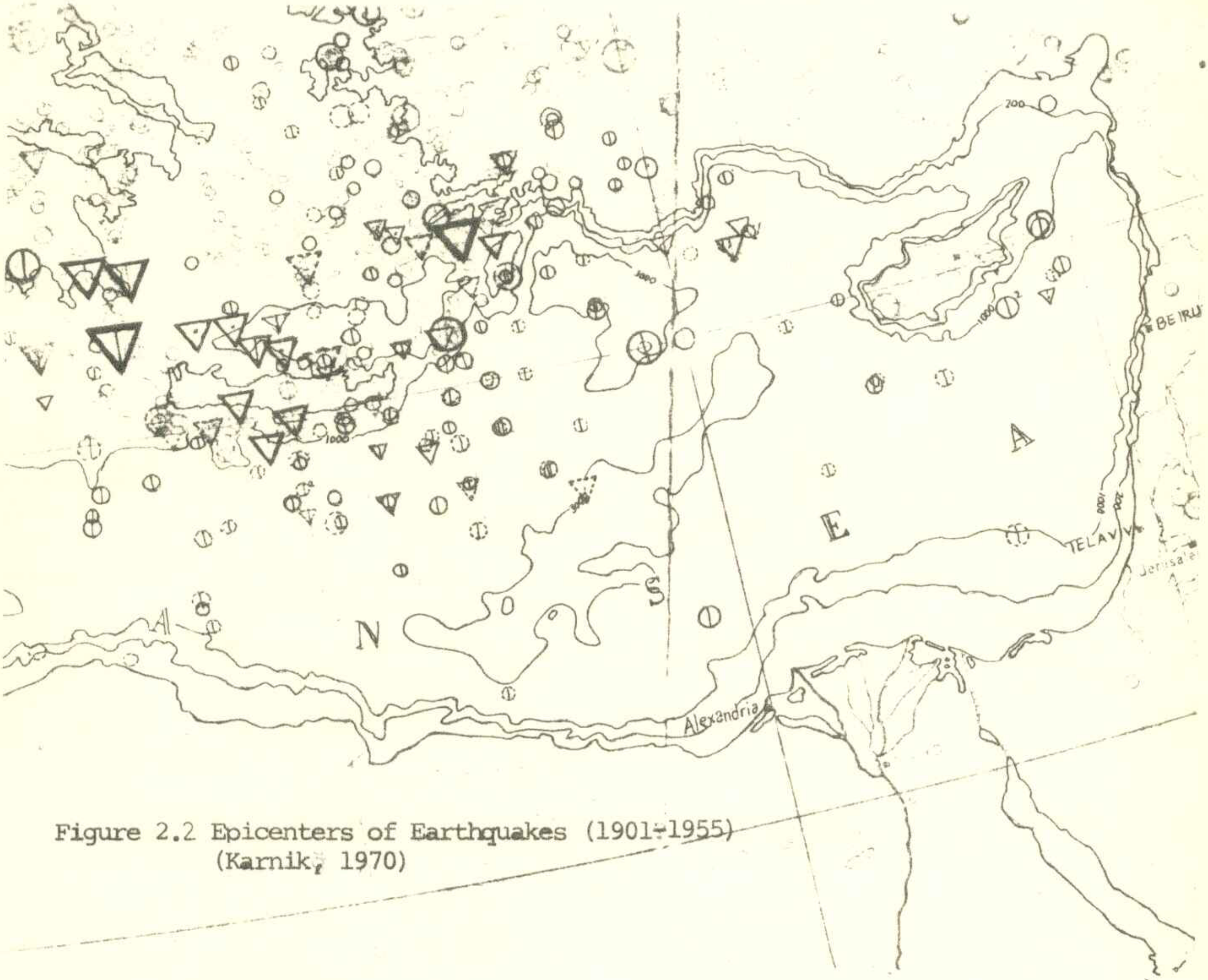

Figure 2.2 Epicenters of Earthquakes (1901-1955)
(Karnik, 1970)

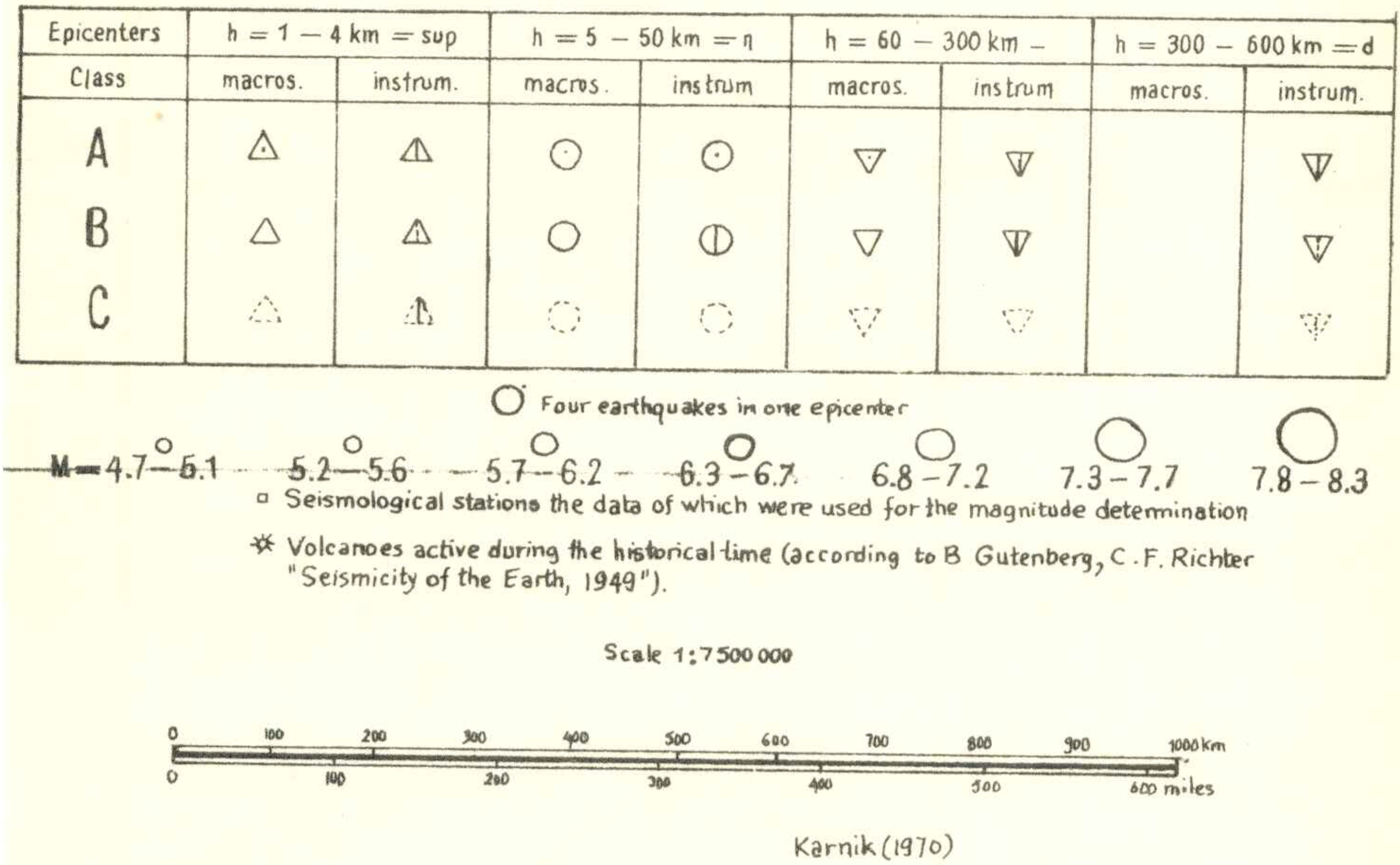

Figure 2.2 (Legend)

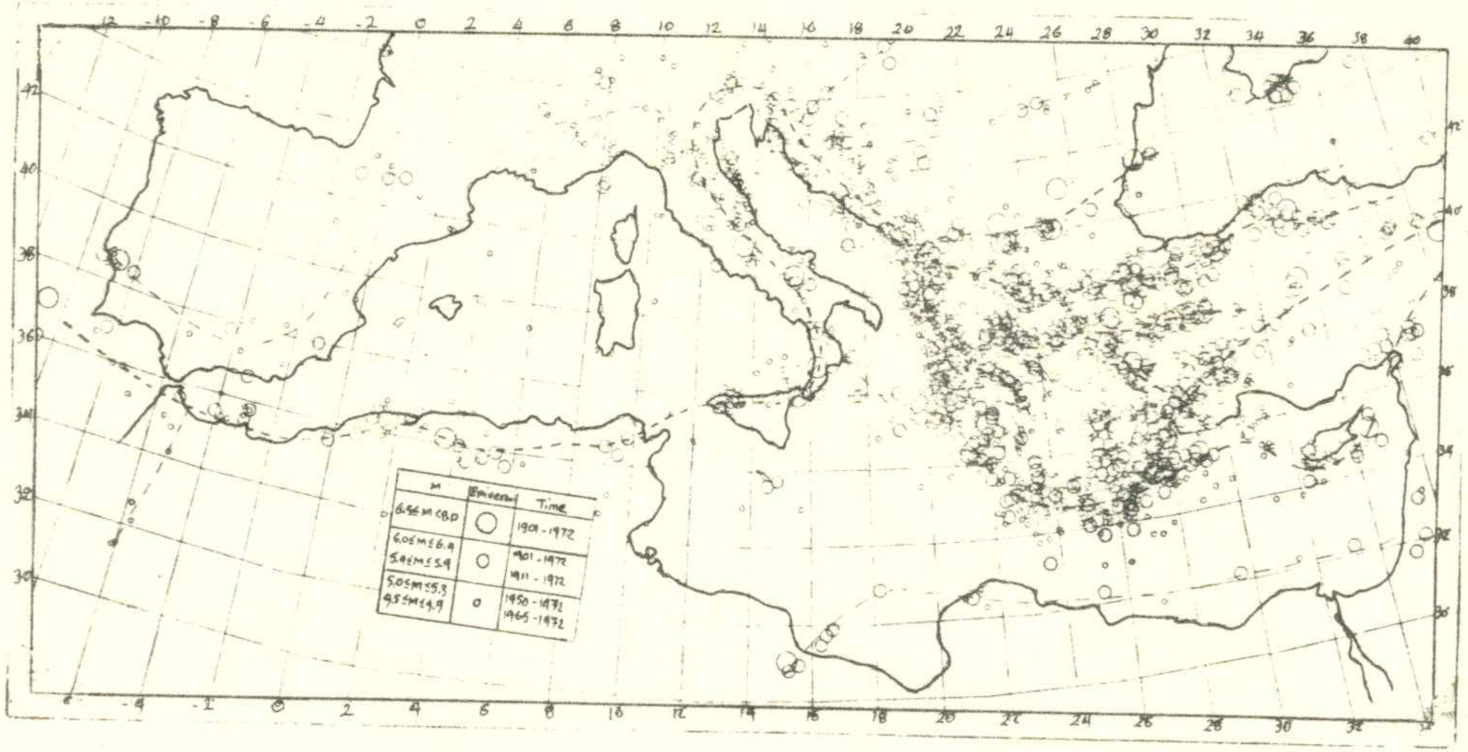

Figure 2.3 Distribution of Epicenters of Shallow Earthquakes Occuring in the Mediterranean Area During 1901-1972 (Papazachos,1974).

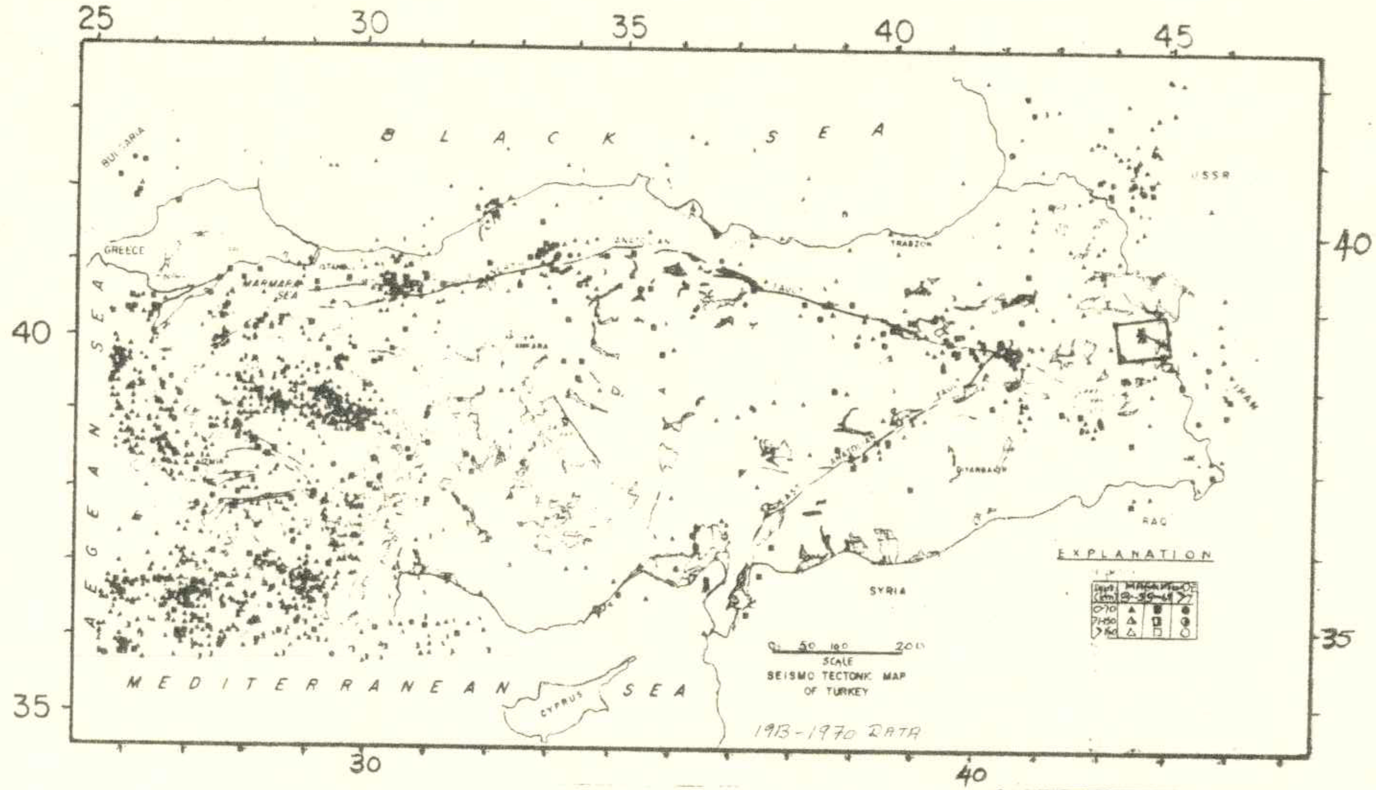

Figure 2.4 Seismo Tectonic Map of Turkey (Toksöz, 1977)

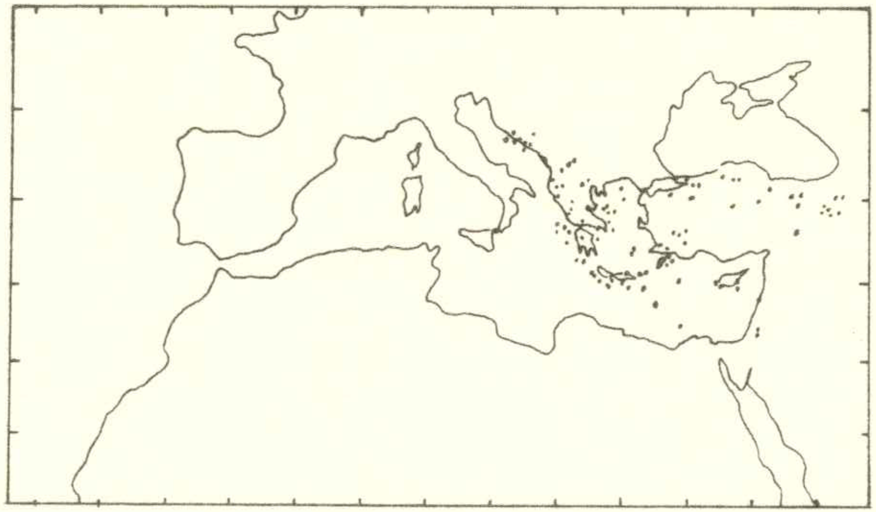

Figure 2.5 Epicenters of Earthquakes since 1925 with Magnitudes Greater than 6 (McKenzie, 1970)

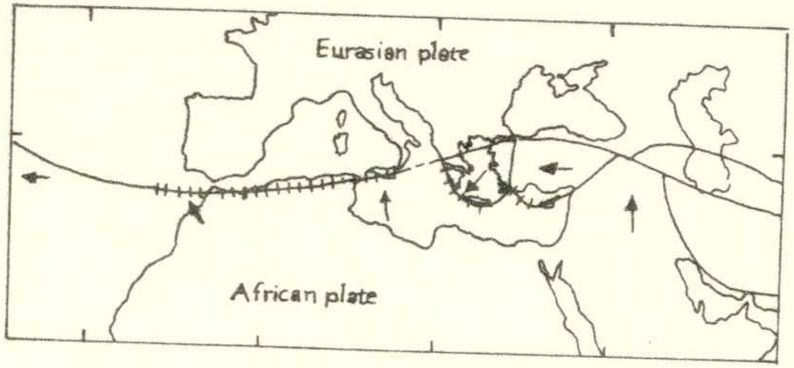

Figure 2.6 The Turkish and the Aegean Plates with Approximate Positions of Plate Boundaries. Arrows Indicate Direction of Motion Relative to the Eurasian Plate. Boundaries Consuming Plates are Shown with Short Lines Perpendicular to Them. (McKenzie, 1970)

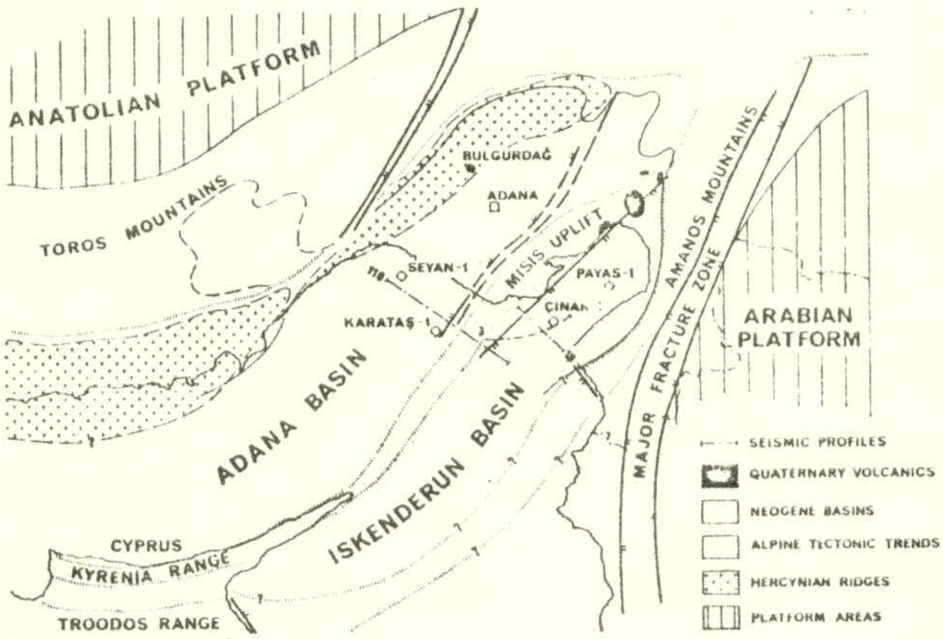

Figure 2.7 The Setting to the East, North and North-East of Cyprus (Beltrandi and Biro, 1975)

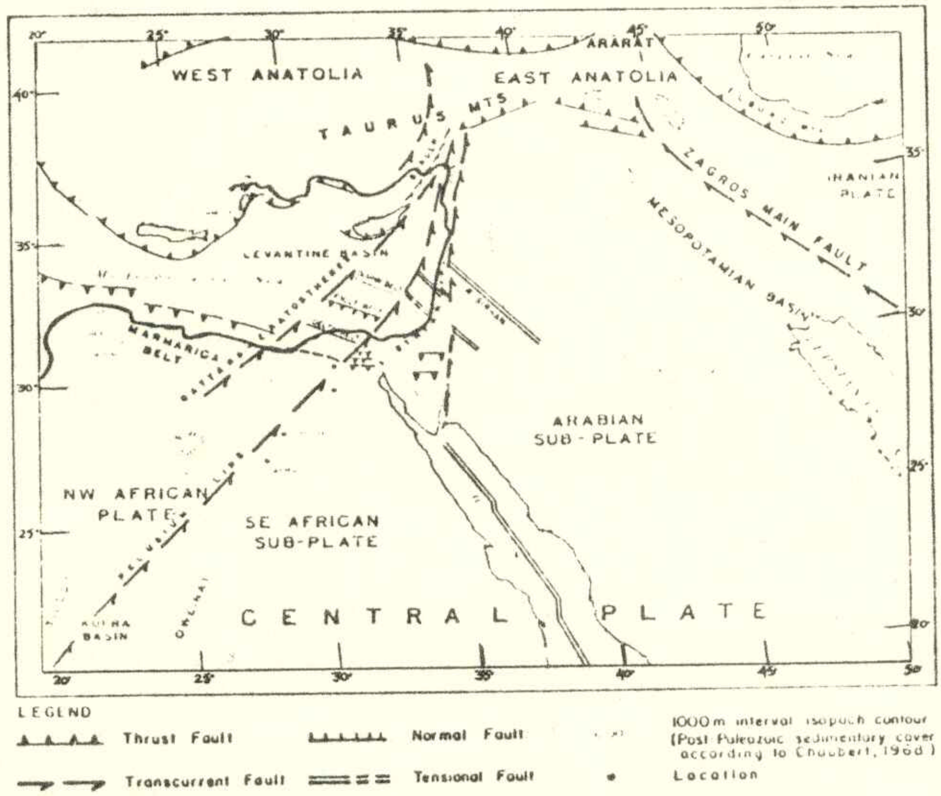

Figure 2.8 Techtonic Sketch Map of Eastern Mediterranean (Neev, 1975)

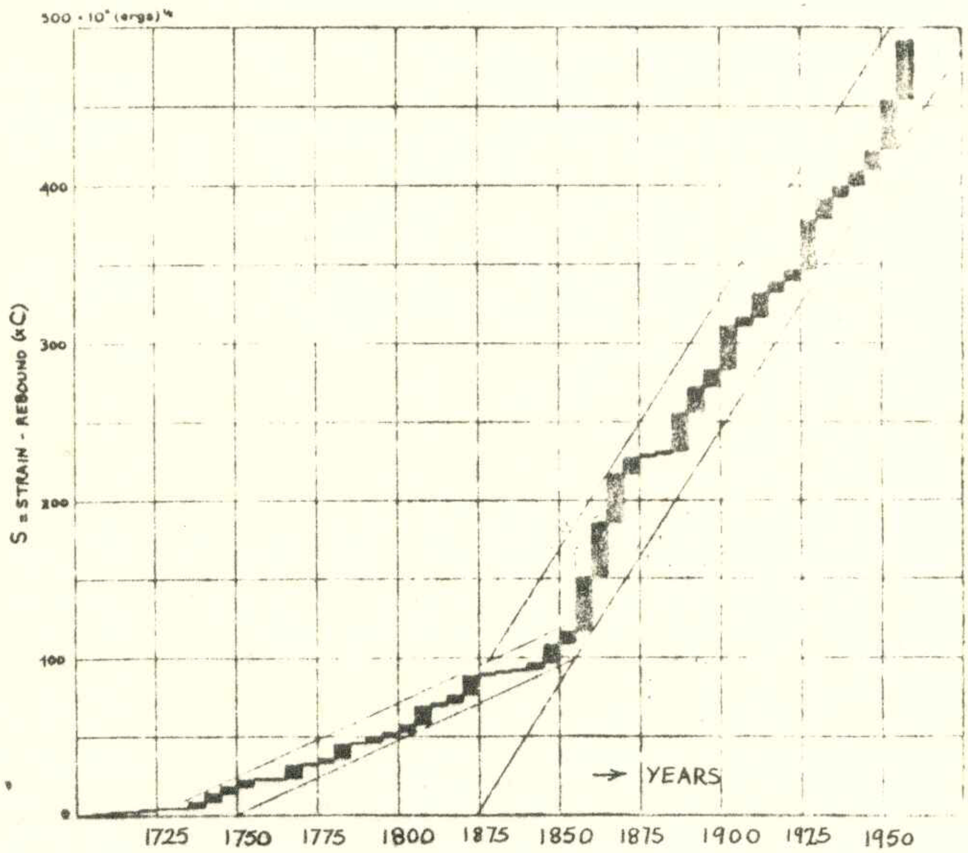

Figure 2.9 Seismic Energy Release in the Aegean Plate and its Vicinity (Galanopoulos, 1963)

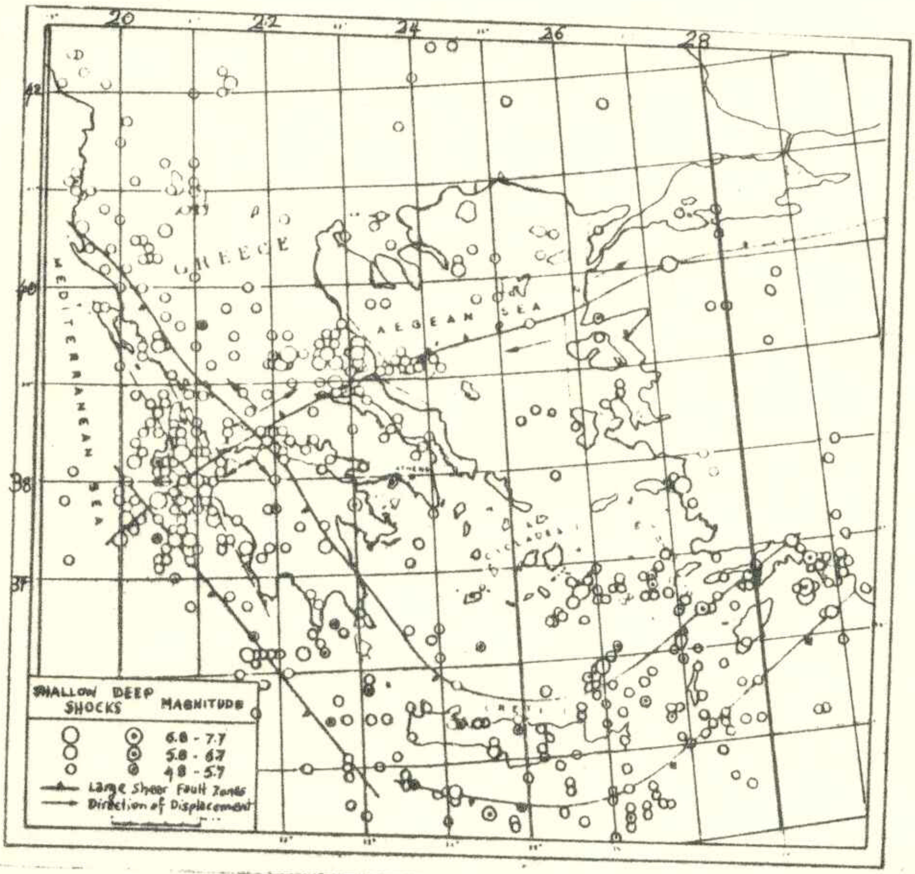

Figure 2.10 Seismo Tectonic Map of the Aegean Plate and its Vicinity (Galanopoulos, 1963)

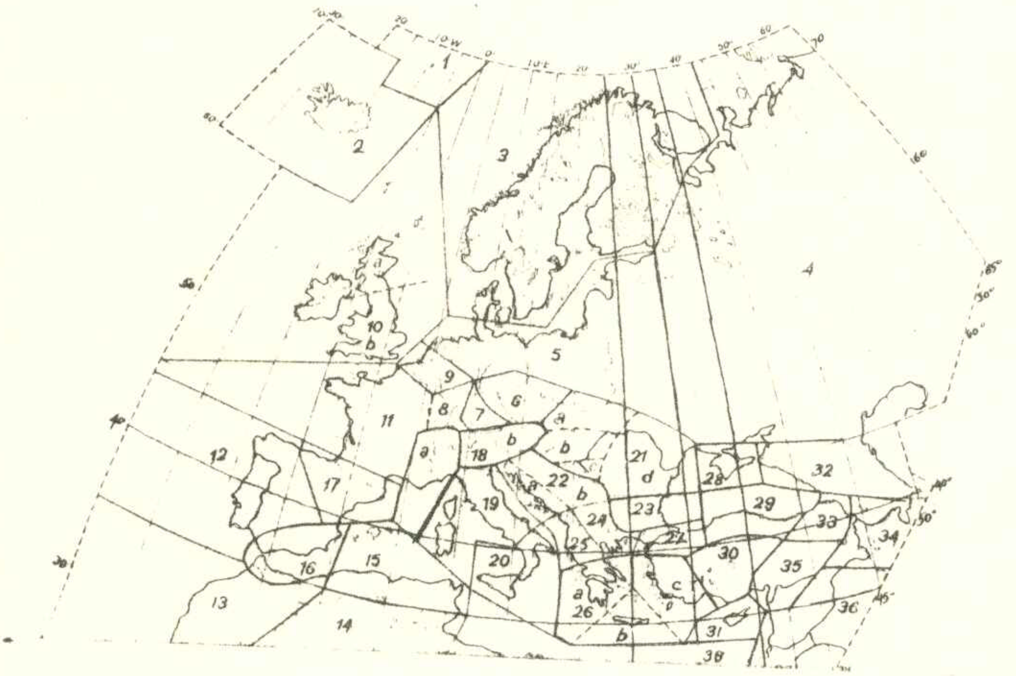

Figure 2.11 Specifications of the Regions Considered by Karnik (1970)

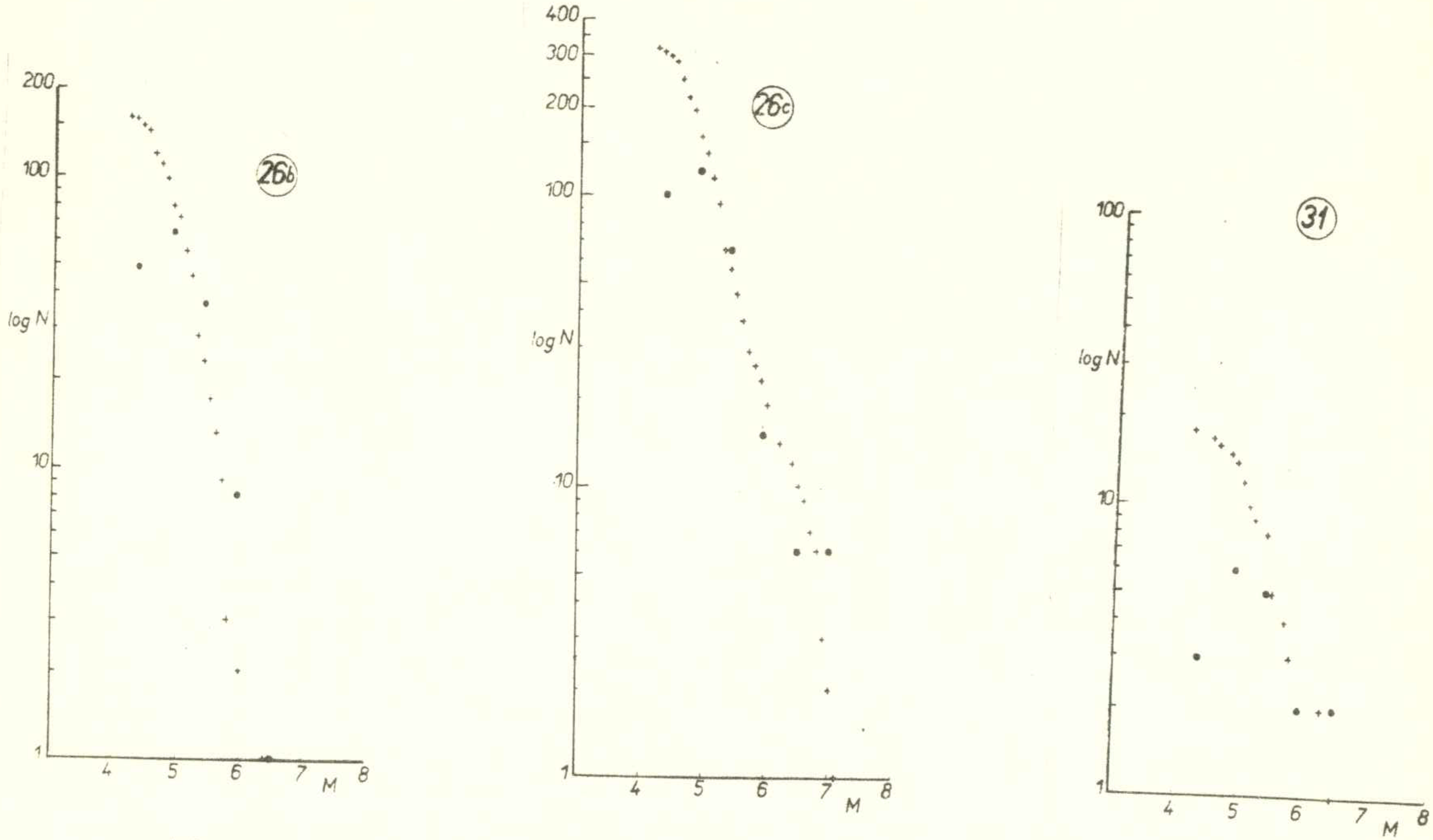

(a) (b) (c)

Figure 2.12 a-c Frequency-Magnitude Relations for Individual Seismic Regions, Crosses correspond to Cumulative Frequencies, Circles to Frequencies within M = 0.5 Period 1901-1955 (Karnik, 1970)

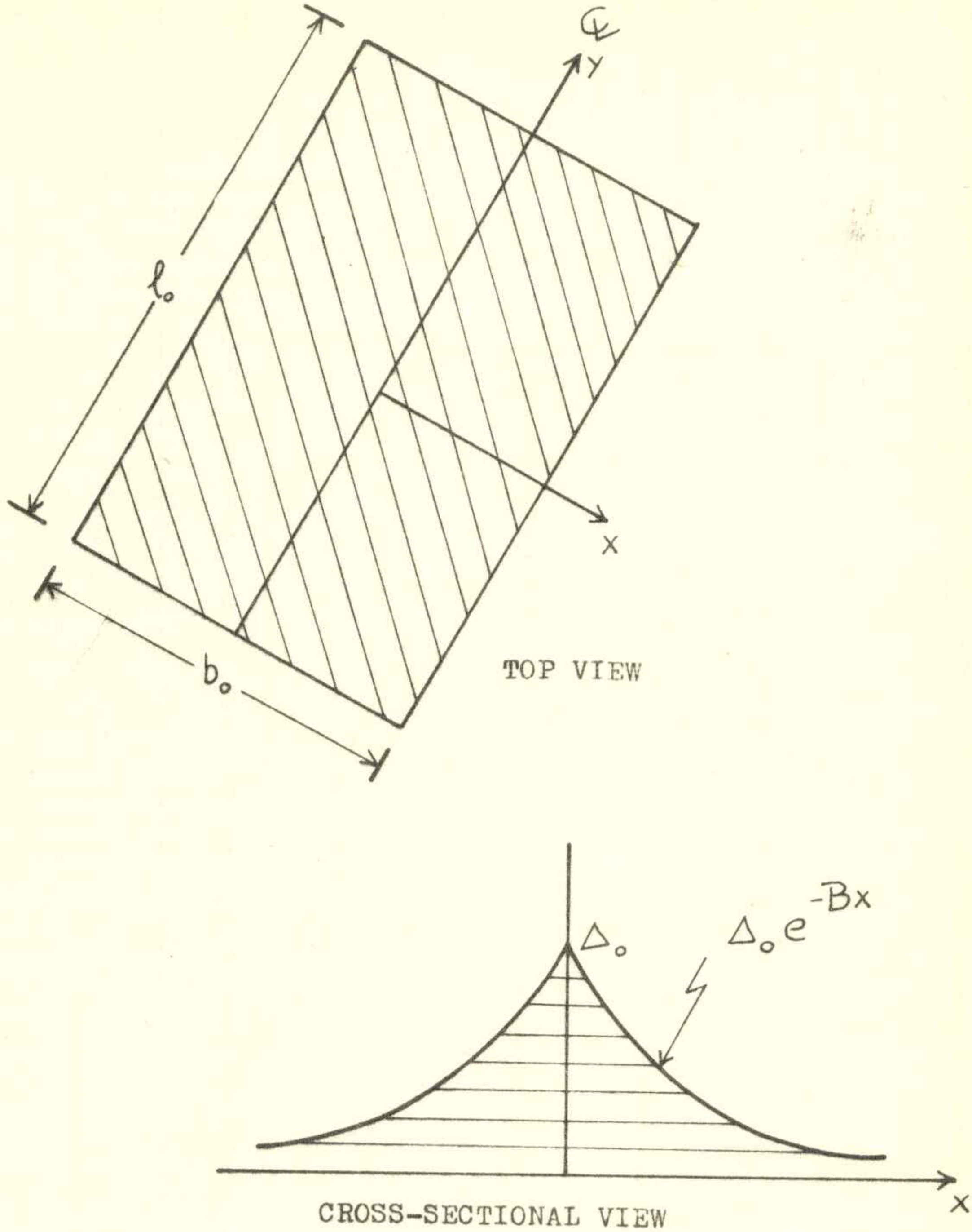

Figure 3.1 Definition sketch for form of ground motion.

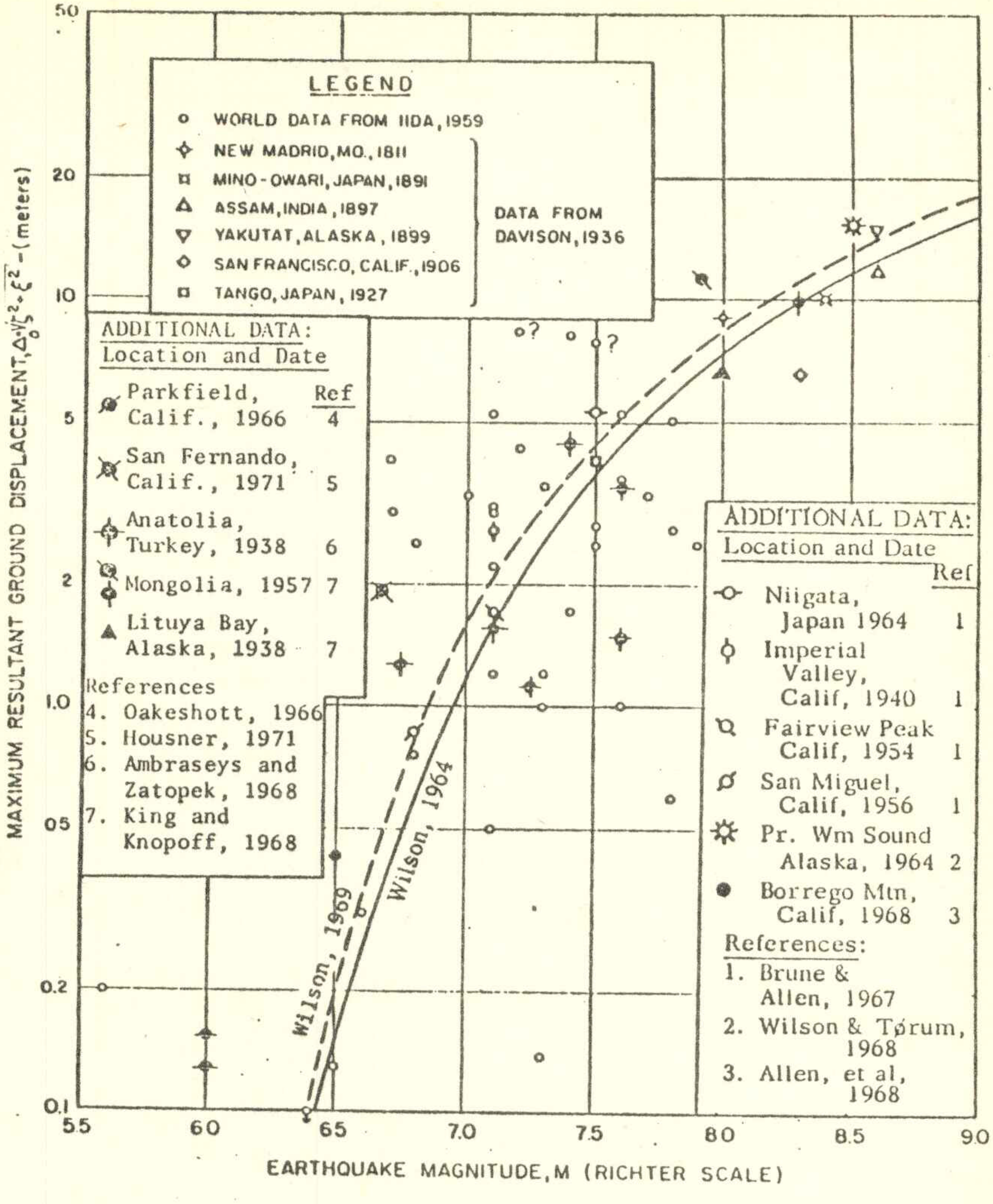

Figure 3.2 Maximum Displacement v.s. Earthquake Magnitude M (Richter).

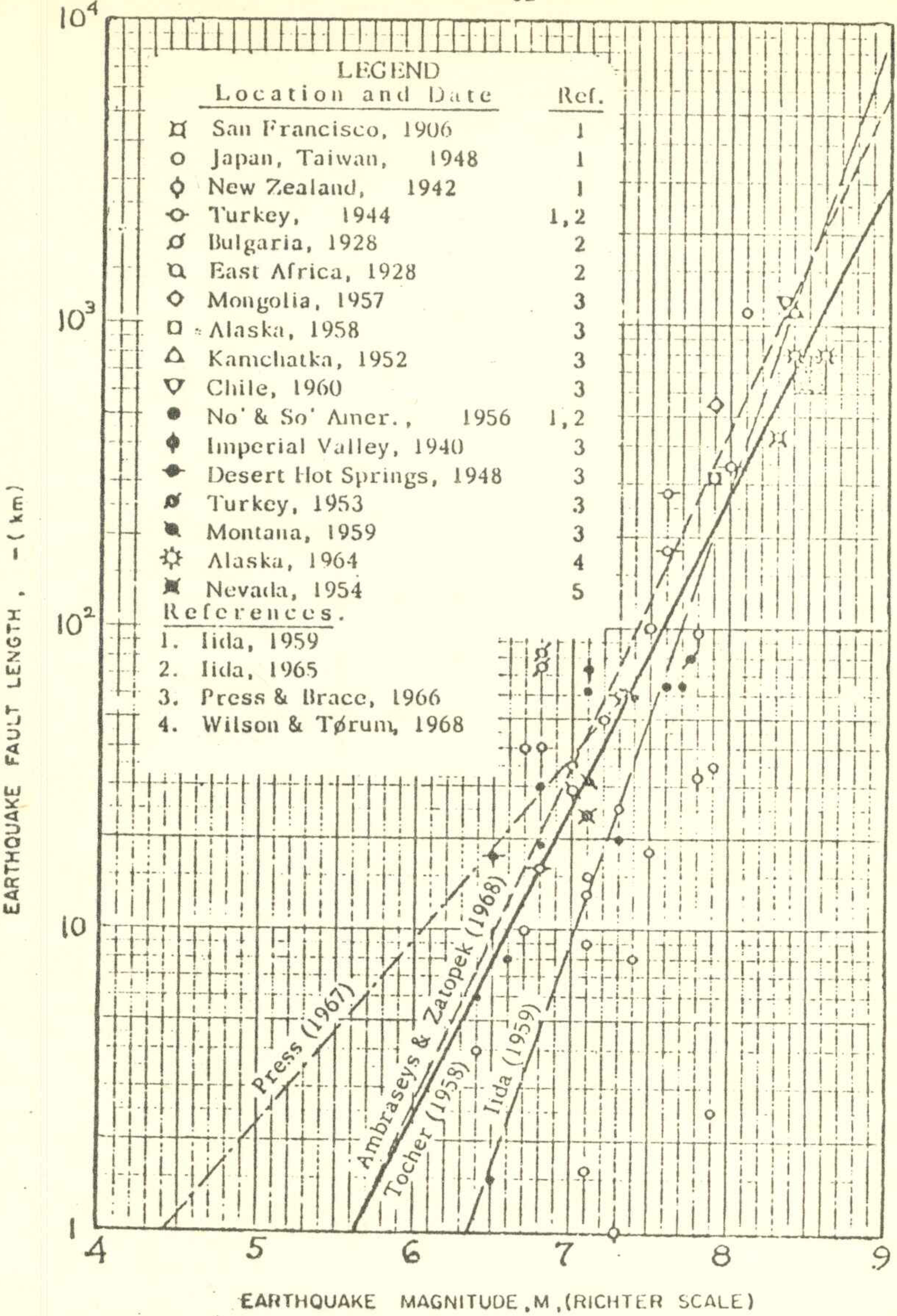

Figure 3.3 Length of Ground Motion v.s. Earthquake Magnitude M (Richter).

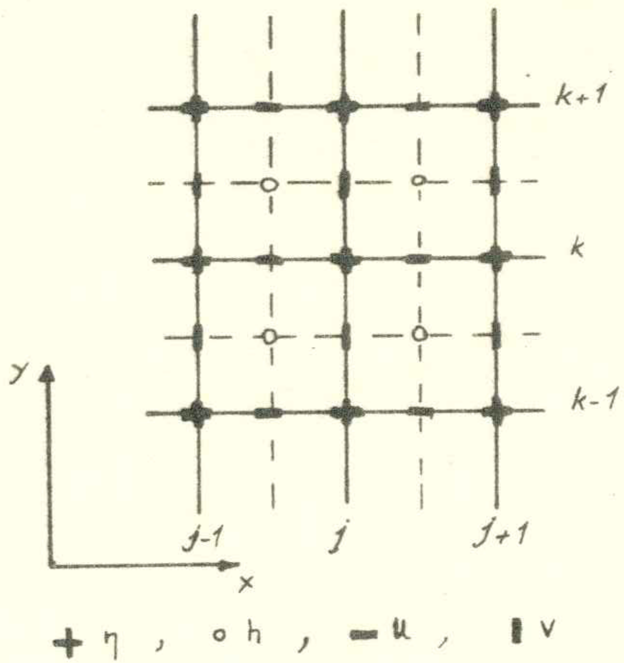

Figure 4.1 SPACE STAGGERED SCHEME

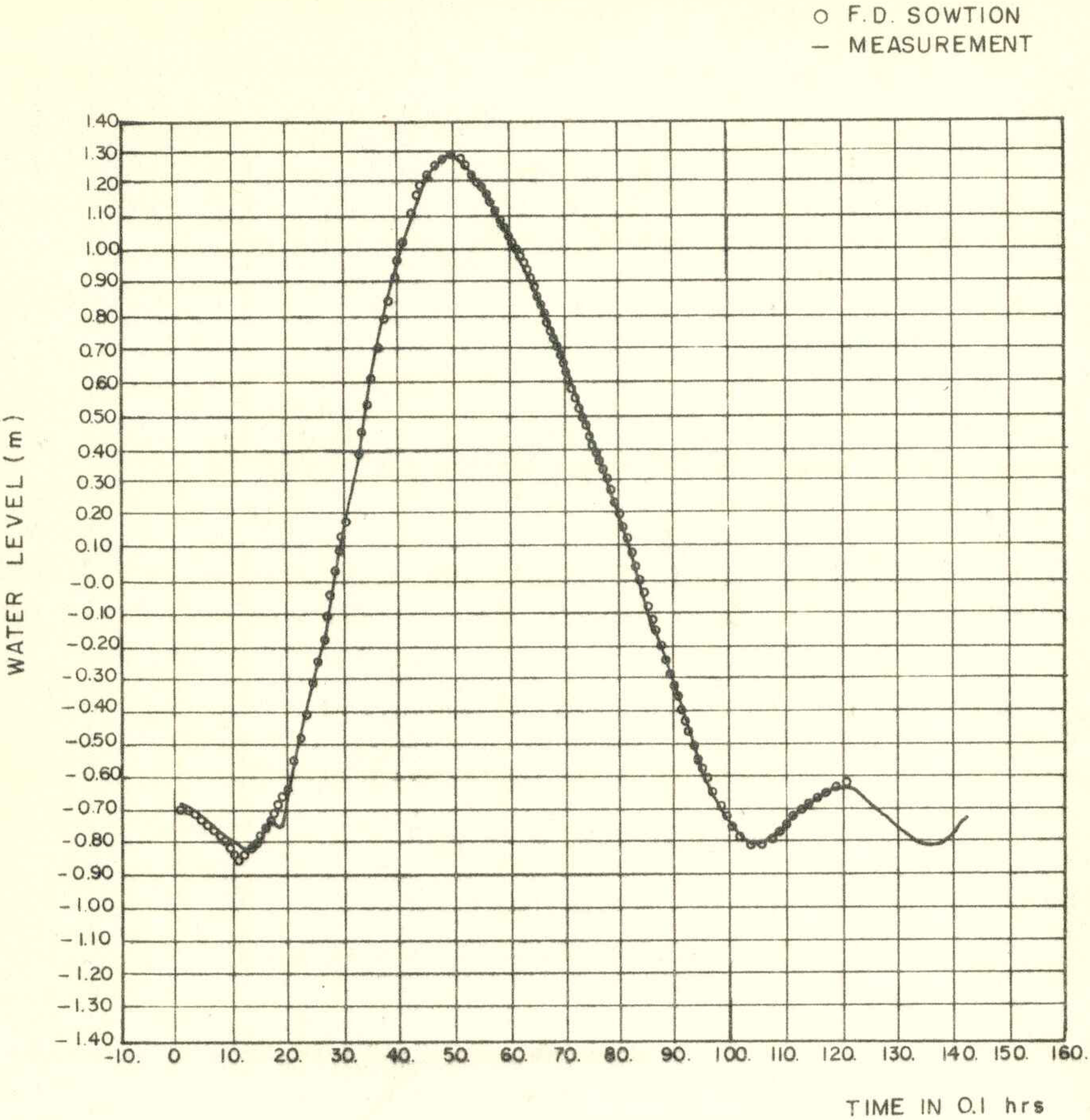

FIGURE 4.2. WATER LEVELS AT N=13 ,M =31.

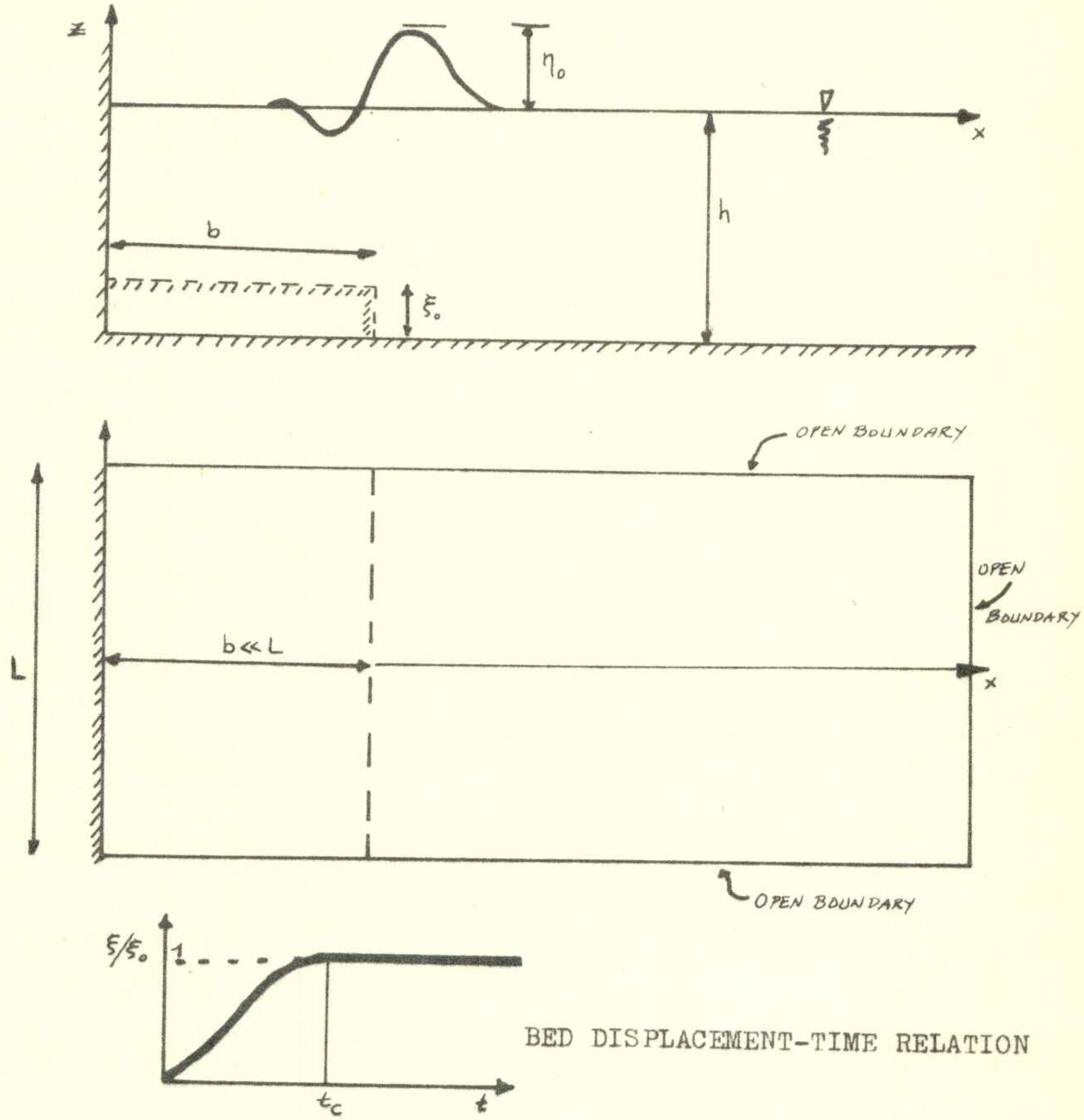

Figure 4.3 SIMULATION OF TWO DIMENSIONAL REGION

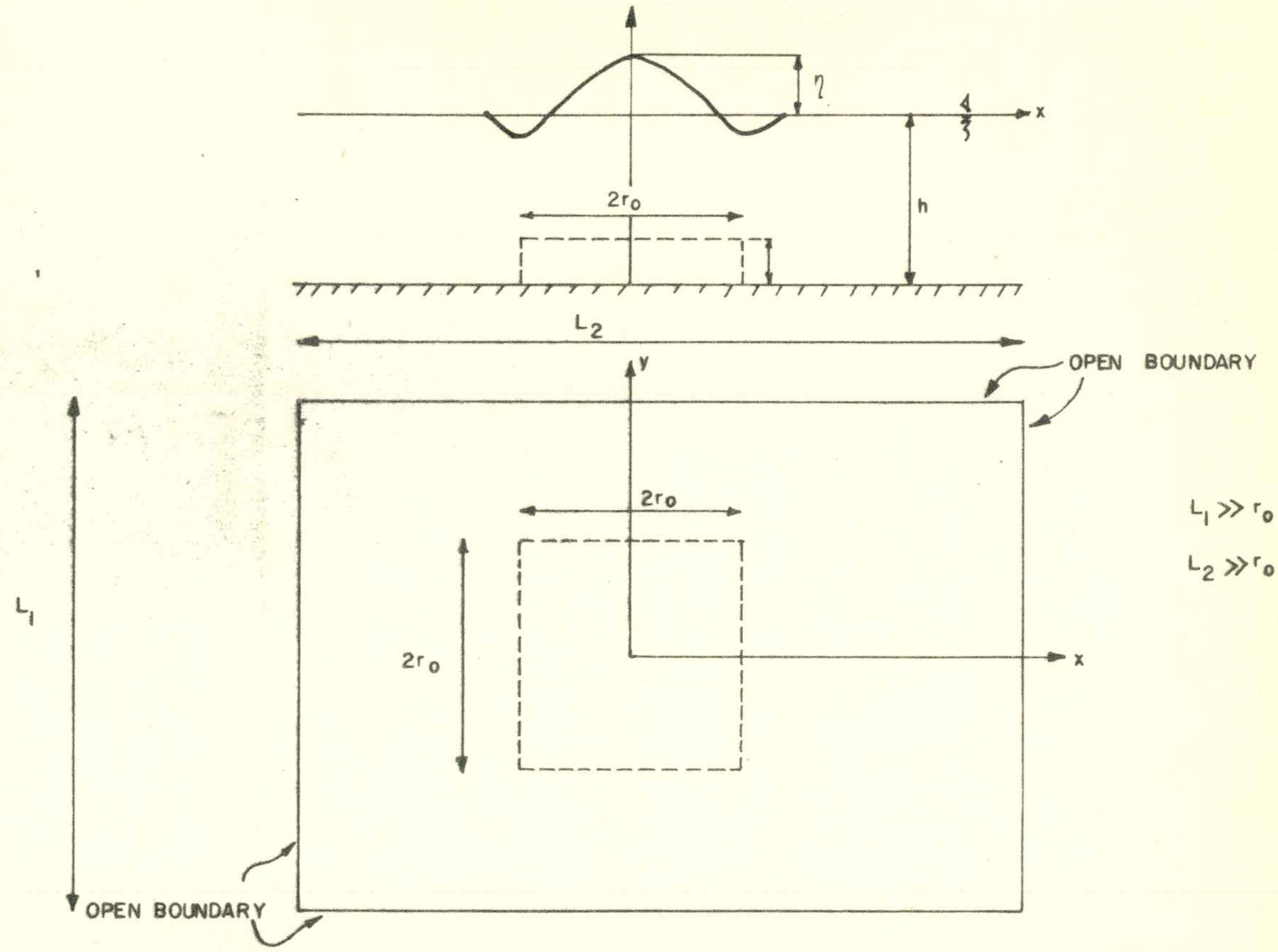

FIGURE 4.4 SIMULATION OF THREE DIMENSIONAL REGION

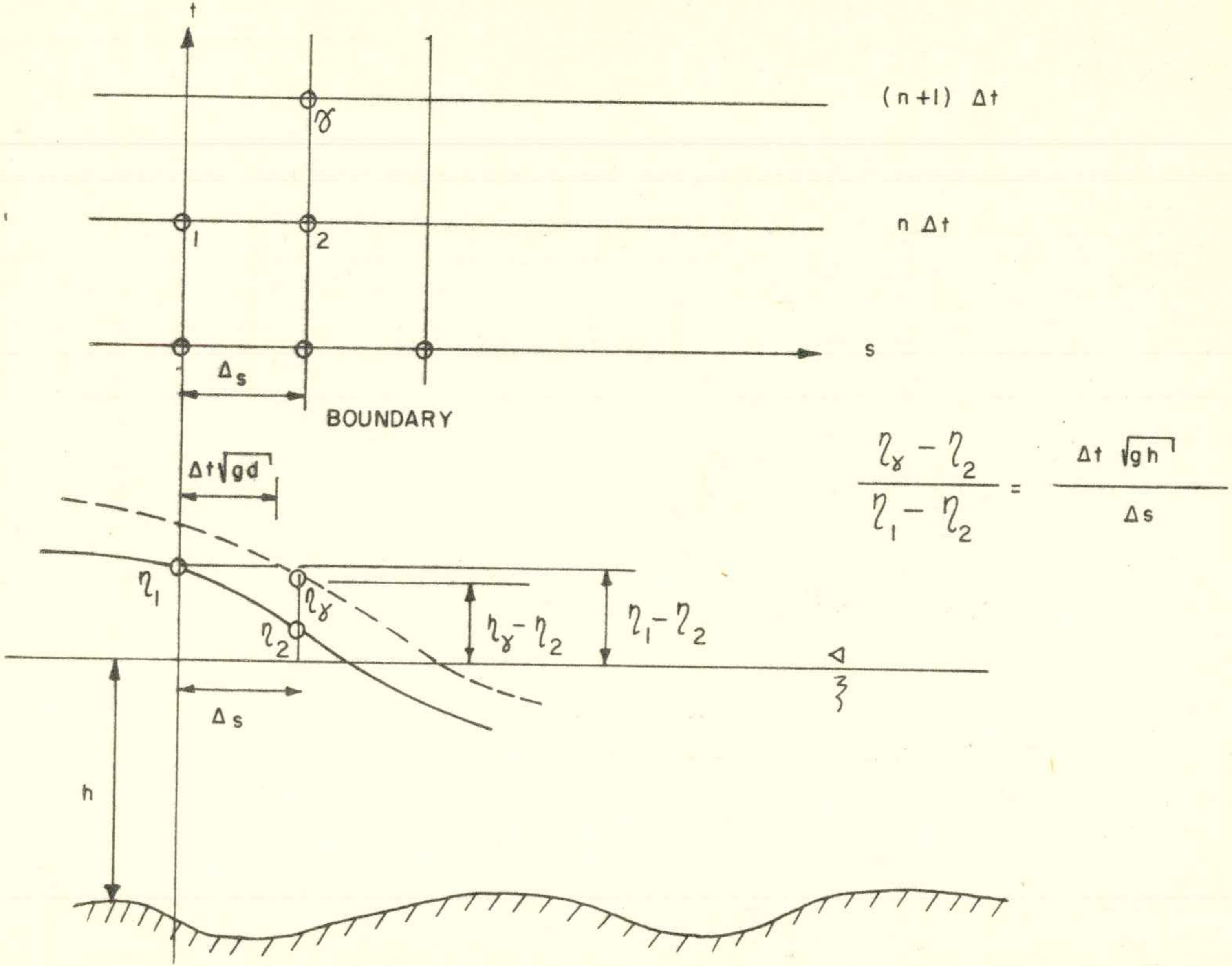

$$\frac{\eta_\gamma - \eta_2}{\eta_1 - \eta_2} = \frac{\Delta t \sqrt{gh}}{\Delta s}$$

FIGURE 4.5. GRAPHICAL REPRESENTATION OF TOTAL TRANSMISSION BOUNDARY CONDITION

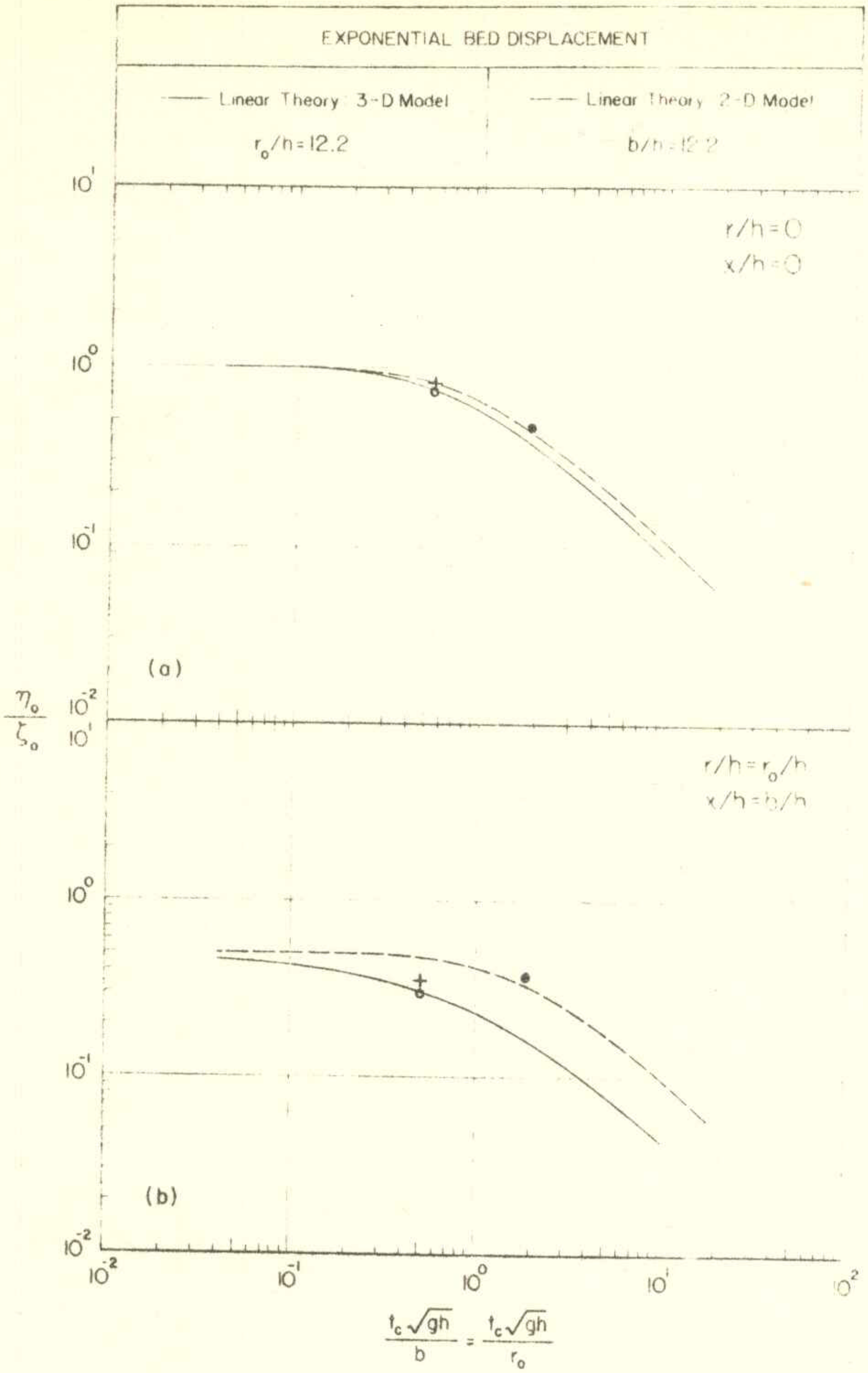

Fig. 4.6 Theoretical variation of relative maximum wave amplitude, η_o/ζ_o, with the time-size ratio, $t_c\sqrt{gh}/r_o$: a) at $r/h = 0$, b) at $r/h = r_o/h$ (Hammack,1972)

o FINITE ELEMENT RESULTS (3. DIM.MODEL)
+ FINITE DIFFERENCE RESULTS (3. DIM.MODEL)
o FINITE DIFFERENCE RESULTS (2. DIM.MODEL)

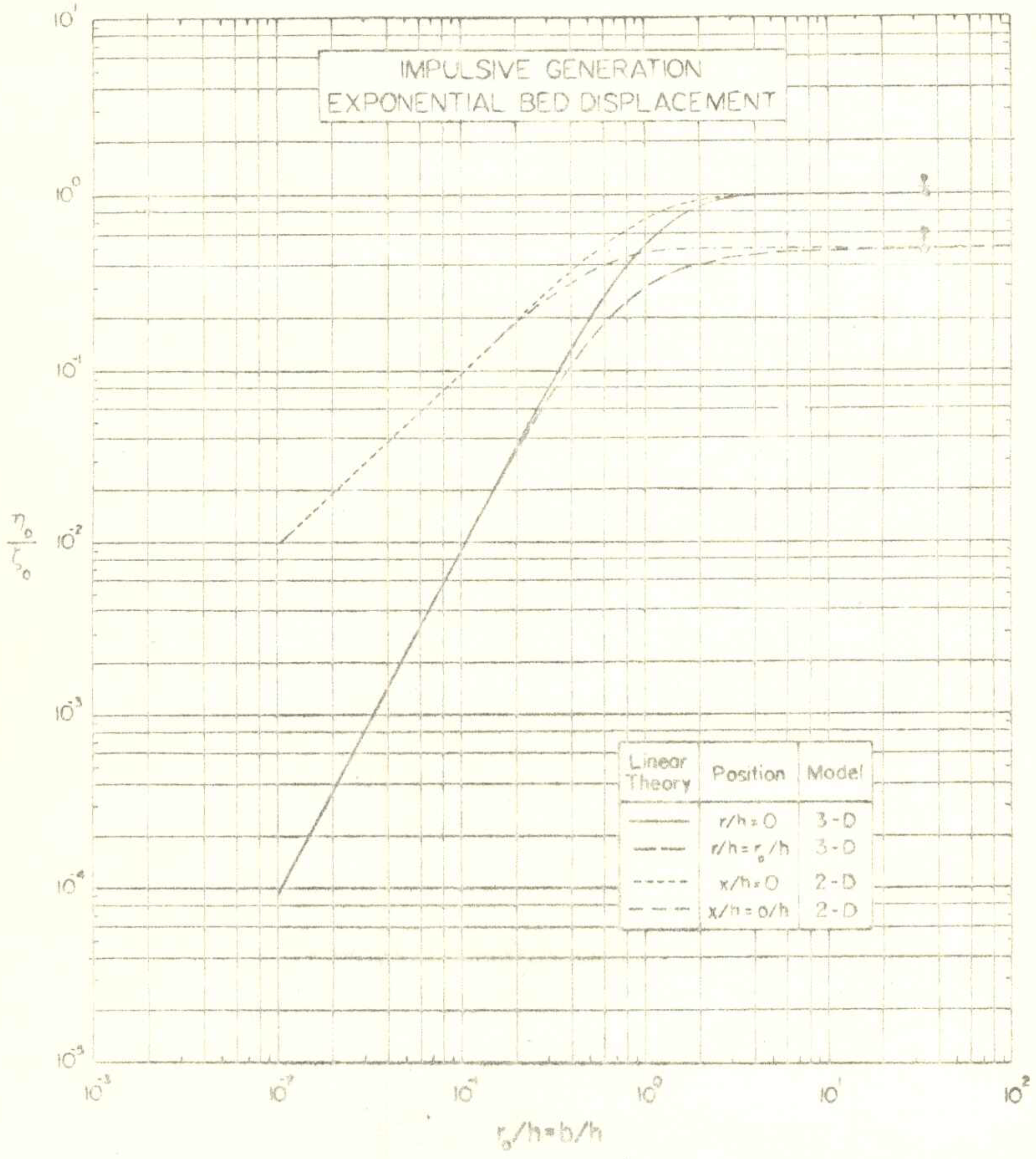

Fig. 4.7 Theoretical variation of relative maximum wave amplitude, η_o/ζ_o, with the disturbance-size scale, b/h and r_o/h, for impulsive bed displacements. (Hammack, 1972)

oFINITE ELEMENT RESULTS (3.DIM.MODEL), +FINITE DIFFERENCE RESULTS (3.DIM.MODEL), oFINITE DIFFERENCE RESULTS (2.DIM.MODEL).

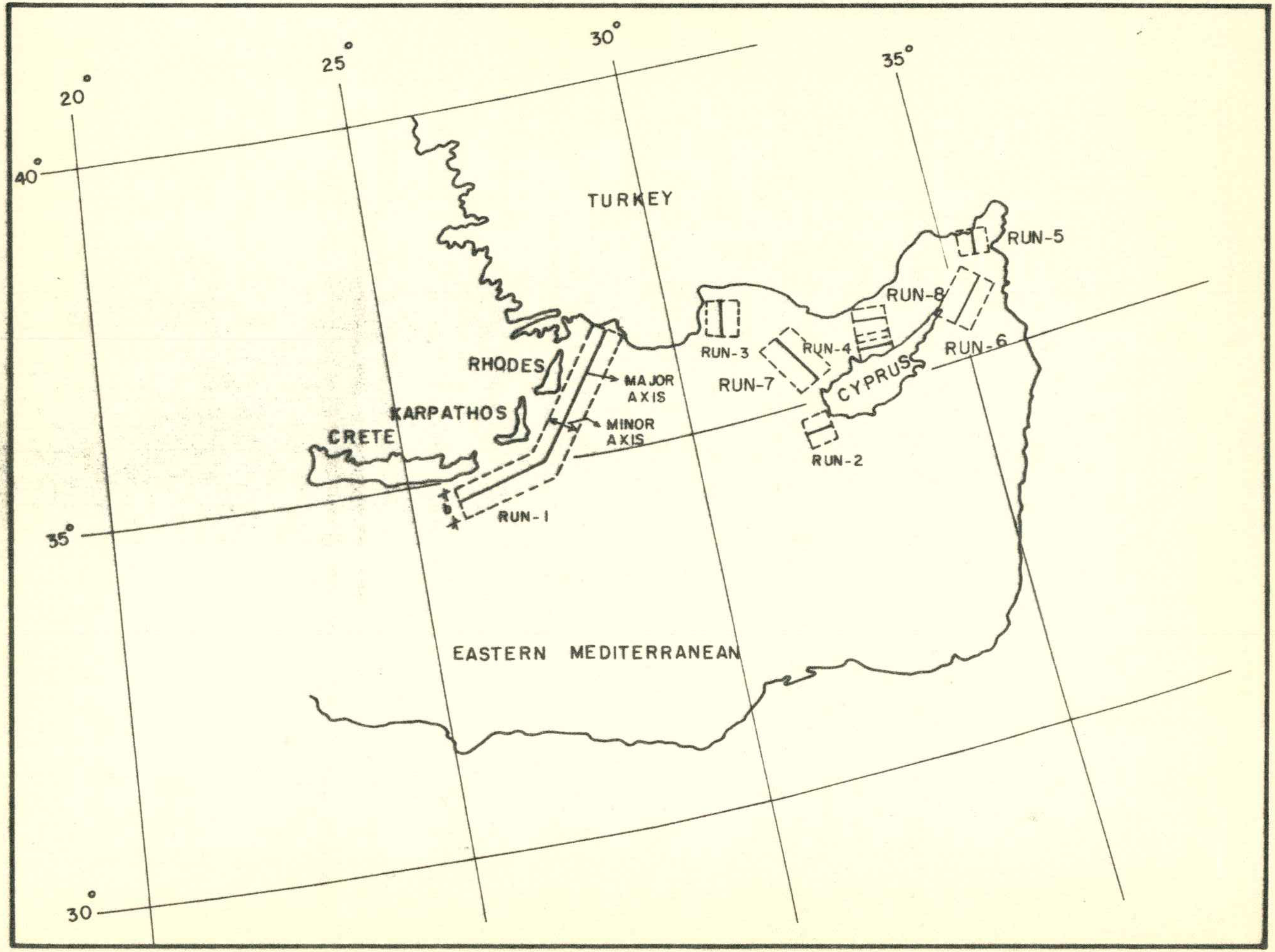

Figure 5.1 LOCATIONS OF EIGHT SAMPLE RUNS IN THE EASTERN MEDITERRANEAN

WATER LEVELS IN FIELD

```
M  N
             111111111122222222223333333333444444444455555555556
    123456789012345678901234567890123456789012345678901234567890

 1  000000000000000000000000000000000000000000000000000000000000
 2  000111110000000000000000000000000000000000000000000000000000
 3  001111111000000000000000000000000000000000000000000000000000
 4  011111111000000000000000000000000000000000000000000000000000
 5  011111111100000000000000000000000000000000000000000000000000
 6  000111111110000011000000000000000000000000000111000000000000
 7  000011111111000011110000000000011111100000011111110000000000
 8  000011111111001111111111100001111111111111111111110000000000
 9  000001111111111111111111100001111111111111111111111000000000
10  000000011111111111111111111111111111111111111111111100000000
11  000000001111111111111111111111111111111111111111111000000000
12  000000000111111111111111111111111111111111111111111111111110
13  000000000111111111111111111111111111111111111111111111111110
14  000000000111111111111111111111111111111111111111111111111111
15  000000000111111111111111111111111111111111111111111111111111
16  000000000111111111111111111111111111111111111111111111111111
17  000000000111111111111111111111111111111111111111111111111111
18  000000011111111111111111111111111111111111111111111111111111
19  000000011111111111111111111111111111111111111111111111111111
20  000000111111111111111111111111111111111111111111111111111111
21  000000111111111111111111111111111111111111111111111111111111
22  000001111111111111111111111111111111111111111111111111111111
23  000001111111111111111111111111111111111111111111111111111111
24  000011111111111111111111111111111111111111111111111111111111
25  000011111111111111111111111111111111111111111111111111111111
26  000011111111111111111111111111111111111111111111111111111111
27  000011111111111111111111101111111111111111111111111111111111
28  000001111111111111111111100111111111111111111111111111111111
29  000000111111111111111111001111111111111111111111111111111111
30  000000001111111111111111100111111111111111111111111111111111
31  000000001111111111111111100011111111111111111111111111111111
32  000000000111111111111111110001111111111111111111111111111111
33  000000000011111111111111111000111111111111111111111111111111
34  000000000001111111111111111100011111111111111111111111111111
35  000000000000011111111111111110000111110111111111111111111111
36  000000000000001111111111111111000111100111111111111111111111
37  000000000000011111111111111110000100001111111111111111111111
38  000000000000011111111111111110000000000111111111111111111111
39  000000000000011111111111111100000000000111111111111111111111
40  000000000000000000111111111111000000000111111111111111111111
41  000000000000000000111111111111000000000111111111111111111111
42  000000000000000000111111111111000000000011111111111111111111
43  000000000000000000111111111111000000000000111111111111111111
44  000000000000000000111111111111000000000000001111111111111111
45  000000000000000000111111111111000000000000001111111111111111
46  000000000000000001111111111111000000000000000111111111111111
47  000000000000000011111111111111000000000000000111111111111111
48  000000000000000001111111111111000000000000000011111111111111
49  000000000000000000111111111111000000000000000001111111111111
50  000000000000000000111111111111000000000000000001111111111111
51  000000000000000000111111111111000000000000000000111111111111
52  000000000000000000111111111110000000000000000000011111111111
53  000000000000000000111111111110000000000000000000001111111111
54  000000000000000000011111111111111000000000000001111111111111
55  000000000000000000011111111111111100000000000111111111111111
56  000000000000000000011111111111111100000000000111111111111111
57  000000000000000000011111111111111100000000000111111111111111
58  000000000000000000111111111111111100000000000111111111111111
59  000000000000000000111111111111111100000000000111111111111111
60  000000000000000001111111111111111111100000001111111111111111
61  000000000000000011111111111111111111110000001111111111111111
62  000000000000000011111111111111111111110000111111111111111111
63  000000000000000111111111111111111111000001111111111111111111
64  000000000000001111111111111111111111111111111111111111111111
65  000000000000011111111111111111111111111111111111111111111111
66  000000000111111111111111111111111111111111111111111111111111
67  000000000111111111111111111111111111111111111111111111111111
68  000000000111111111111111111111111111111111111111111111111111
69  000000000111111111111111111111111111111111111111111111111111
70  000000001111111111111111111111111111111111111111111111111111
71  000000011111111111111111111111111111111111111111111111111111
72  000000011111111111111111111111111111111111111111111111111111
73  000000011111111111111111111111111111111111111111111111111111
74  000000111111111111111111111111111111111111111111111111111111
75  000001111111111111111111111111111111111111111111111111111111
76  000001111111111111111111111111111111111111111111111111111111
77  000001111111111111111111111111111111111111111111111111111111
```

Figure 5.2 Computer Map of Eastern Mediterranean (Mesh Size 5.5x5.5 km^2)

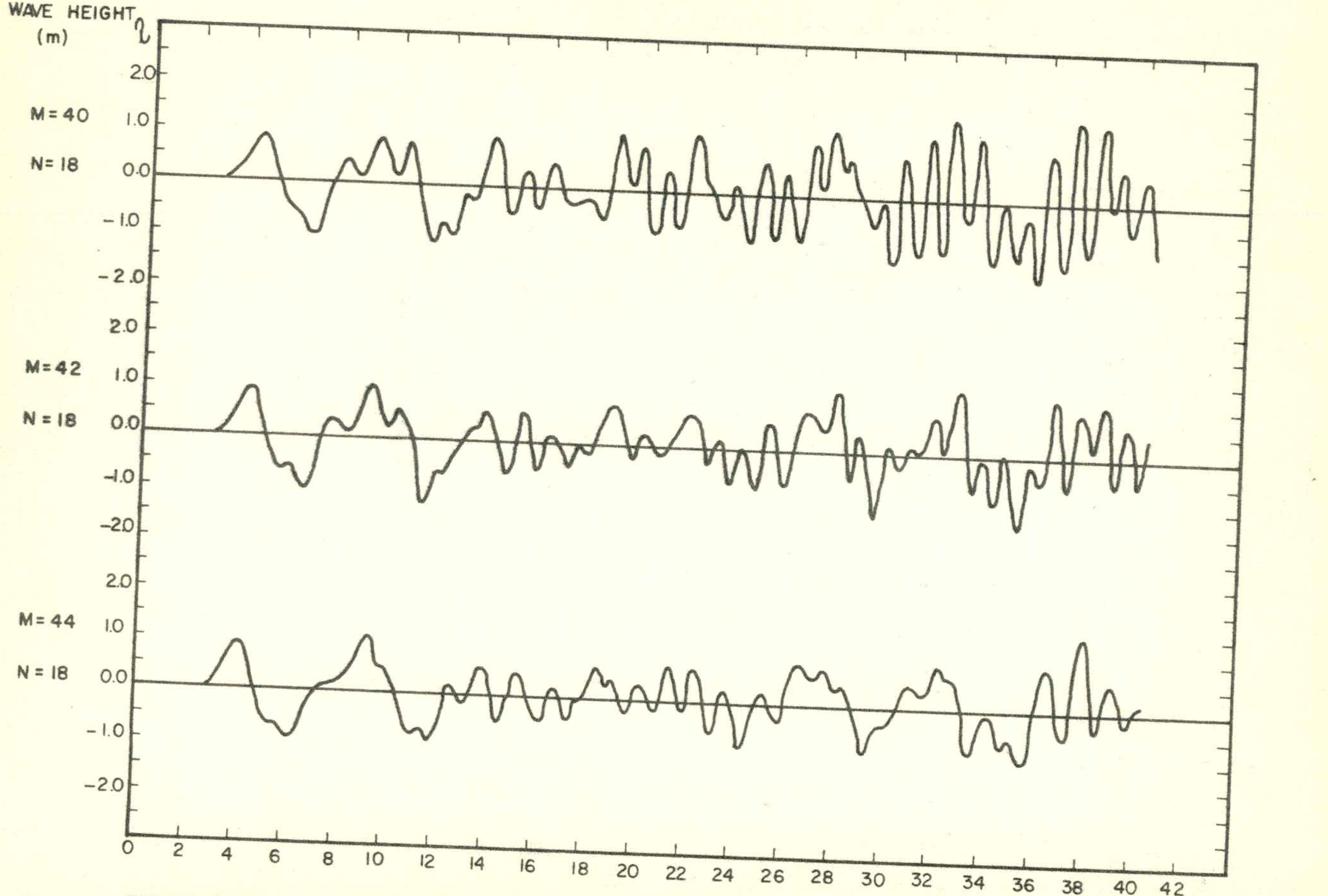

FIGURE 5.3. RESULTS OF RUN-I, SOUTH EAST OF GRECIAN ARCHIPELAGO
M=42, N=18 CORRESPONDS TO AKKUYU BAY ENTRANCE

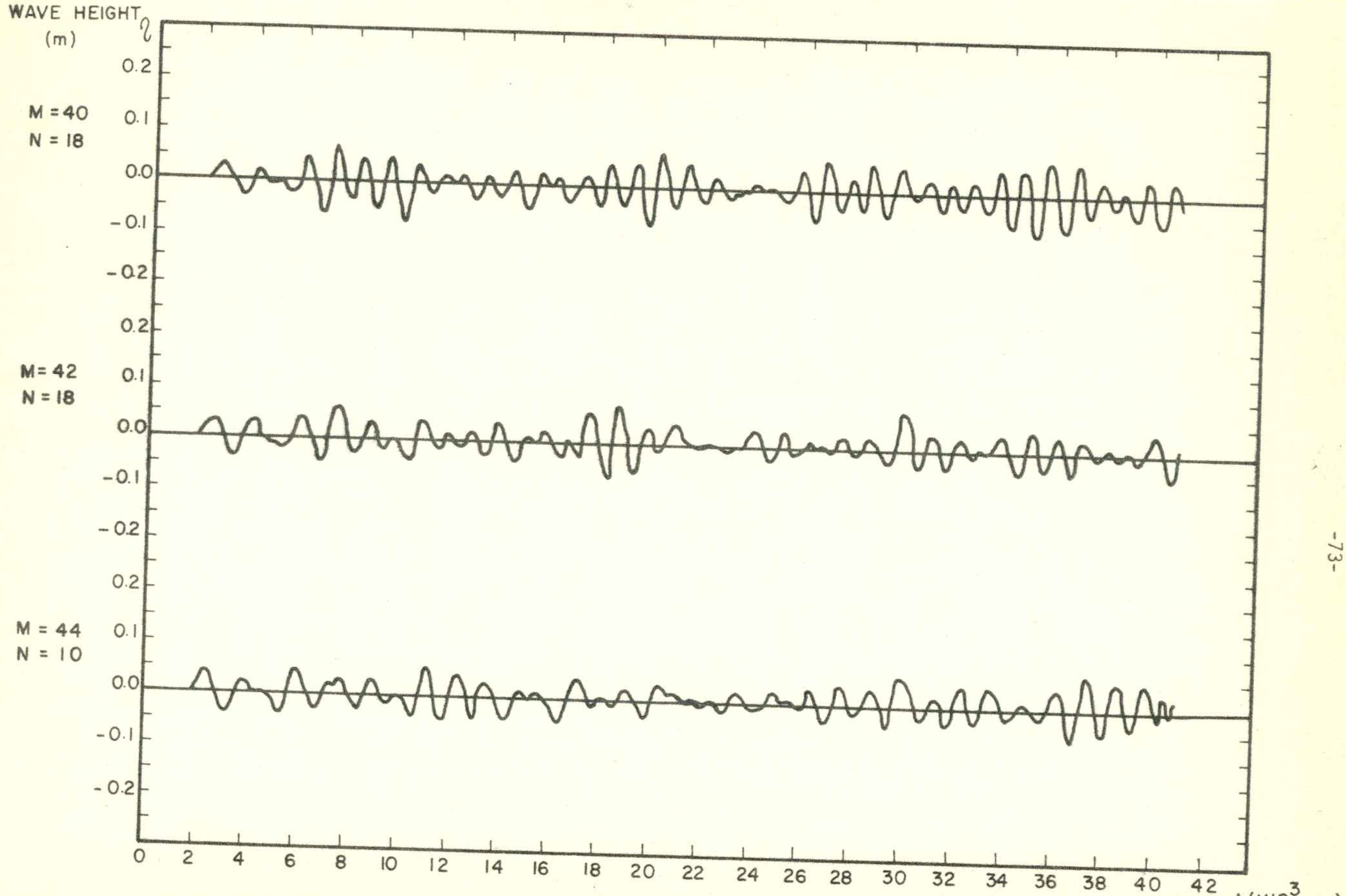

FIGURE 5.4. RESULTS OF RUN- 2, SOUTH WEST CYPRUS
M=42, N = 18 CORRESPONDS TO AKKUYU BAY ENTRANCE

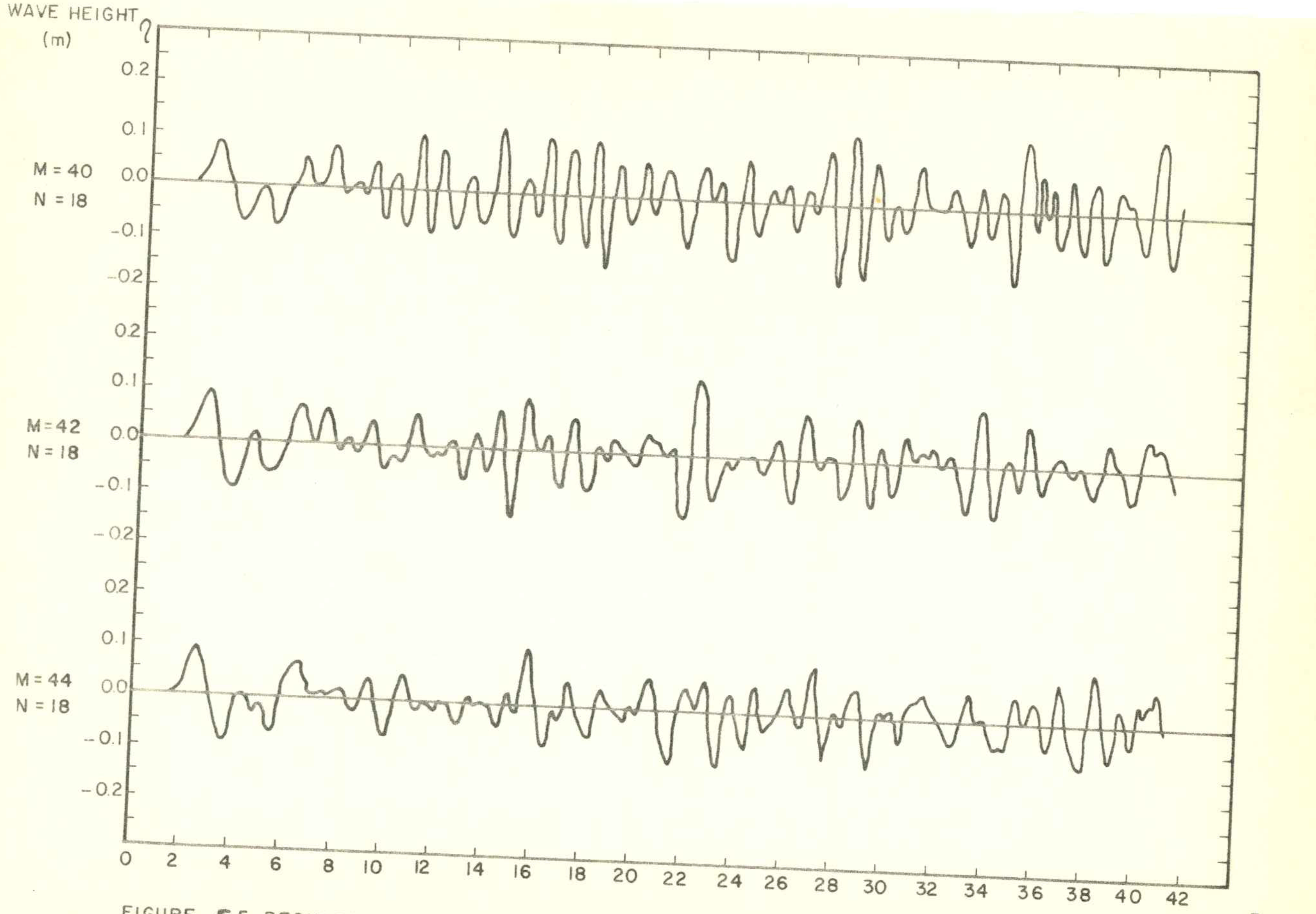

FIGURE 5.5. RESULTS OF RUN-3, ANTALYA BAY.
M = 42, N = 18 CORRESPONDS TO AKKUYU BAY ENTRANCE

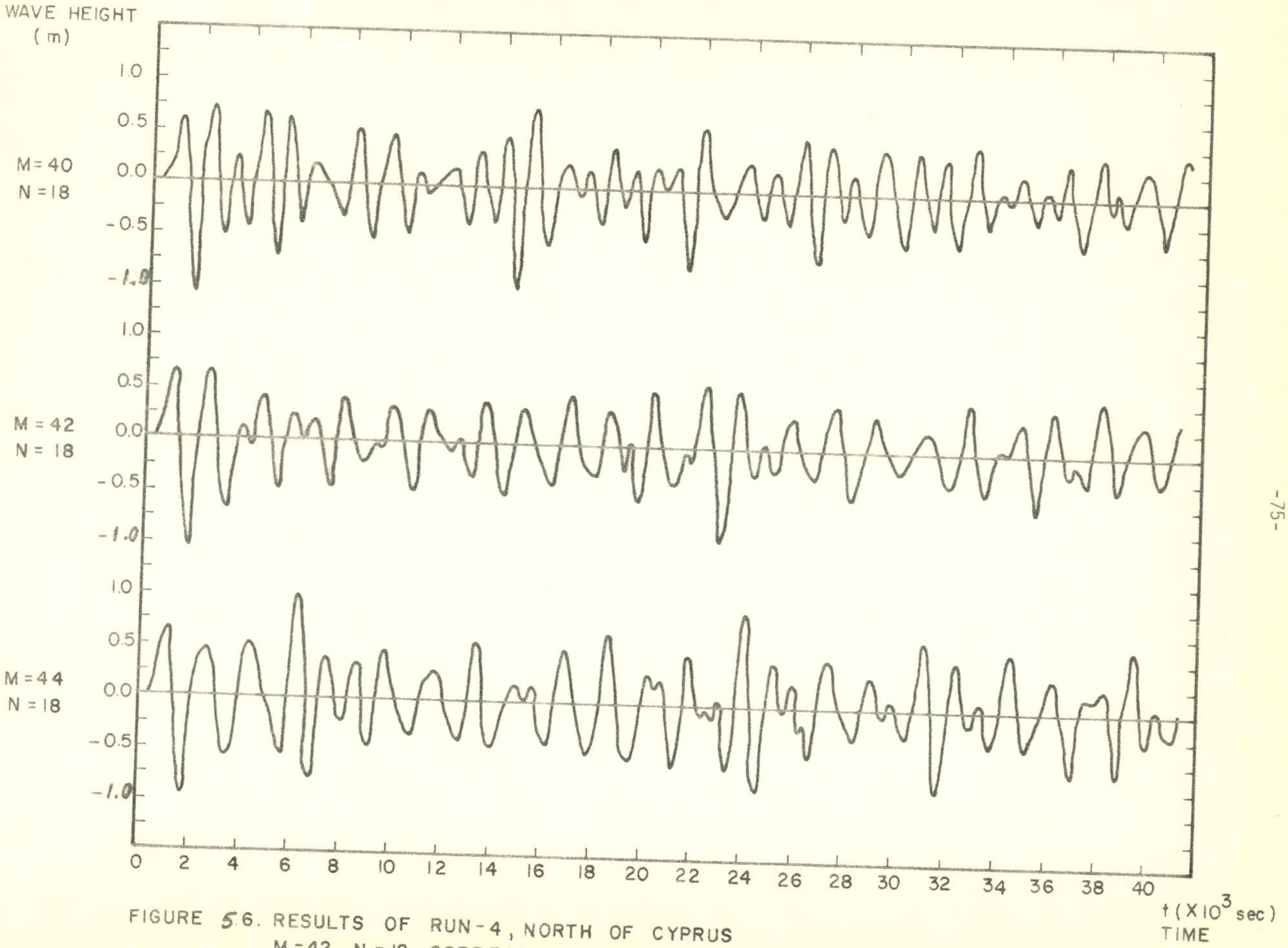

FIGURE 5.6. RESULTS OF RUN-4, NORTH OF CYPRUS
M=42, N=18 CORRESPONDS TO AKKUYU BAY ENTRANCE.

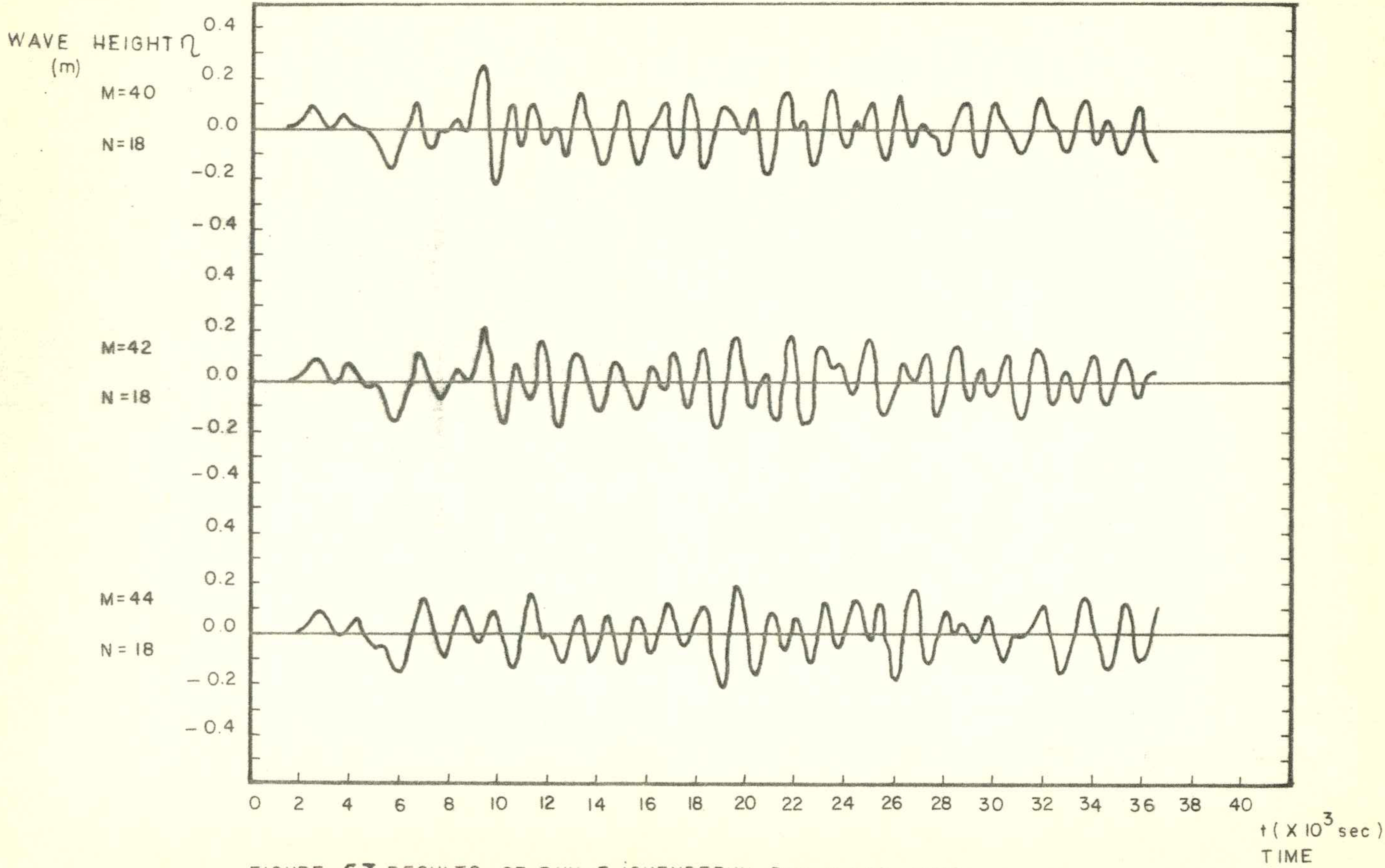

FIGURE 5.7. RESULTS OF RUN-5, İSKENDERUN BAY M = 42 , N = 18
CORRESPONDS TO AKKUYU BAY ENTRANCE

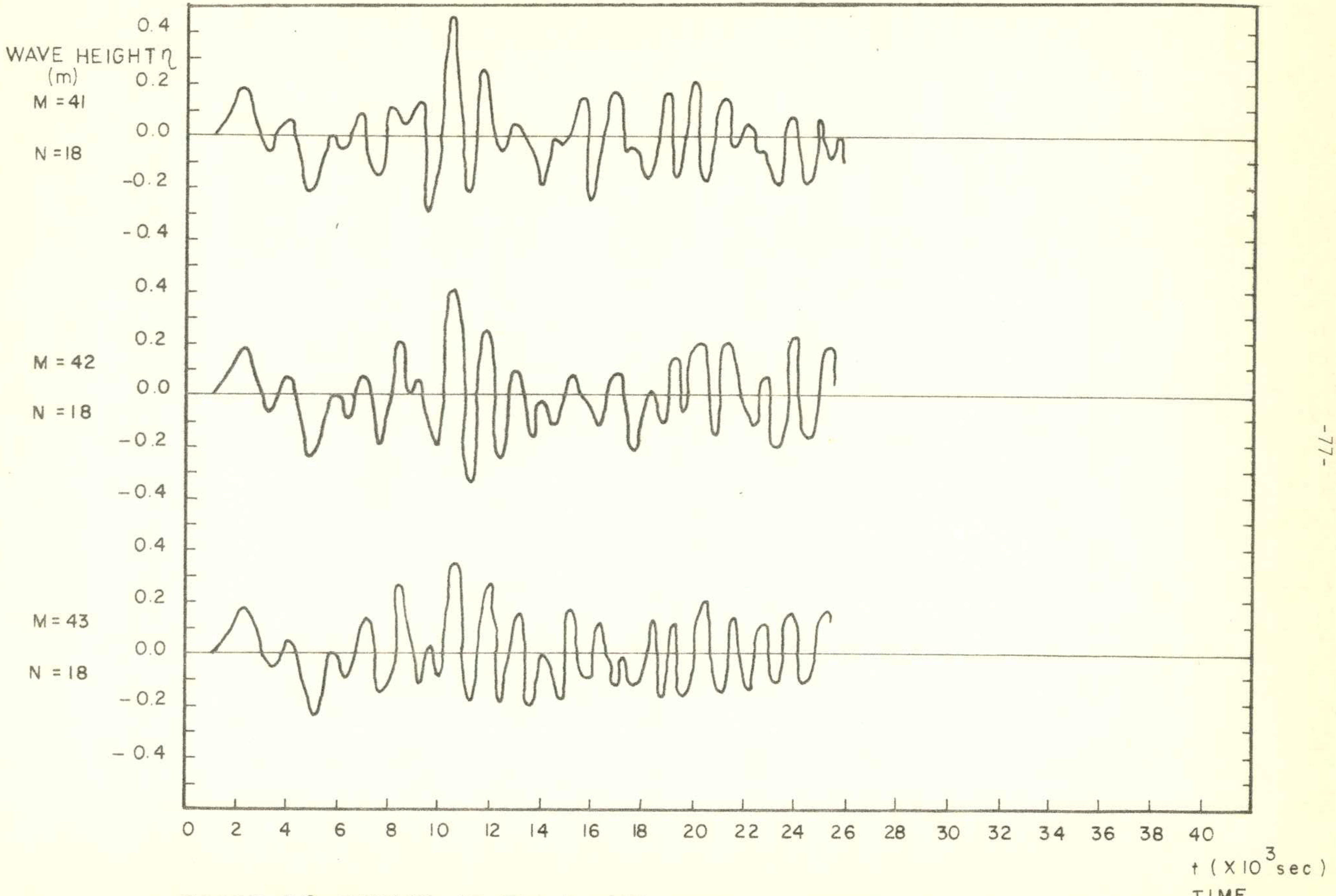

FIGURE 5.8 : RESULTS OF RUN-6, NORTH EAST OF CYPRUS
M = 42 , N = 18 CORRESPONDS TO AKKUYU BAY ENTRANCE

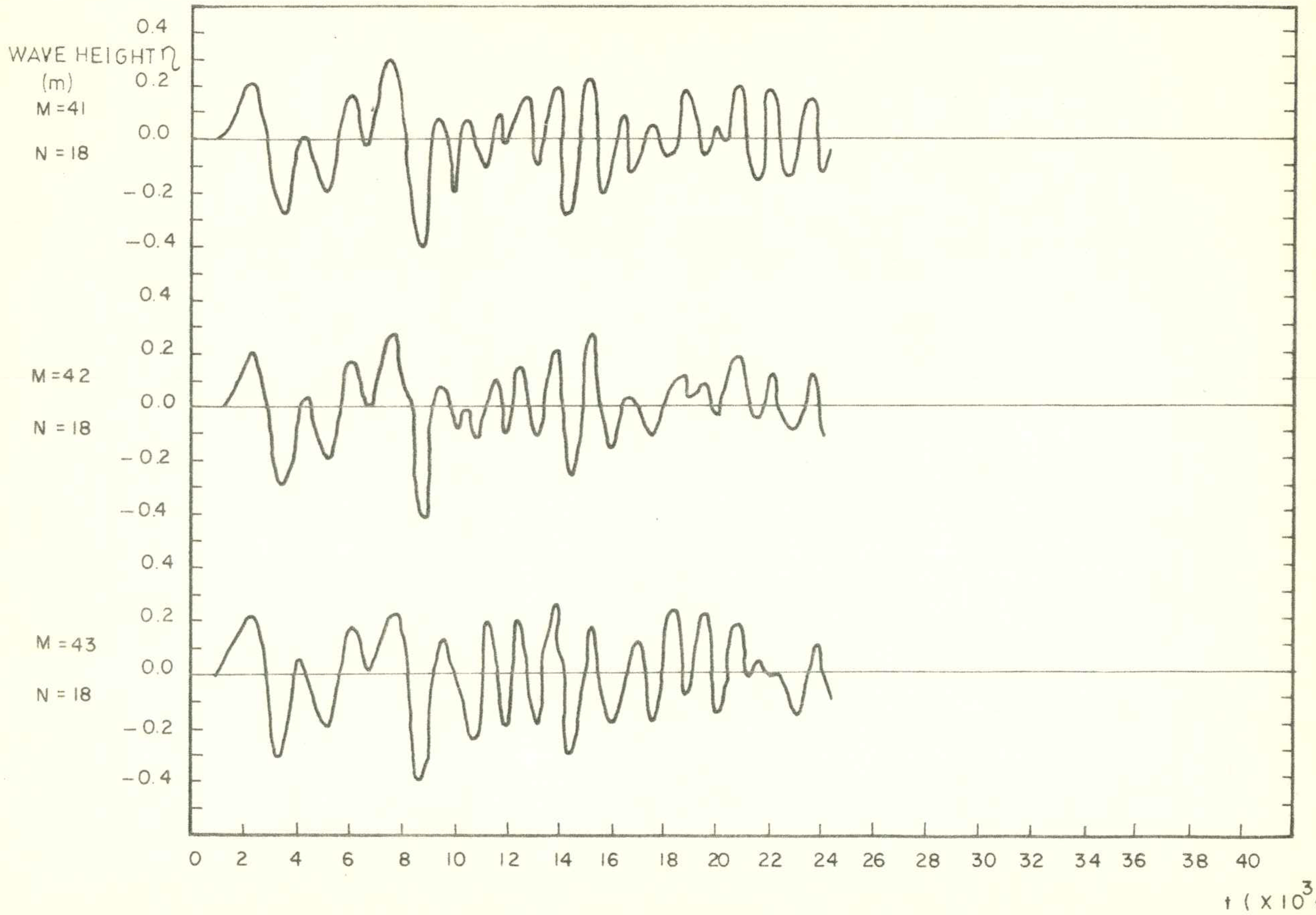

FIGURE 5.9 : RESULTS OF RUN-7, NORTH WEST OF CYPRUS
M=42 , N=18 CORRESPONDS TO AKKUYU BAY ENTRANCE

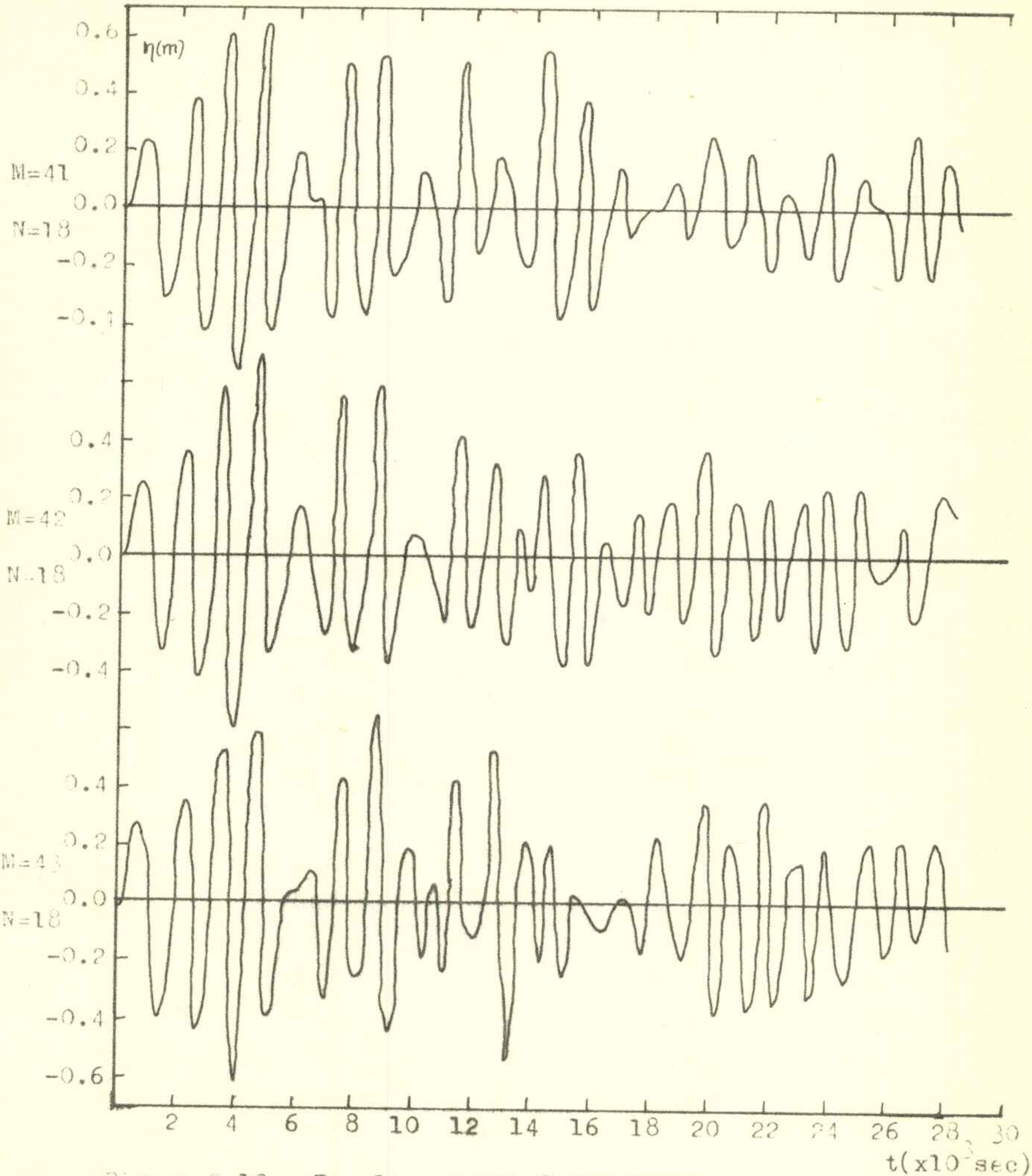

Figure 5.10 Results of RUN-8 MID REGION BETWEEN ASIA MINOR AND CYPRUS, M=42, N=18 CORRESPONDS TO AKKUYU BAY ENTRANCE

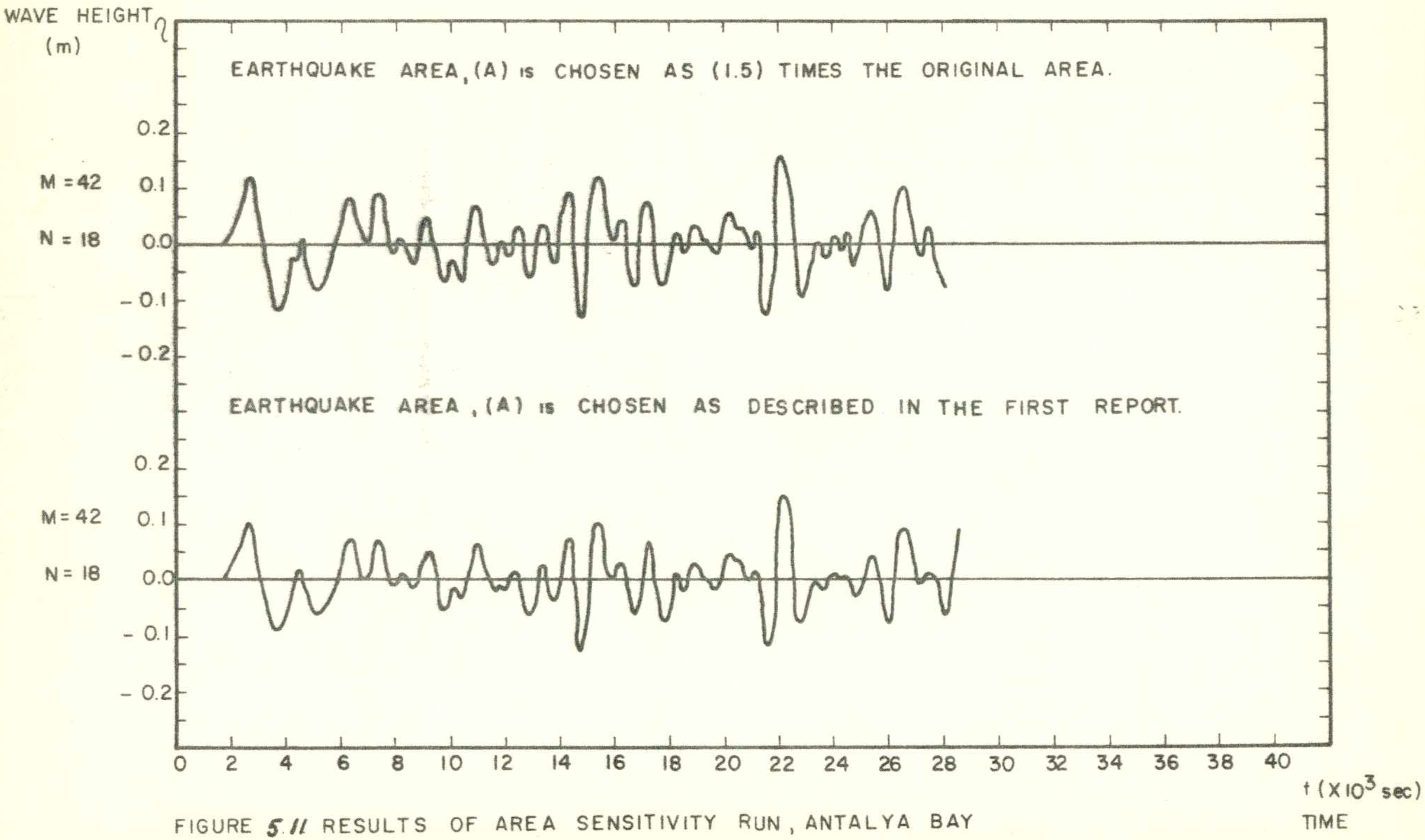

FIGURE 5.11 RESULTS OF AREA SENSITIVITY RUN, ANTALYA BAY
M = 42, N = 18 CORRESPONDS TO AKKUYU BAY ENTRANCE

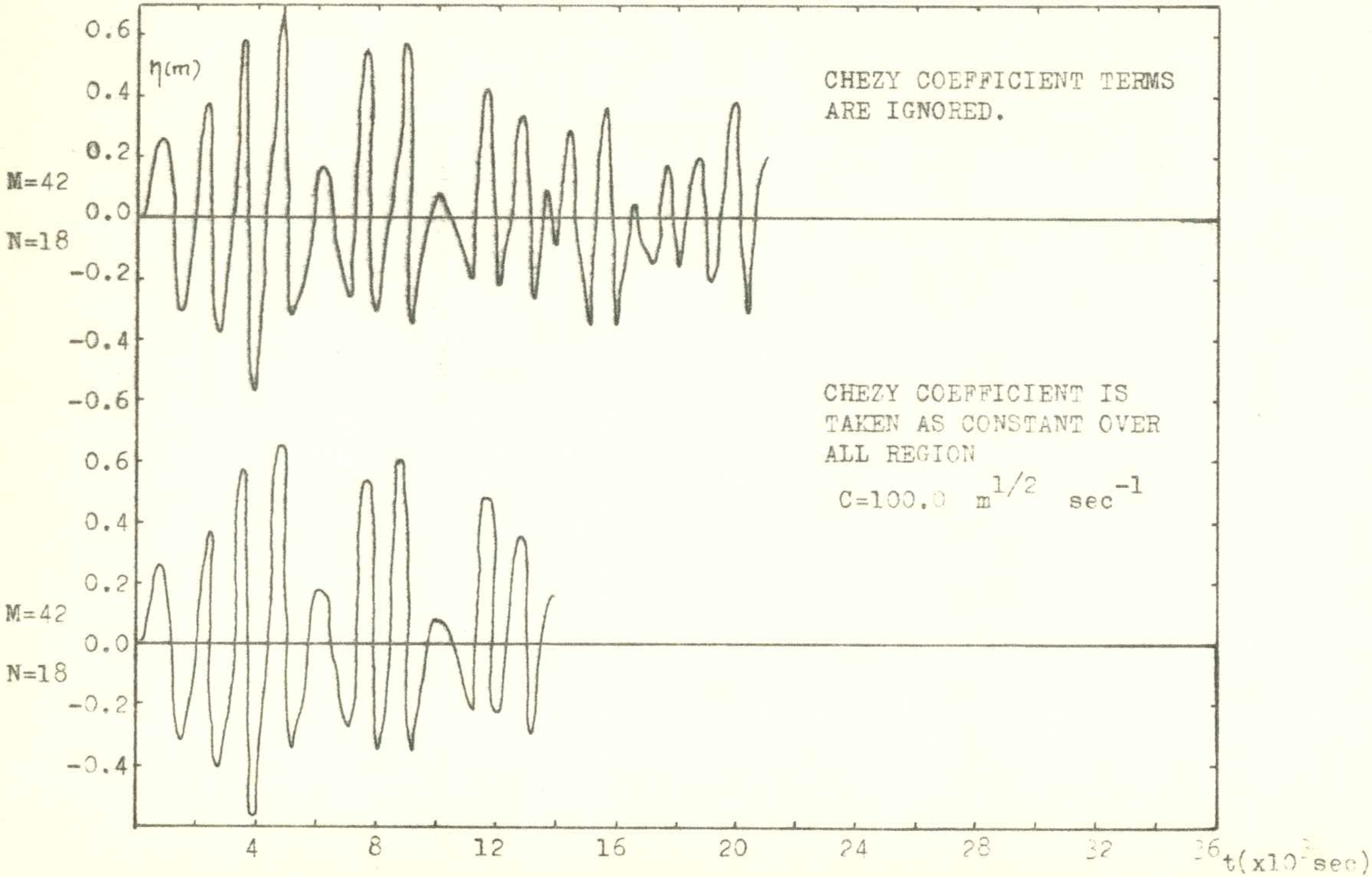

Figure 5.12 RESULTS OF CHEZY COEFFICIENT SENSITIVITY RUN
(DUPLICATION OF RUN-8)

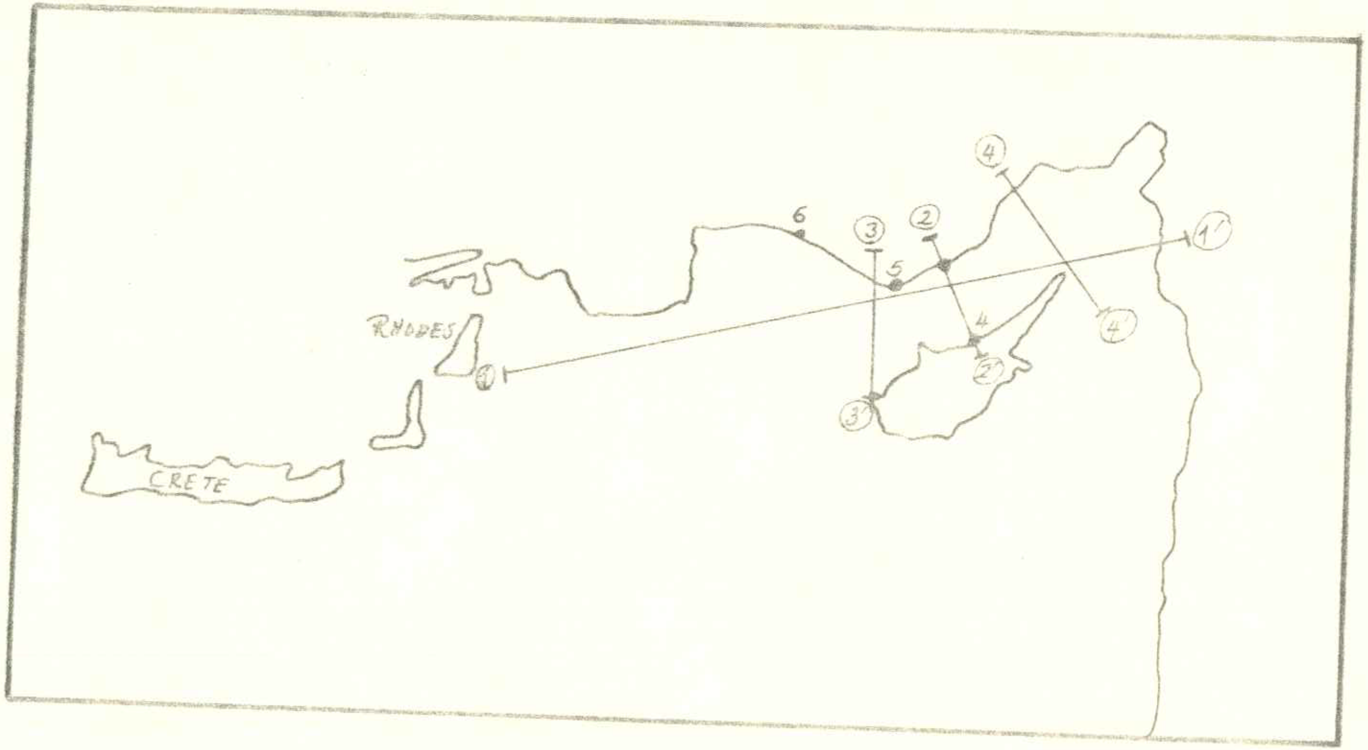

Figure 5.13 Sections and Locations where space-time history of the Surface Motions are given.

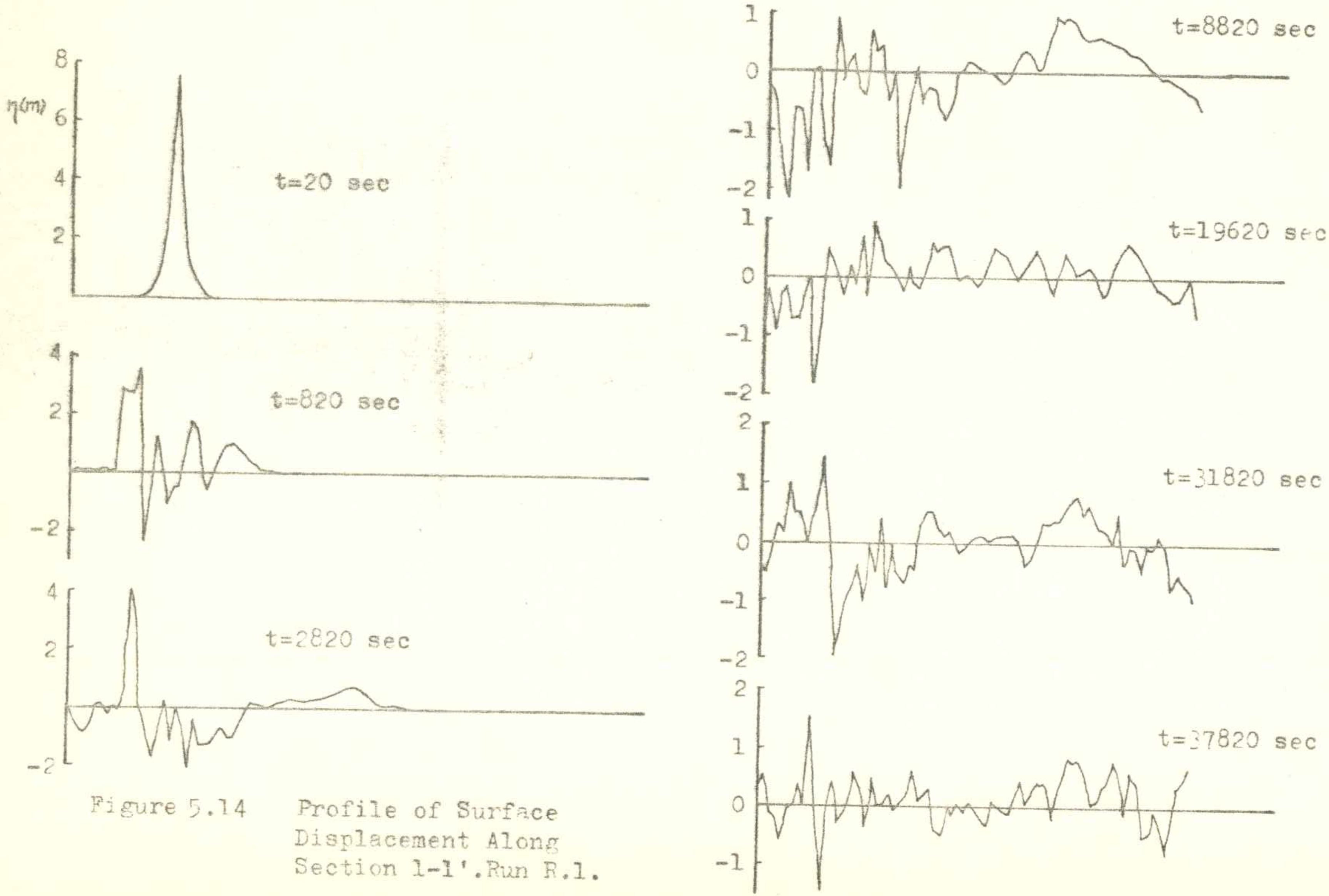

Figure 5.14 Profile of Surface Displacement Along Section 1-1'. Run R.1.

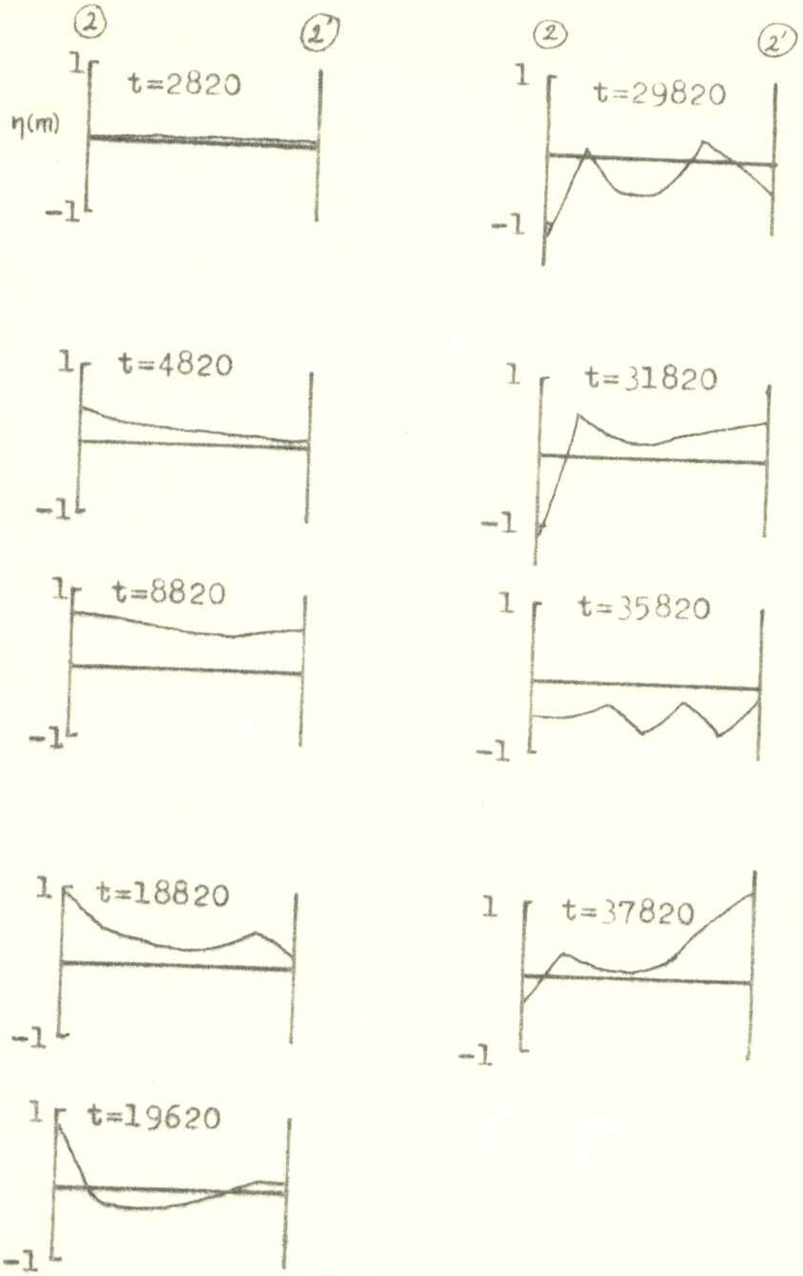

Figure 5.15. Transverse Profile of Surface Displacement

Between Akkuyu and Cyprus (Section 2-2'). Run R.1. Time t is in seconds

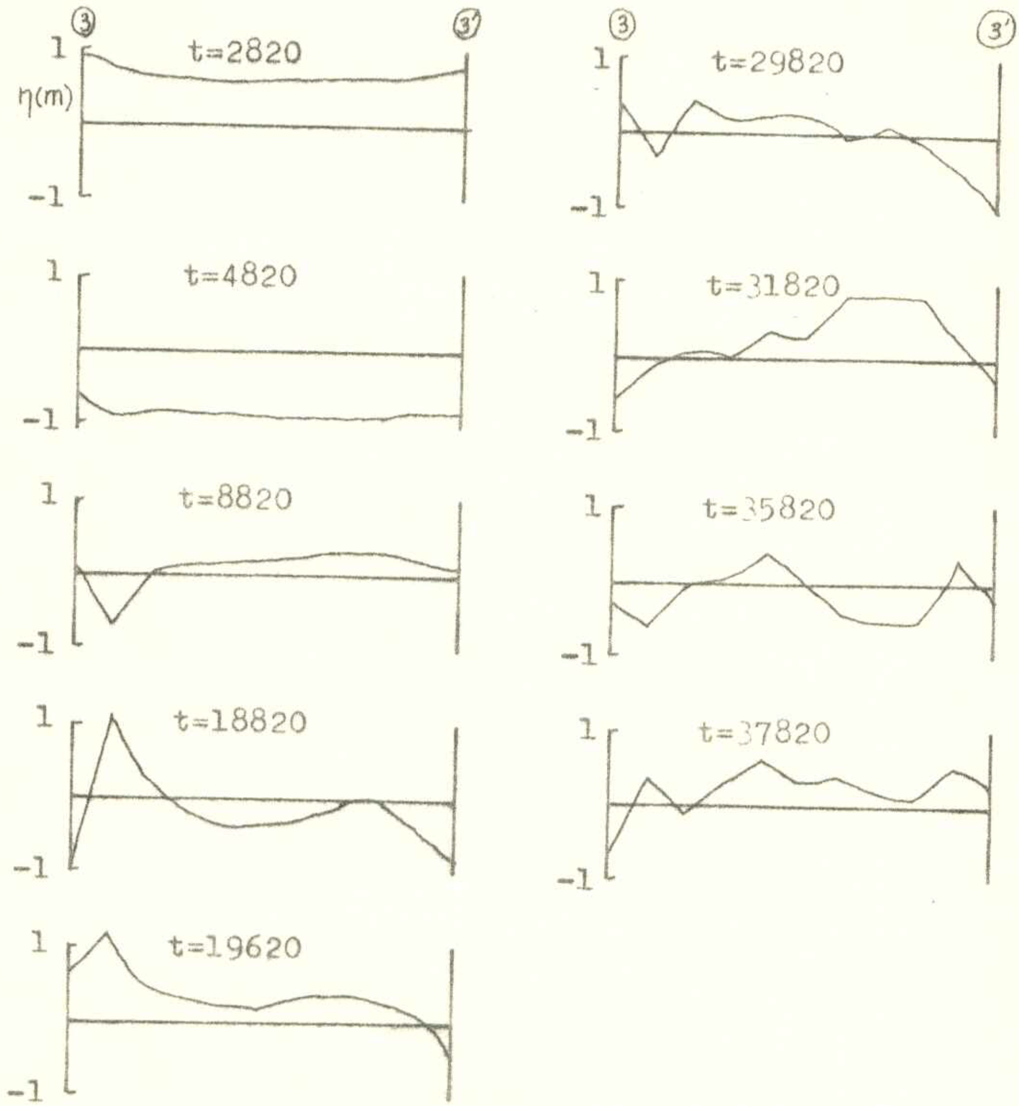

Figure 5.16 Transverse Profile of Surface Displacement Along Section (3-3'). Run R.1. Time t is in seconds.

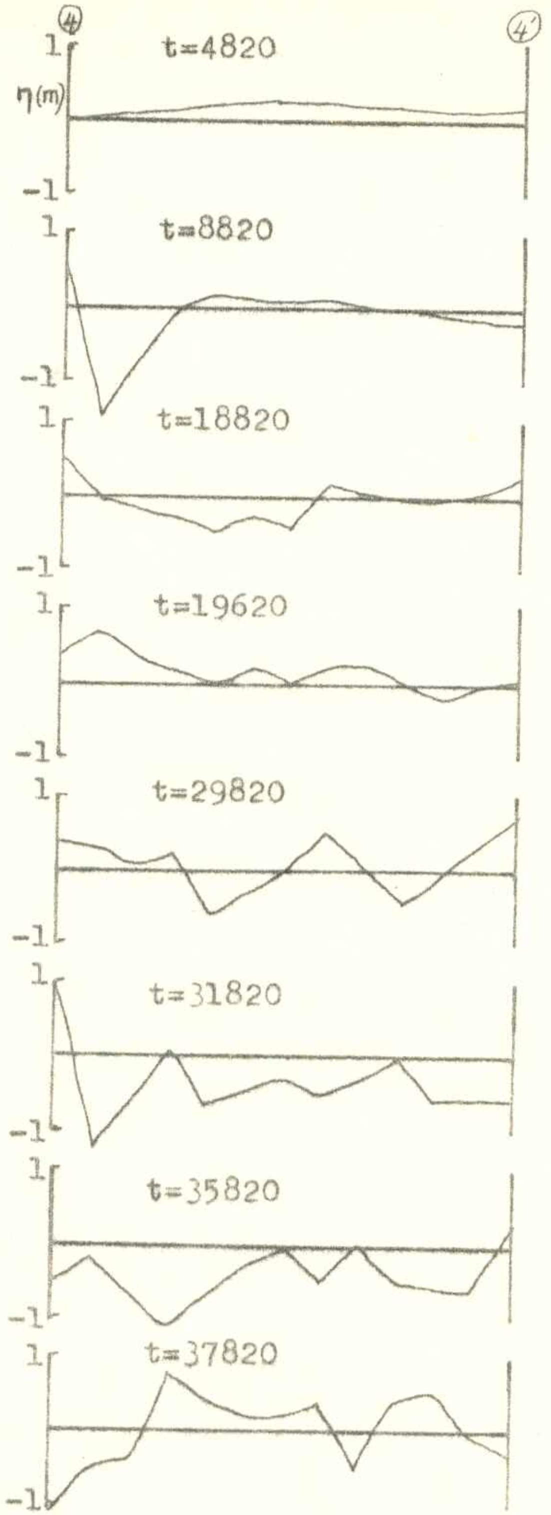

Figure 5.17 Transverse Profile of Surface Displacement Along Section (4-4'). Run R.1. Time t is in seconds.

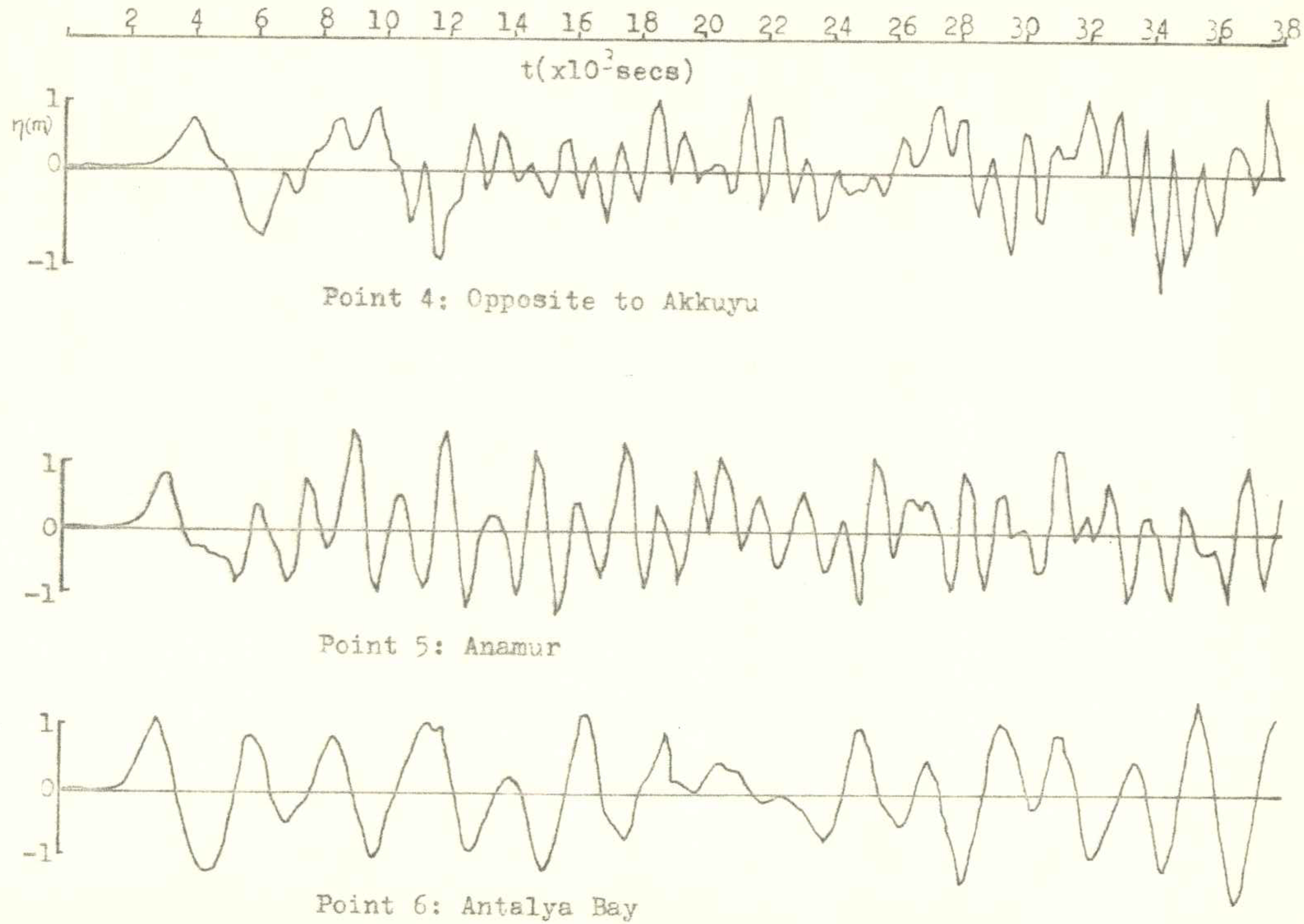

Figure 5.18 Time History of Surface Displacement at Points 4, 5 and 6. Run R.1.

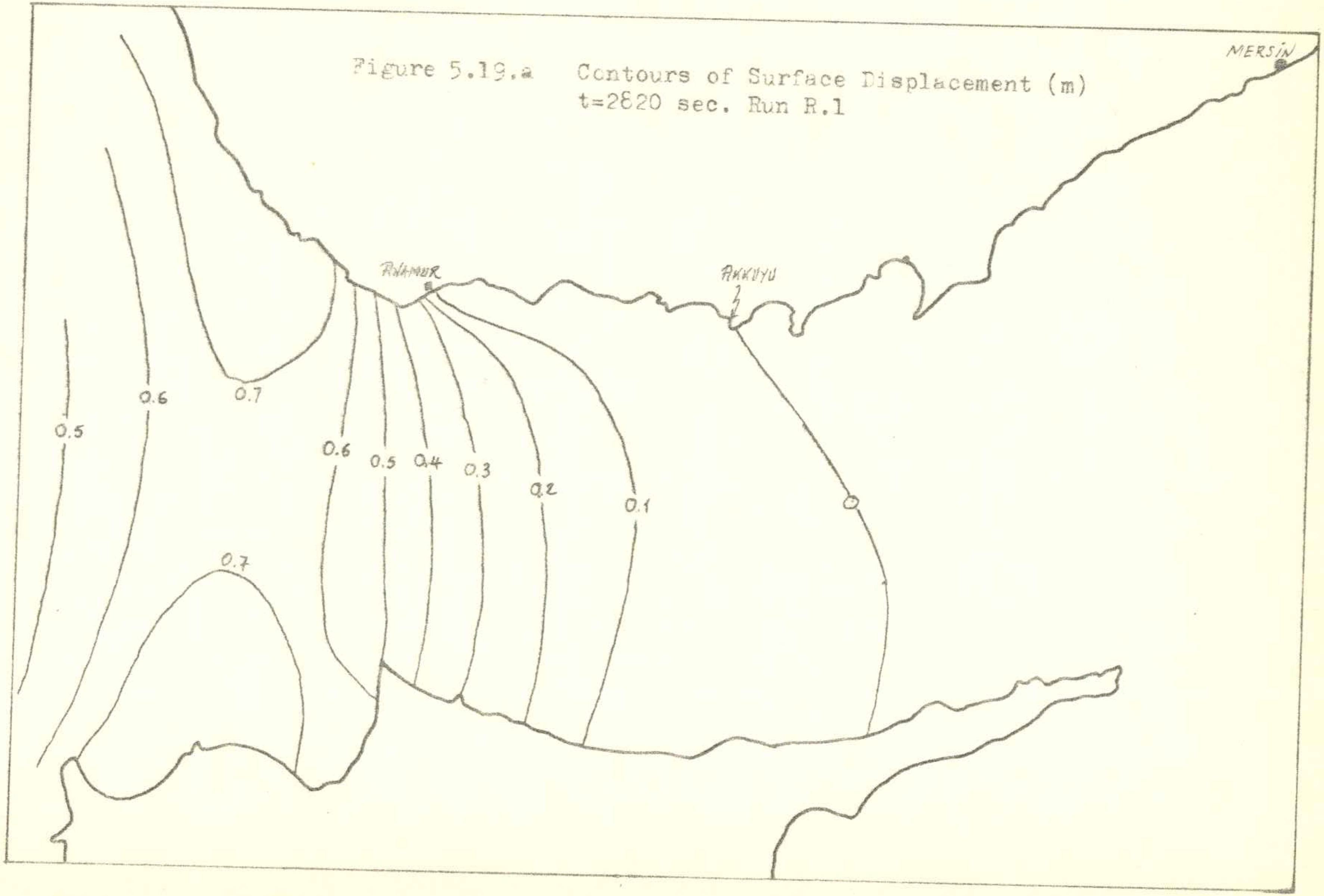

Figure 5.19.a Contours of Surface Displacement (m)
t=2820 sec. Run R.1

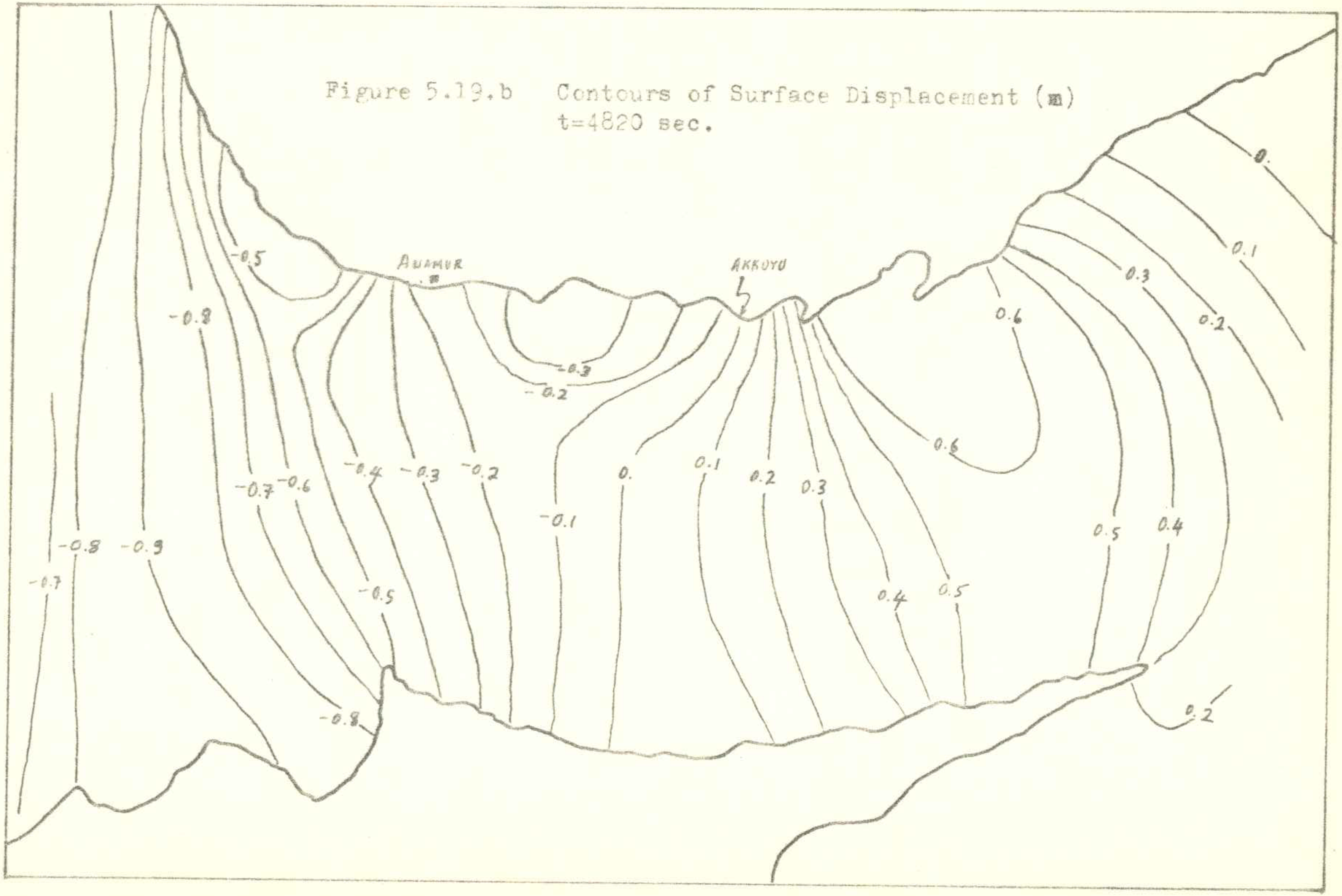

Figure 5.19.b Contours of Surface Displacement (m)
t=4820 sec.

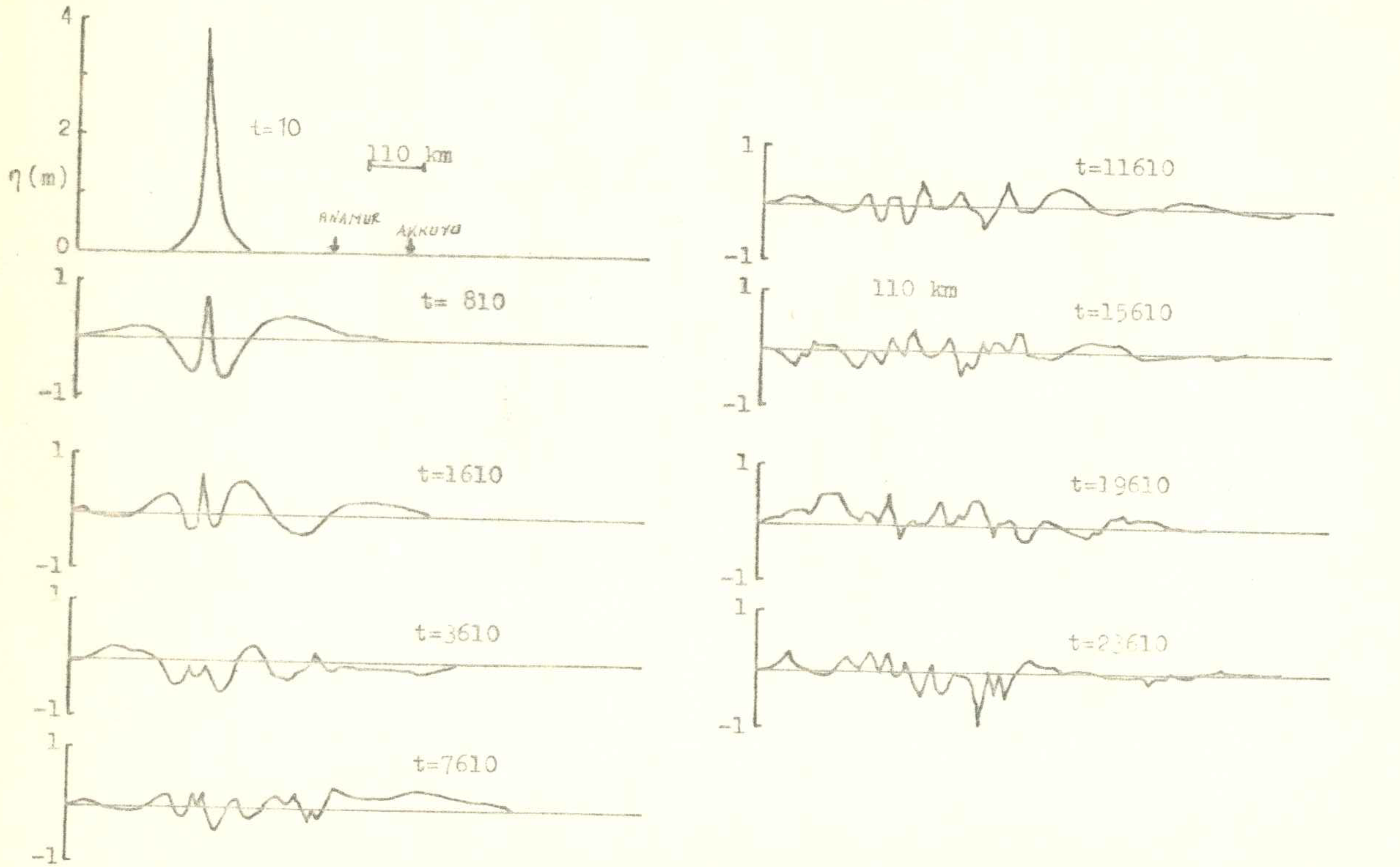

Figure 5.20 Profile of Surface Displacement Along Section 1-1'. Run R.7
Time t is in seconds.

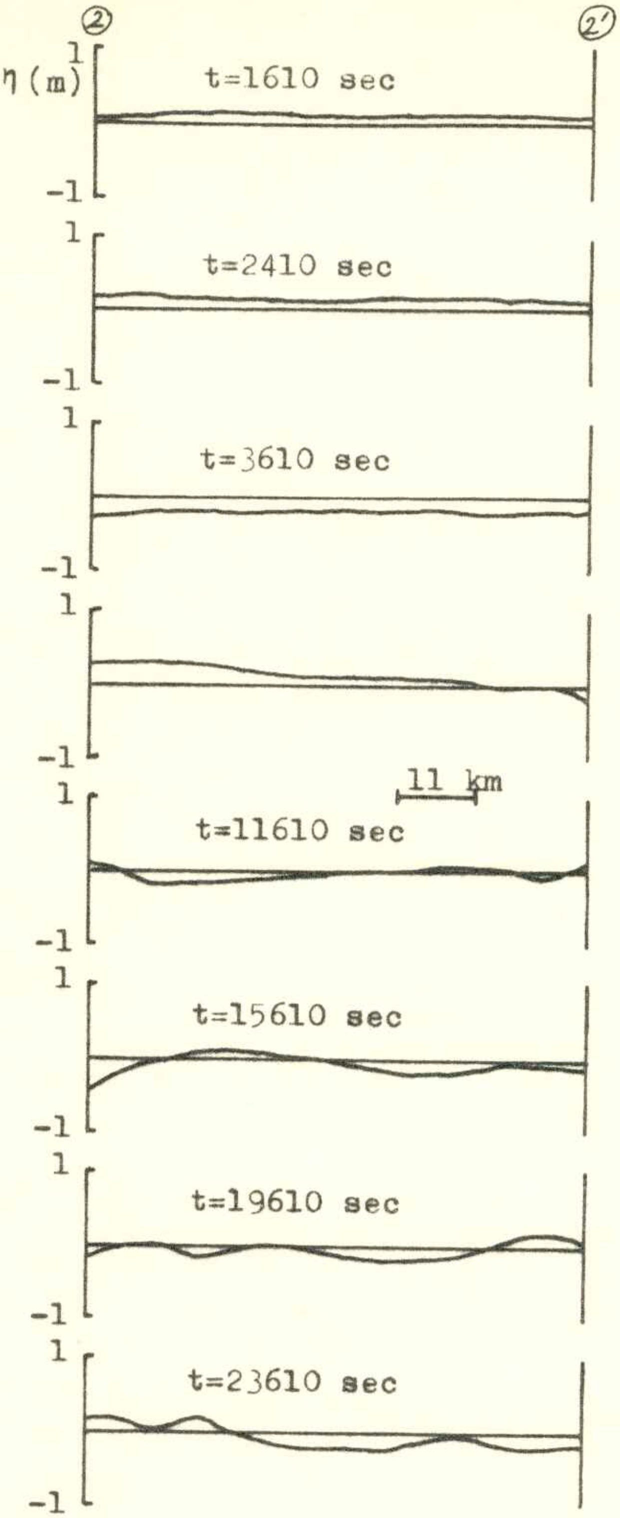

Figure 5.21 Transverse Profile of Surface Displacement Between Akkuyu and Cyprus (Section 2.2'). Run R.7

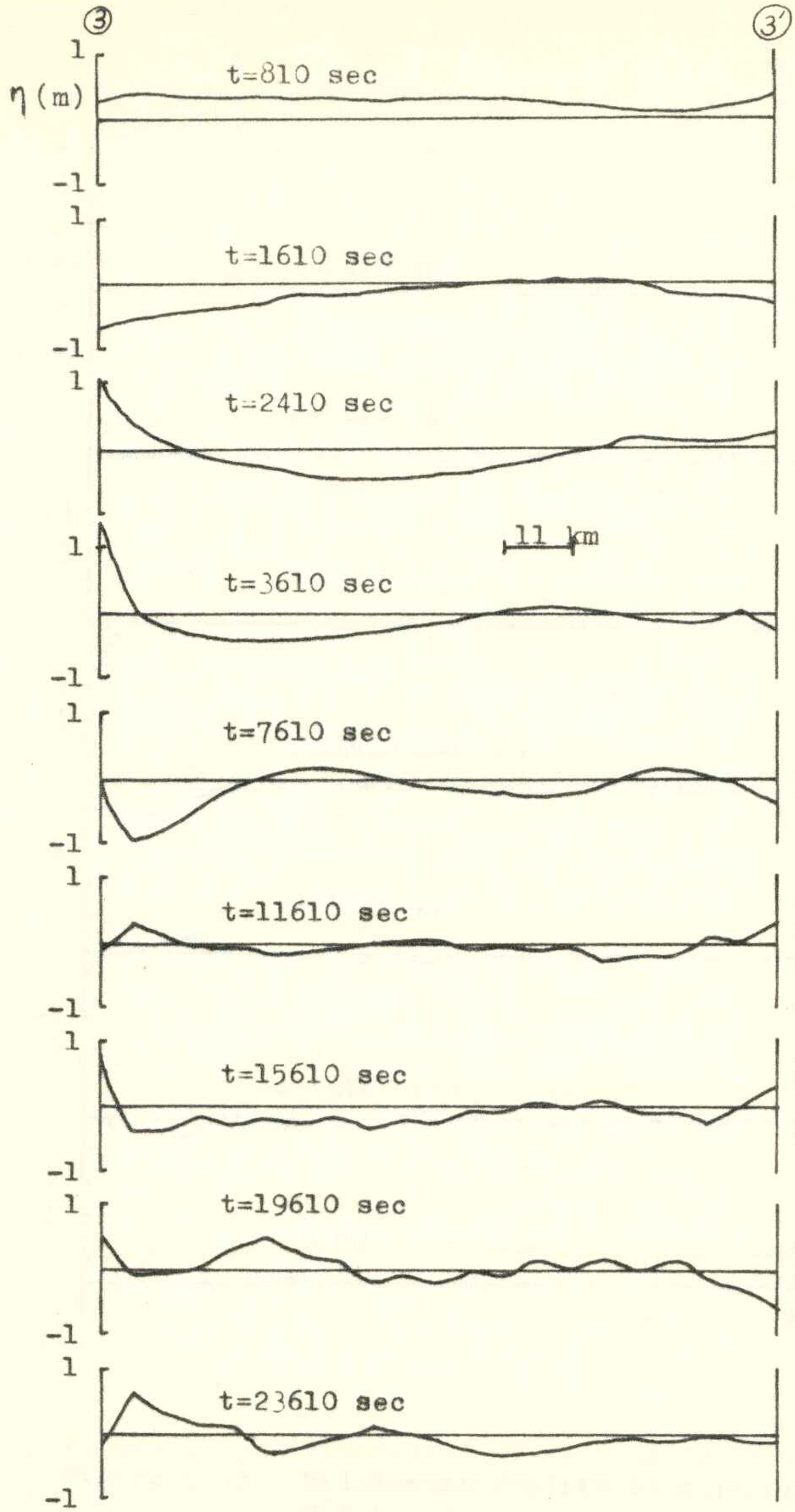

Figure 5.22 Transverse Profile of Surface Displacement Along Section (3-3'). Run R.7

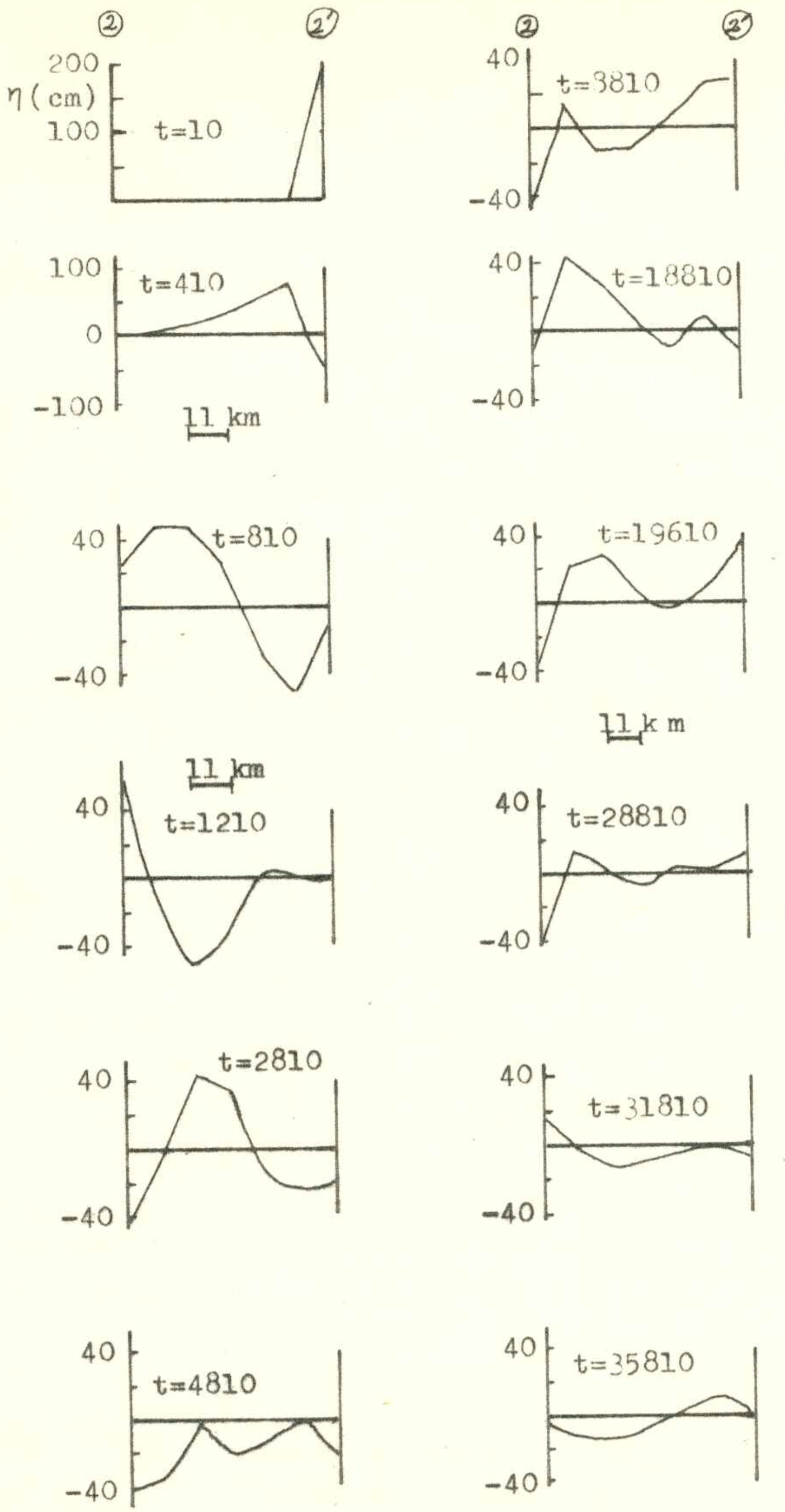

Figure 5.26 **Transverse Profile** of Surface **Displacement** Along Section (2-2'). **Run 4. Time** t is in seconds.

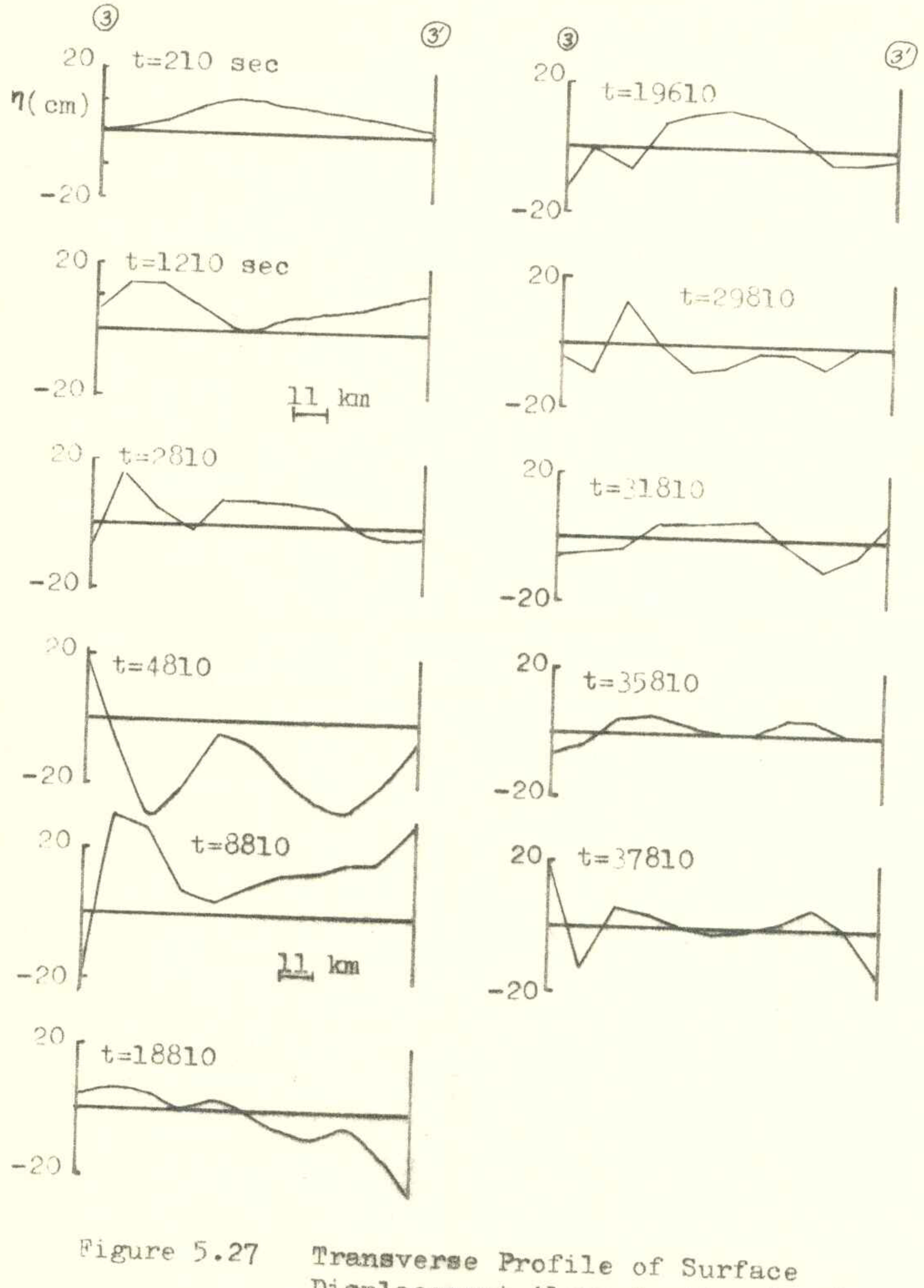

Figure 5.27 **Transverse Profile of Surface Displacement Along** Section (3-3).

Run R.4. Time t is in seconds.

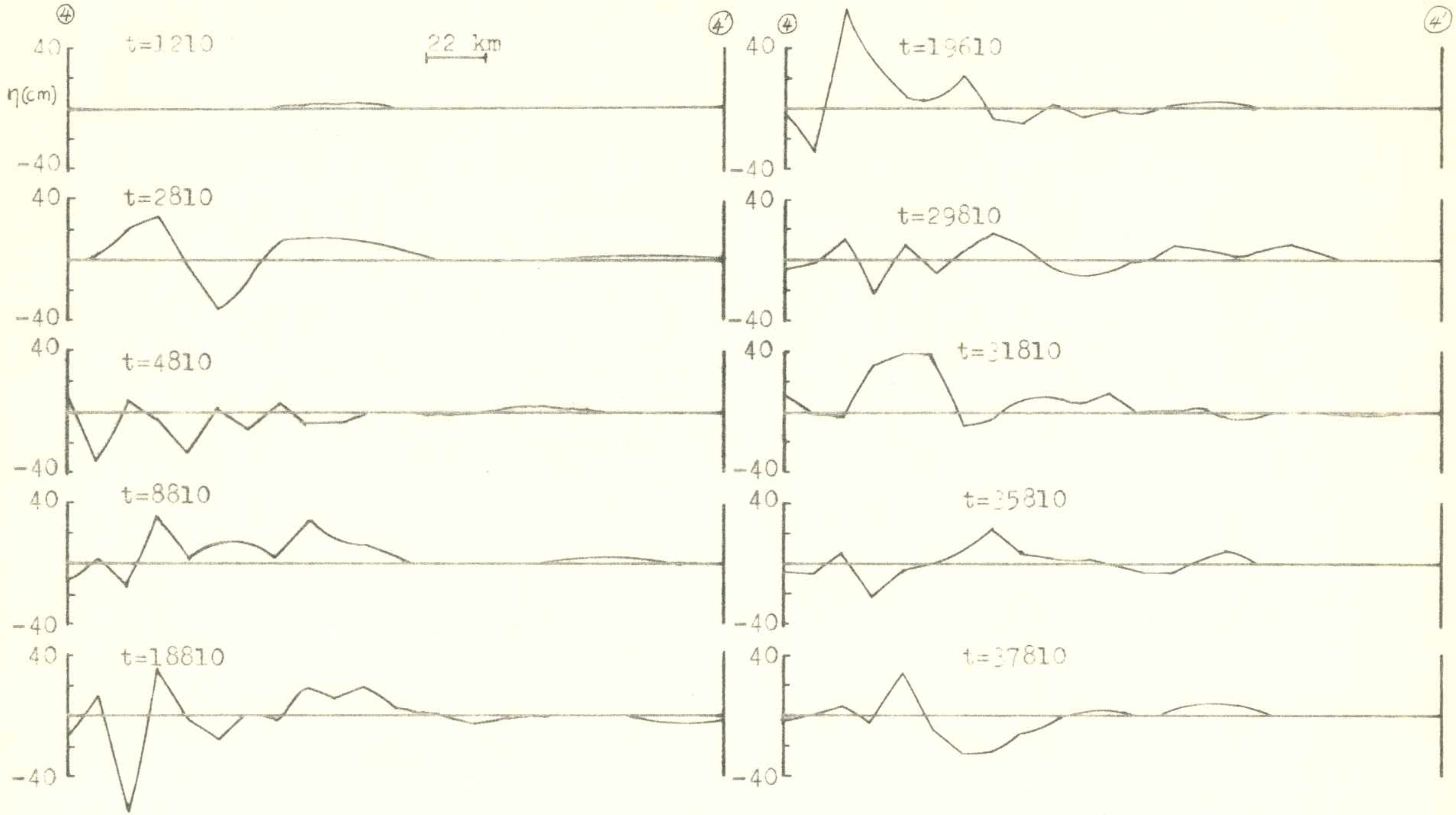

Figure 5.28 Transverse Profile of Surface Displacement Along Section (4-4'). Run 4. Time t is in seconds.

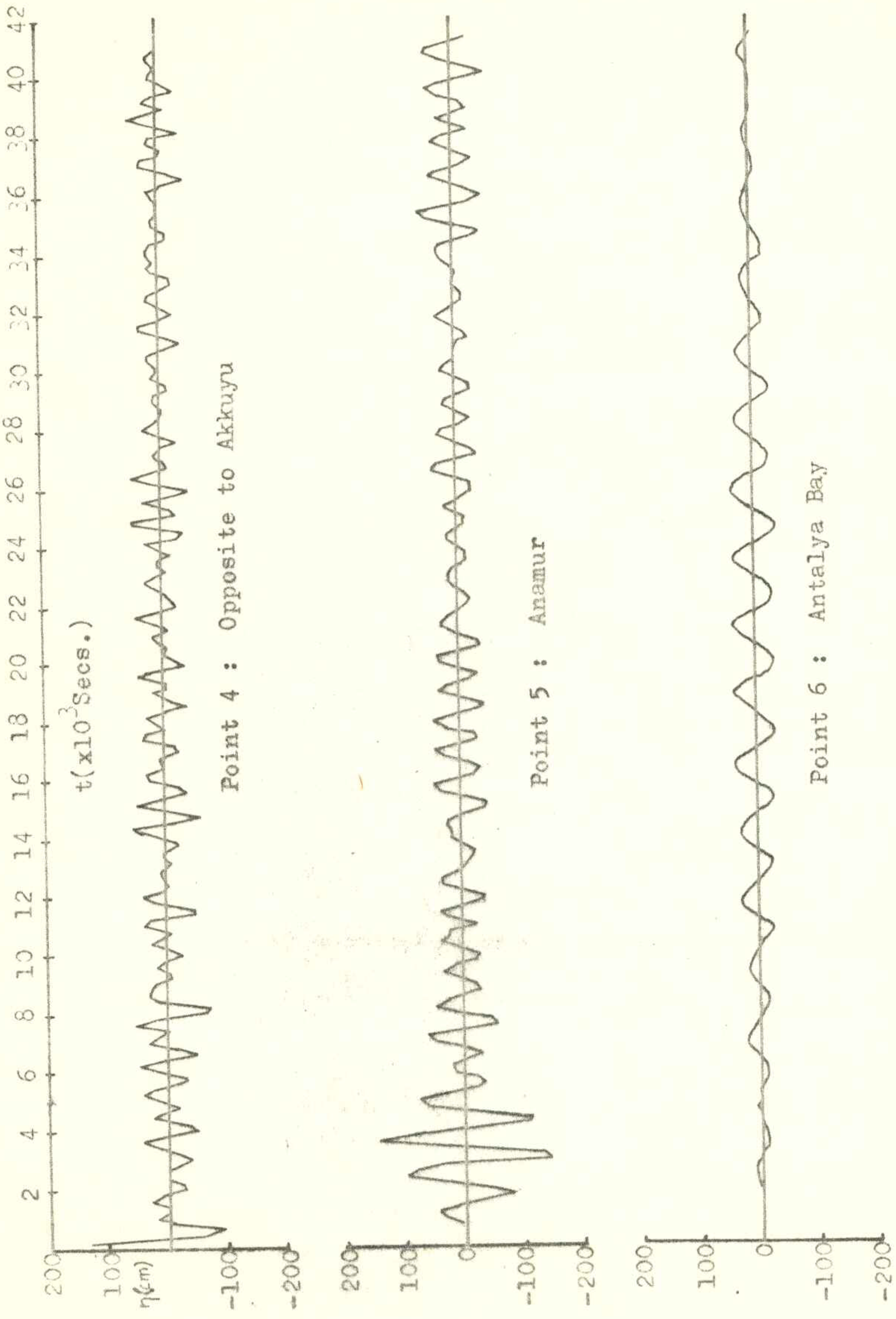

Figure 5.29 Time History of Surface Displacement at Points 4, 5 and 6.

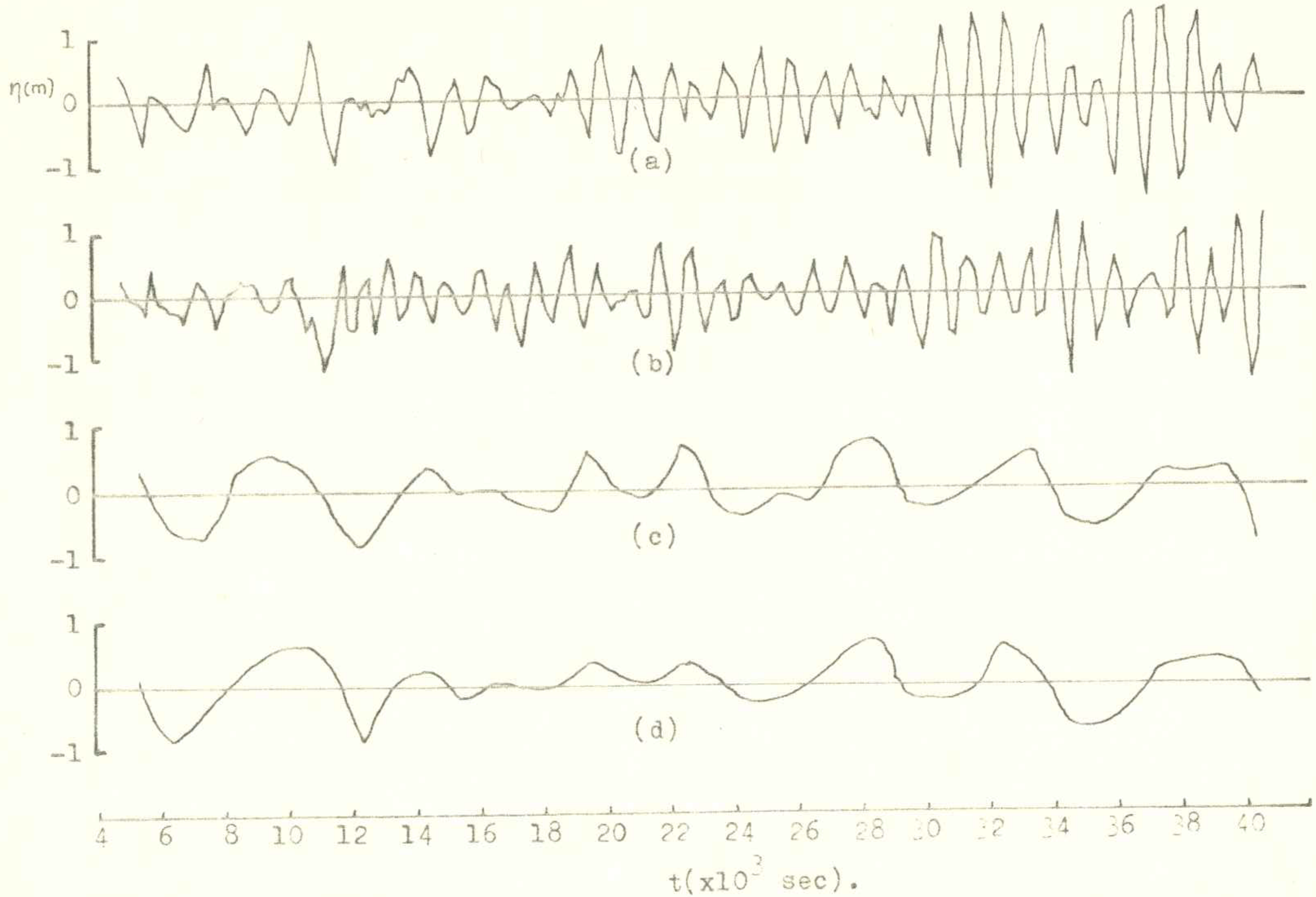

Figure 5.30 High Passed (5 Pt.Averaging) Surface Motions at Akkuyu (a) and at Point 4 Opposite to Akkuyu. The Corresponding Low Passed Series are Shown in (c) and (d). Run R.1.

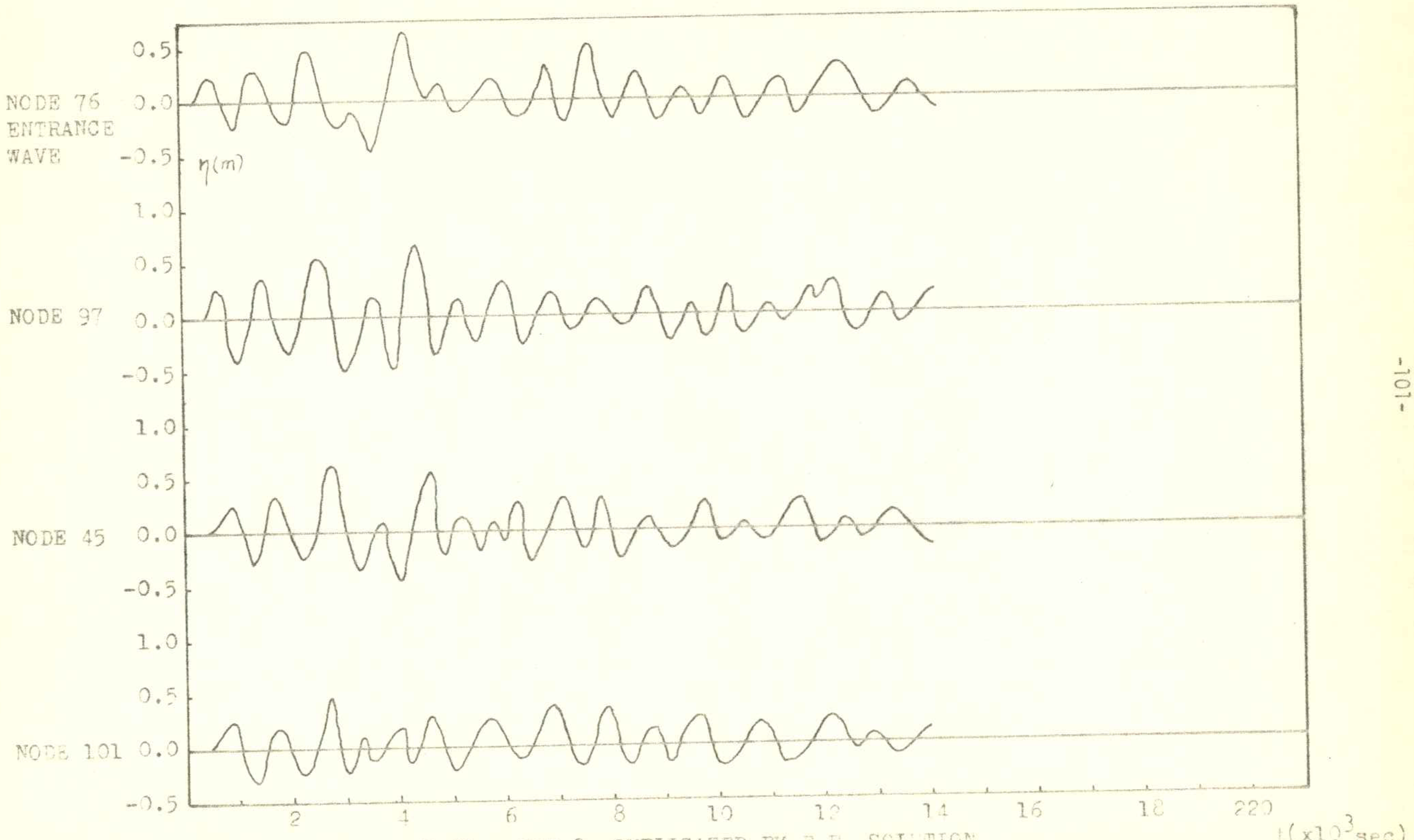

Figure 5.31 RUN-8 DUPLICATED BY F.E. SOLUTION.

TABLE. 2.1

(Reproduced from Van Dorn,1965)

NUMBER AND DISTRIBUTION OF LARGE TSUNAMIS

Dates	Atlantic	Mediterranean	Pacific
Before 1500	2	9	9
1500-1800	14	8	62
1800-	13	6	148
Total events	29	23	219

TABLE: 2.2

TSUNAMI CATALOGUE
OF EASTERN MEDITERRANEAN

(Ambraseys, 1962)

1. II millenium B.C. Syrian coasts (vi?).
2. 1410±100. North coast of Crete Grecian Archipelago (vi?).
3. 1365±5. Syrian coasts, Ugarit near Minet-el-Beida (vi?).
4. c. 1300. Ionian coasts and towns in Asia Minor, Troad (v?).
5. c. 760. Coasts of Israel and Lebanon.
6. c. 590. Coasts of Lebanon. Sur (Tyre) (vi?).
7. c.525. Coasts of Lebanon, Saida.
8. 479 Winter. Chalcidice. Isthmus of Kassandra, Potidaea (iii).
9. 426 Summer. Euboean and Malian Gulfs, Phthiotian coasts (v-) Euboean coasts (iv), Island of Skopelos (iii).
10. 373 Winter. Gulf of Corinth. Helice (v).
11. c.330* . Eastern Sporades Islands. Island of Chryse.
12. 222*. Island of Rhodes. City of Rhodes.
13. 138. Coasts of Israel and Lebanon. Between Acre (Ptolemais) and Sur (iv).
14. 58. Albanian coasts. Durazzo (Dyrrhschion) (iii).
15. 23±3. Egyptian coasts between Alexandria and Pelusium (iii). A seismic sea-wave probably connected with the 26 B.C. earthquake in Cyprus.
16. 46* A.D. South Coasts of Crete.
17. 62. South coasts of Crete. Lebena (iii).
18. 76* Cyprus, Kition. Paphos and Salamis.
19. 142. Island of Rhodes. Rhodes (iv). Islands of Kos, Seriphos and Syme (iii).
20. 262. South coasts of Asia Minor (iv).
21. 315. Dead Sea (iii).
22. 342. Cyprus, Farnagusta. 155.

TABLE: 2.2

(continued)

23. 344. Dardanelles and Niksar (Neocaesaria) (iv), Thracian coasts (iii).

24. 348. Syrian coasts. Beirut (iii?). Arwad Islands (iii?) 182 (p.199).

25. 362. Dead Sea, Jordanian coasts (iii?).

26. 365. July 21. Eastern Mediterranean Methone, Epidaurus, Crete (iv), Beeotian coasts, Adriatic coasts, Epirus, Alexandria[1], Sicily (iii-).

27. 447 November. Sea of Marmara. Marmara Islands. Dardanelles, and the coasts of Marmara (iv-), Constantinople (iii).

28. 450 January. Sea of Marmara, Constantinople (iii). Lycosthenes mentions an inundation of the sea but we find no mention of it in contemporary chronicles.

29. 542 Winter. Sea of Marmara. Thracian coasts and Gulf of Edremit (iv).

30. 551 Spring. Malian Gulf. Achinos, Tarphe (iv-).

31. 551 July 9. Syrian coasts. Votrys near Jubeil (Byblos) (iii+), Tarabulus (Tripolis) Beirut (iii-).

32. 554 August 15. Southwest coasts of Asia Minor, Mandalya Bay, Island of Kos, Sporades Isls (iv-).

33. 740 October 26. Sea of Marmara, Izmit, Iznik Lake. Thracian coasts of Marmara (iii).

34. 746 January 18. Syrian and Egyptian coasts (iii-).

---

1 According to Hoff (p.182), probably not Alexandria in Egypt, but Alexandria Troas in Asia Minor.

TABLE: 2.2
(continued)

35. 792. Gulf of Venice, coasts of Istria and Jugoslavian coasts of the Adriatic sea (iv).

36. 803 December 19. Gulf of Iskenderun. Masisa coast (iii).

37. 859 November. Syrian coasts, near Samandag (iii).

38. 811.* Coasts of Israel and Egypt, from Acre to Alexandria.

39. 957. Caspian Sea (iii).[2]

40. 975 October 26. Constantinople and Thracian coasts (iii).

41. 991* April 5. Coasts of Syria.

42. 1034 January 4. Coasts of Lebanon and Israel. Acre (iv).[3]

43. 1039* January. Constantinople.

44. 1050* Grecian Archipelago. Thera (Santorin). Most probably a misprint for 1650.

45. 1068 March 18. Coasts of Israel at Holots Ashod and Yavne (iv).

46. 1202 May 22. Syrian coasts (v), Cyprus (iv), Egypt (iii).

47. 1222 May. Cyprus. Limassolland Paphos (iv).

48. 1273 September. Albanian coasts. Durazzo (iii).

49. 1303 August 8. Egyptian coasts (v-), Syrian coasts (iv). Crete (iv?).

---

[2] It is not clear whether it should be the Caspian Sea or the Persian Gulf. In the various MSS this is given as the "Great Sea" cf.171, 87. We believe, however, that here it should mean the Caspian Sea. It is very probable that the changes in the level of the Caspian, some of which there is reason to believe have occurred within the historical era, and the geological appearances in the district, indicating the desertion by the Sea of its ancient bed, had led Omar El'Aalem (X-th century A.D.) to his theory of a general lowering of the waters of the Caspian. See 124 (vol.1,p.406).

[3] Perrey (1850) and others date this event in 1032 A.D.

TABLE: 2.2
(continued)

50. 1303 December. Crete (iv), Southwest coasts of Peloponnesus and Rhodes (iii), Egyptian coasts and Adriatic Sea (iii?). 35

51. 1332 February 12. Sea of Marmara. Constantinople (iii+).

52. 1344 October 14. Sea of Marmara. Thracian coasts (iv), (L=2 km).

53. 1389 March 20. Island of Chios (iii).

54. 1403 November 16. Syrian coasts, Asia Minor south coasts (iii).

55. 1481 May 3. Rhodes (iii), (H=6'), (L=200').

56. 1489. South coasts of Asia Minor. Antalya (iii).

57. 1494 July 1. Crete. Herakleion (Candia) (ii+).

58. 1508 May 29. South coasts of Crete (iii-), north coasts (iii).

59. 1509 September 14. Constantinople (iii).

60. 1534. Coasts of Israel. Jaffa (iii). Not found in contemporary writers.

61. 1546 January 14. Coasts of Israel and Lebanon. From Gaza to Jaffa (iii+).

62. 1612 November 8. North coasts of Crete (v-).

63. 1629. March 9. Islands of Cythera and Crete (iii?).

64. 1633 November 5. Zante, South coasts (iii-) on the promontory of Agios Sostis.

65. 1646 April 5. Constantinople (iii).

66. 1650 October 9. Thera (vi), west coasts of Patmos (H=100'), east coasts (H=90'), Ios (H=60'), Sikinos (v) Kea, Crete (iv-).

TABLE: 2.2
(continued)

67. 1667 April 6. Dalmatian coasts. Dubrovnik (Ragusa) (iii+).

68. 1667 November 30. Asia Minor. Smyrna (ii).

69. 1672* April. Islet of Stanchio. No wave accompanied the subsidence of the islet.

70. 1688 July 10. Asia Minor. Smyrna (ii).

71. 1723 February 21. Ionian Islands. Leukas (iii?).

72. 1732. Ionian Islands. Corfu (ii-).

73. 1748 May 14. North Peloponnesus. Aigion (iii).

74. 1750 September 17. Adriatic Sea. Fiume (iv).

75. 1752 July 21. Syrian coasts (iii?).

76. 1759 October 30. Coasts of Israel and Lebanon. Acre (H=8') (iv-).

77. 1766 May 22. Constantinople (ii).

78. 1791 November 2. Ionian Islands. Between Zante and the mainland (iii-).

79. 1802 January 4. Adriatic Sea. Fiume (iii).

80. 1804 June 8. Northwest coasts of Peloponnesus. Patras (iii). ($38\frac{1}{4}$ N - $21\frac{3}{4}$ E, I = IX, M = ?, d = n).

81. 1817 August 23. Gulf of Corinth. Aigion (iii+). ($38\frac{1}{4}$ N - $22\frac{1}{4}$ E, I = X, M = ?, d = n).

82. 1818* January. Athens. Mallet (p.212+114) mistakes the event before mentioned.

TABLE: 2.2
(continued)

83. 1821 January 6. Gulf of Corinth. Alcyonic Sea (iv).
($37\frac{3}{4}$ N - $21\frac{1}{4}$ E, I = X, M = ?, d = n).

84. 1823 August 20. Dalmatian coasts. Dubrovnik (iv-).

85. 1825 January 19. Ionian Islands. Leukas, between the islet of Sessoula and east coasts of the island (iii?).
($38\frac{3}{4}$ N - $20\frac{3}{4}$ E, I = XI, M = ?, d = n).

86. 1829 May 23. Constantinople (ii).

87. 1833 January 19. Albanian coasts. Valona and Saseno Isle (iv-).

88. 1835 July 12. Ionian Islands. Zante (ii).

89. 1837 January 1. Syrian and Israeli coasts of Tiberias (iv).

90. 1843 September 14. Dalmatia. Dubrovnik, Gruz (Gravosa) (iv).

91. 1844 March 3. Dalmatia. Dubrovnik (iii).

92. 1844 March 23. Dalmatia. Dubrovnik (ii).

93. 1845 August 16. Dalmatia. Dubrovnik, Gruz (iii).

94. 1851 February 28. Asia Minor. Fetiye (iii) (H = 2').

95. 1851 April 3. Asia Minor. Fetiye (iii) (H = 6').

96. 1851 May 23. Khalki Isle, Rhodes (ii).

97. 1851 October 12. Albanian coasts, Valona (H = 2') (iii).

98. 1852 May 12. Asia Minor, Smyrna (iii).

99. 1852 September 8. Asia Minor. Smyrna (iii).

100. 1853 August 18. Euboean Gulf (iii+).
($38\frac{1}{4}$ N - $23\frac{1}{2}$ E, I = IX, M = ?, d = n).

101. 1855 February 13. Asia Minor, Fetiye (iii).

TABLE: 2.2
(continued)

102. 1856 November 13. Eastern Sporades. Chios (iii+).
($38\frac{1}{4}$ N - $26\frac{1}{4}$ E, I = IX, M = ?, d = n).

103. 1859* October 20. Piraeus (ii-). Most probably a strong seiche.

104. 1861 December 26. Gulf of Corinth. Northeast coasts (H = 7') (iv-) South coasts (iii). ($38\frac{1}{4}$ N - $22\frac{1}{4}$ E, I = XI, M=?, d=n).

105. 1866 January 2. Albanian coasts. Valona, Himara (iv).

106. 1866 January 6. Albanian coasts. Valona, Narta (iii).

107. 1866 February 2. Eastern Sporades. Chios (iii).

108. 1866 February 6. South coasts of Peloponnesus. Island of Kythera (H = 26') (iv).

109. 1866 March 3. Albanian coasts. Valona (iii).

110. 1866 March 6. Albanian coasts. Himara, Kanina (iv).

111. 1866 March 13. Albanian coasts. Himara, Kanina (iii).

112. 1867 September 20. South coasts of Peloponnesus, Gythion (iv), Crete, Herakleion (iv), Ionian Islands, Syros (iii), Southeast coasts of Italy (ii+). ($36\frac{1}{2}$ N-$22\frac{1}{4}$ E, I=IX, M=?, d=n).

113. 1869 December 28. Albanian coasts. Valona (iii).
($38\frac{3}{4}$ N - $20\frac{3}{4}$ E, I = XI, M = ?, d = n). 210 (nr.1883).

114. 1870 June 24. Alexandria (iii).

115. 1870 July 29. Adriatic Sea. Island of Vis (Lissa) (iii).

116. 1878 April 19. Sea of Marmara, Izmid (iii).

TABLE: 2.2
(continued)

117. 1883 June 27. Ionian Islands. Corfu (iii).
($39\frac{1}{2}$ N - 20 E, I = VI, M = ?, d = n).

118. 1886 August 27. South coasts of Peloponnesus. Messenia, Pylos (iii); Asia Minor, Smyrna (ii).
(37 N - $21\frac{1}{4}$ E, I = XI, M = ?, d = i).

119. 1887 October 4. Gulf of Corinth. South coasts, Xylokastro (iii), between Xylokastro and Sykia (L=65'). ($38\frac{1}{4}$N-$22\frac{3}{4}$E, I = VIII, M = ?, d = n).

120. 1893 February 9. Sporades Islands. North coast of Samothrace. (H = 3') (iii+), Alexandroupolis (H = 3', L = 130') Thracian coasts (iii). ($40\frac{1}{2}$N - $25\frac{1}{2}$E, I = IX, M = ?, d = n).

121. 1893 June 14. Albanian coasts. Valona, Himara (iii).

122. 1894 April 27. Euboean Gulf. Atalanta Bay (H = 10') (iv), West and Northwest coasts of Euboean Gulf (iii).
(38.7 N - 23.1 E, I = XI, M = ?, d = n).

123. 1894 July 10. Constantinople (iii).

124. 1898 December 3. Ionian Islands.Zante (ii+).
($37\frac{3}{4}$ N - 21 E, I = VII, M = ?, d = n).

125. 1899 January 22. Messenia, Kyparissia, Marathos (iii).
($37\frac{1}{4}$ N - $21\frac{3}{4}$ E, I = IX, M = ?, d = n).

126. 1902 July 5. Salonika (ii-). ($40\frac{3}{4}$N - $23\frac{1}{4}$E, I=IX, M=?, d=n).

127. 1908 December 28. Lybian Sea. 90 Miles north of Alexandria (v), Egyptian coasts (ii).

128. 1914 November 27. Ionian Islands. Leukas (H = 11') (iv+).
($38\frac{3}{4}$ N - $20\frac{1}{2}$ E, I = X, M = $6\frac{1}{4}$, d = n).

TABLE: 2.2
(continued)

129. 1915 August 7. Ionian Islands. Between Cephalonia and Leukas (iii+). ($38\frac{1}{2}$ N - $20\frac{1}{2}$ E, I = IX, M = $6\frac{1}{4}$, d = n).

130. 1920 December 18. Albanian coasts. Valona (iv), Saseno (v-).

131. 1928 March 31. Asia Minor. Smyrna (ii).

132. 1928 April 23-25. Grecian Archipelago; Piraeus, Chalkis, Nauplion, Alexandroupolis (H = 2') (ii); Crete, Chania, Karystos (H = 3') (ii+); Crete (H = 7') (iii+).

133. 1928 May 3. Eastern Greece. Strymonic Gulf (ii). 71.

134. 1932 September 26. Gulf of Hierissos. Chalcidice (ii+). ($40\frac{1}{2}$ N - $23\frac{3}{4}$ E, I = X, M = 6.9, d = n).

135. 1947 October 6. South Peloponnesus. Methone in Messenia (ii+). (36.9 N - 22 E, I = IX, M = 7, d = 28) 105, 113.

136. 1948 February 9. Dodecanese. Island of Karpathos (L = 3000') (iv). ($35\frac{1}{2}$ N - 27 E, I = IX, M = 7.1, d = 40).

137. 1948 April 22. Ionian Islands. Leukas (H = 3') (iv-). ($38\frac{1}{2}$ N - $20\frac{1}{4}$ E, I = X, M = 6.4, d = n).

138. 1956 July 9. Grecian Archipelago. Amorgos (H = 100'), Astipalaea (H = 67'), Pholegandros (H = 33'), Patmos (H=13'), Kalimnos (H = 12'), Crete (H = 10'), Tinos (H = 9').(v to iii). (36.9 N - 26 E, I = IX, M = 7.8, d = 20?).

139. 1956 November 2. Magnessia. Volos (H = 4') (ii+) ($39\frac{1}{2}$ N - 23 E, I = VII, M= $5\frac{3}{4}$, d = n).

140. 1959* February 23. North and west coasts of the Grecian Archipelago. Salonika (H = 3'), Salamis (H=1) Leros (H=1), Crete (H=2'). No earthquake shook was recorded. Most probably a seiche.

141. 1961* June 6. Grecian Archipelago. Crete (H=3'), Volos(H=1'), Leros (H = 1'). Probably strong seiche.

MODIFIED SIEBERG SEISMIC SEA-WAVE INTENSITY SCALE
(AFTER AMBRASEYS, 1962)

i. Very light. Wave so weak as to be perceptible only on tide-gauge records.

ii. Light. Wave noticed by those living along the shore and familiar with the sea. On very flat shores generally noticed.

iii. Rather strong. Generally noticed. Flooding of gently sloping coasts. Light sailing vessels carried away on shore. Slight damage to light structures situated near the coast. In estuaries reversal of the river flow for some distance upstream.

iv. Strong. Flooding of the shore to some depth. Light scouring on man-made ground. Embankments and dikes damaged. Light structures near the coast damaged. Solid structures on the coast injured. Big sailing vessels and small ships drifted inland or carried out to sea. Coasts littered with floating debris.

v. Very strong. General flooding of the shore to some depth. Quay-walls and solid structures near the sea damaged. Light structures destroyed. Severe scouring of cultivated land and littering of the coast with floating items and sea animals. With the exception of big ships all other type of vessels carried inland or out to sea. Big bores in estuary rivers. Harbour works damaged. People drowned. Wave accompanied by strong roar.

vi. Disastrous. Partial or complete destruction of man-made structures for some distance from the shore. Flooding of coasts to great depths. Big ships severely damaged. Trees uprooted or broken. Many casualties.

TABLE 2.3a. Magnitude M v.s. Return Period T in Regions 26b and 26c. Numbers in parantheses refer to periods extrapolated from the largest observed value.

M	5.0	5.5	6.0	6.5	7.0	7.5	8.0
T (Region 26b)	1.92	4.35	16.66	111.11	(1333)	-	-
T (Region 26c)	1.49	2.15	3.77	8.33	22.22	(76.92)	(357.14)

TABLE 2.3b. Calculated and Observed Magnitudes and Return Periods in Regions 26b and 26c.

Region	26b	26c
$\hat{M}$ (calculated)	6.5	7.6
$\hat{M}$ (observed)	6.4	7.1
$\hat{T}$ (observed)	111	29

TABLE 3.1. F.D.M. DATA

RUN		R.1	R.2	R.3	R.4	R.5	R.6	R.7	R.8	R.9	R.10
Magnitude		8.0	6.75	7.0	7.0	7.0	7.5	7.5	7.0	7.0	7.0
Fault Length, L (km)		350.0	40.0	55.0	55.0	55.0	120.0	120.0	55.0	55.0	55.0
Max.Ground Disp. (m)		8.0	1.2	2.0	2.0	2.0	4.0	4.0	2.0	2.0	2.0
Duration (sec)		10.0	5.0	5.0	5.0	5.0	5.0	5.0	5.0	5.0	5.0
Equv. Diam. D (km)		229.0	47.3	63.1	63.1	63.1	105.0	105.0	63.1		63.1
Source Area (km^2)		41218.4	1758.3	3126.7	3126.7	3126.7	8812.4	8812.4	3126.7	4690.0	3126.7
Equiv.Width, b (km)		117.8	44.0	55.0	55.0	55.0	73.43	73.43	55.0	85.3	55.0
Exp. Const., B		0.102	0.272	0.217	0.217	0.217	0.163	0.163	0.217	0.141	0.217
1/2 Time Step, Δt (sec)		100.0	100.0	100.0	100.0	100.0	200.0	200.0	200.0	100.0	200.0
Coordinates of Main Fault.	Start	36°15'N 29°05'E	34°25'N 32°15'E	36°35'N 31°05'E	35°30'N 33°45'E	36°00'N 35°25'E	35°05'N 34°25'E	35°15'N 31°50'E	35°47'N 33°45'E	36°35'N 31°05'E	35°47'N 33°45'E
	Corner	34°30'N 26°55'E									
	End	34°30'N 25°55'E	34°25'N 31°55'E	36°30'N 31°05'E	35°30'N 33°10'E	36°32'N 35°25'E	35°40'N 35°25'E	36°15'N 31°14'E	35°47'N 33°10'E	36°30'N 31°05'E	35°37'N 33°10'E
Description		Normal	Normal	Normal	Normal	Normal	Normal	Normal	Normal	Area Run	Fric.Run

TABLE 7.1

Design Storm Surge and Storm Wave Setup

TYPE	Ret. Per. (yrs)	Wind speed (m/s)	St. Surge (m)	H_s (m)	H_{max} (m)	Wave Setup (m)	T_s (sec)
Design Wind (DW)	10^2	25	0.04	6	8	1.2	10
Design Basis Extreme Wind (DBEW)	10^4	35	0.06	12	14	2.3	13
Extreme gusts	-	50	0.25	14†	18†	3.7†	15†

† - a duration of 6 hrs is used in these calculations.

TABLE 7.2.

Design Events

Prob.of Occurrence	Storm Surge + Wave Setup + Tide(m)	Tsunami + Tide (m)	Tsunami + Tide + Storm Surge + Storm Wave Setup (m)
10^{-2}	1.9	-	-
10^{-4}	3.1	3.9	-
10^{-8}	-	-	7.0

APPENDIX - A

EARTHQUAKE DATA

TABLE I-A

CATALOGUE OF SHOCKS AND TSUNAMIGENIC EVENTS IN THE EASTERN MEDITERRANEAN

(1800 - 1900)

1802, ?,	($34^{o}N, 36\frac{1}{4}^{o}E$), R.37, I_o V II? At Bikaa, Baalbek and in several localities in Lebanon, moderate damage (SAM, PK), not in (KAD, SNP).
1804, June 8,	03^h, $38\frac{1}{4}^{o}N$, $21\frac{3}{4}^{o}E$, h-n, R.26a, I-IX, three shocks (GG,CAM), I-VIII-IX (GGK,GG), I_o-X-XI (MF), I_o-VIII(MJD). Almost complete destruction of Patrai, causualties many houses overthrown, violent in (Zante) Zakinthos and in Monrea (GG, MMC), destructive tsunami (ANS).
1805, July 3,	At sunrise, $36^{o}N$, $24^{o}E$, R.26b, I_o-VII, h-i, r-810 km (GG, MMC,SAM), I_o-VII(MJD), I_o-IX (MF). Crete, "the towns of Khania (Chania) and Rethimmon suffered most damage" (MMC), felt in Sicily and at Napolu (BI).
Between 1810-1815	($35^{o}N$, $24\frac{1}{4}^{o}E$, R.26b, I_o-VIII?) a strong shock destroyed allegedly the monastery Asomatos (GG).
1810, Febr.16,	$35\frac{1}{2}^{o}N$, $25^{o}E$, R.26b, I_o - IX, h-i, r-110 km (GG), I_oXI-XII(MF), I_o-X(CAM). The town Iraklion was ruined and 2000 persons perished (MMC, SAM, PAP), many houses collapsed ($\frac{1}{3}$), 200 victims, large shaken area (GGK,GG,PAP, MMC,ANC,MJD), felt strongly in Malta, at Napoli and in N.Africa (PAP), slightly in Cyprus (ANC).
1815,Dec.,?,	$35^{o}N$, $25\frac{3}{4}^{o}E$, R.26b, I_o-IX, h-n; not mentioned in (PAP). S. and E.Crete shaken, a greater part of Ierapetra destroyed, solid houses in Itea also destroyed as well as the monastery Acrotiriani (GG,SAM), serious damage at Toplu (GGK).

TABLE I-A
(continued)

1817, Aug.23,	08^hUT, $38\frac{1}{4}^o$E, R.26a, I_o-IX-X, h-n, I_o-IX (GG), I_o-IX-XI (GGK), I_o.X-XI (MF). A complete destruction of Aiyion (Aigion), subsidence of terraian (GG), the town of Vostitsa was destroyed, strongly felt at Pasrai, weakly at Korinthes (Korint), tsunami swept the downtown section of Aiyion and the Cape Aliki (ANS), many violent shocks during the following 8 days (GG,MMC, PAP),
1821, Jan.6,	18^h45^m, $37\frac{3}{4}^o$N, $21\frac{1}{4}^o$E, R.26a, I_o-IX-X, h-n, I_o-X (GG), I_o-VIII-X (GGK). Much damage was done in the villages around the town of Zatkinthos, the town of Sala in Morea was almost entirely destroyed by these shocks and those of December, numbers of people perished beneath the ruins (MC,MMC, PAP, MCA), destructive tsunami at Patrai (GGK, ANS).
1822, Aug.13,	20^h, 36^oN, 36^oE (PK), I_o-XI (SAM, SNP), I_o-X-XI (ONB), isos, map in (SAM), p.35. Destructive earthquake, particularly at Antakya (Antiochia) and Halab (Aleppo) two thirds of the town destroyed, thousands of inhabitants perished, less damage at Djesr and Ladhiqiya (Latakia) tsunami at Beirut, Jerusalem, Iskenderun and in Cyprus (ANC,MMC, KAD, SNP, PAP, ONB, CAM).
1822, Sept.5,	36^oN, 36^oE, R.35, I_o-X?, I_o-X-XI (ONB). Another dissatrous shock at Halab (Aleppo) which destroyed what had resisted the former one, more than 20,000 persons are said to have lost their lives (MMC, CA,).
1831, April. 3,	37^oN, 27^oE, R.26c, h-n, I_o-VII? (GG), I_o-V-VII (GGK). A sequence of strong shocks in the Samos island caused a rockfall which killed 7 persons (MMC, GGK).

TABLE I-A
(continued)

1834 May, 23,	06^h, 31^oN, $35\frac{1}{2}^oE$, R.37, I_o-IX, I_o-X (SNP), I_o-VII (MJD), isos, map in (SMP). At Jerusalem several churches, the city wall, many houses and cisterns seriously damaged, a minaret collapsed, at Bethlehem much damage to monasteries, many people killed, at Deir Mar Saba a tower cracked, large blocks of asphalt floated on the Dead Sea (KAD, MMC). The epicenter was in the district of Lisan, the pleistoseismal area extended from south of the Dead Sea to Kerak, Jenin, Amman and the Judean Hills. Causalties, houses ruined in Nablus, damaged houses at Karak, serious damage at Gasa, some damage at Jerusalem and Bethlehem, some faulting in the Lebanon and in Baqa (Baka) (SNP).
1837, Jan.1,	03^h, 33^oN, $35\frac{1}{2}^oE$, R.37, I_o-X (PK, CAM), I_o-XI (SAM, KAD, SNP), I_o-IX, isos, map (ANS, PK). Destructive earthquake with epicenter near Safad where all houses on steep slopes fell, fissures in the ground, 5000 victims, destructive effects (IX-X) at El Jish, Er Reina, Ein Zeitun, Tiberias (city walls overthrown, the lake swept the shores (700 victims), Sejera IX?, Siden VIII-IX, Sur VIII-IX Hunin VIII?, Quaditta and Lubya severe, Nazareth VI-VII, Nabumsstrong, Kafr, Kanna V, Tsippori, Jerusalem, Bethlehem. Hebron moderate, many casaulties (KAD). Devastation from Beirut (Beyrouth) to Safad, deep fissures in solid rock, new hot springs (PAP, MMC). Epicenter probably in Tiberias depression. Beirut not particularly heavy, Nazareth great cracks in houses, Jericho slight, Tiberias city ruined, Esh Sham (Damascus) city affected, Hauran and Gaulan considerable (SNP). Strong tsunami along Syrian-Israeli coasts of Tiberias (ANS).

TABLE I - A
(continued)

1837, March 20,	08^{o}UT, $37\frac{1}{2}^{o}$N, $23\frac{1}{2}^{o}$E, R.26a, h-n, I_o VII-VIII, I_o-VII (GG), I_o-VI-VII (GGK), I_o-VIII (MJD), I_oIX(CAM), I_o-IX-X (MF), r-210 km (GG). In the island of Idhra (Ydra) some houses were thrown down and others were injured, damage in the islands of Paros, Syros, Spetai and Thira (Santorin) felt also in the interior of Greece at Kalamai (Kalamata) and Messini (PAP, MMC, GGM), in Athinai blocks of marble fell down (GGK).
1838, Date?,	Jaffa, (Tel-Aviv), great destruction, probably identical with Jan.1, 1837 (KAD,PK).
1840, Oct. 30,	38^{o}N, 21^{o}E, h-n, P.26a, I - IX-X(MJD), I_o-IX(GG), I^{o}-X (MP, CAM), I_o-VII - X (GGK). "This shock was the most destructive of ever felt in Zakinthos (Zante)", one village was ruined, the buildings with foundations on limestone escaped well, the island of the Trente-Nova (?) sank into the sea (MMC, PAP), felt in Ipiros (Epeiros) (MCA), alltogether 1271 houses collapsed (35 at Zante), 12 persons perished, most destruction at Skulikadon and Agios Demetrios (St.Dimitros) (GGK).
1843, Oct.18,	$36\frac{1}{4}^{o}$N, $27\frac{1}{4}^{o}$E, R.26c, h-n, I_o-IX? (GG), I_o-VII-IX (GGK), 36^{o}N, 28^{o}E, I_o-X-XI (ONB). Earthquake in Rodhos (Rhodes) most violent in the island of Khalki, houses thrown down, rockslide, casualties (SAM, SAE, PAP).

TABLE I - A
(continued)

1846, March, 28,	15^h, 36^oN, 25^oE, h-i, R.26b, I_o-VII-VIII (GGK,MJD), I_o-VII, r-1100 km (GG), I_o-IX-X (MF). Considerable damage in Kriti (Crete), 100 houses at Iraklion (Heraklion) heavily injured, at Khania 20 houses injured, severe in Maita and Gizo, felt in S.Sporades, in Rhodes, in Syria, at Iskandariya (Alexandria) and Al Quahira (Cairo), in the direction to the west over Greece, Zakininus (Zante), Sicily, Leece and Napoli (SAM, BI, SF).
1846, June, 10,	36^oN, 22^oE, h-n, F.26a, I_o-X, r-417 km (GG). I_o-XI (MF), I_o-X (CAM), isos, map in (GGK).
1851, Febr.28,	15^h, $36\frac{1}{4}^oE$, R.26c, I_o-IX (GG), I_o-VIII - IX (GGK), I_o-IX-X (MJD), I_o-X (CAM), I_o-VI (EGU). Destructive shock in Rodhos (Rhodes), Makri and Kayı (Levisi) in Asia Minor sufferedl largly, earthslides in Bubadağ destroyed 14 villages (GG, SAM, LC, SF), tsunami at Fethiye much higher on April 3 (ANS) according to (LC) destructive aftershocks on March 5 (Makri) April 3 (Makri), April 4 (Rodhos).
1852, May 12, Sept. 8,	Rather strong tsunamis at Smyrna (ANS).
1852, Oct. 19,	03^h25^m, (36^o6^oN, 29.1^oE), R.26, I_o-VII? M-5.5 (ONB). Fethiye, at Çeşme a "terrible" shock (PL, PAT).
1855, March 2,	38.8^oN, 27.2^oE, R.26c, I_o-VII? (ONB), I_o-IX (CAM). Felt at Izmir (Smyrna), the village Macri (Makri?) sank by 105 feet (PAT).

TABLE I - A
(continued)

1856, Oct.12,	00^h45^m, $35\frac{1}{2}^oN$, 26^oE, h-i, R.26c, I_o-X-XI, (GGK), I_o-XI, r-1450 km (GG, MF, SAM), I_o-X (CAM), I_o-IX-X (PK, MJD), isoeismal maps in (SAM) p.46.91. A earthquake catastrophe in Krimi (Crete), at Iriklion (Heraklion), only 18 houses from the total of 3620 houses remained inhabitable, 538 victims, Sitia almost completely destroyed, heavy damage at Ierapari (Hierapetra) and Gulf of Meracellou (Mirabello), at Khania, in Karpathos all houses damaged, in Rhodes 8 villages heavily injured, elevation of the coast, casulaties, tsunami, slight damage observed in Thira (Santorin), Makri, Gpzp, Kiren. Cyprus, S.S ria, N.Palastia, delta of the Nile, very large shaken area extending up to Palermo, Napoli, Ancona, Zara, Athinia, Bursa? (SAM, PAP, BI), disaster at Ioannina (Janinna) (a relais shock?) (MCA).
1861, Dec.26,	16^h49^mUT, $38\frac{1}{4}^oN$, $22\frac{1}{4}^oE$, R.26, h-n, I_o-X-XI (GGK), I_o-XI (GG, MF), I_o- IX (CAM), I_o-VIII (MJD), M-$7\frac{1}{2}$ (GGE), isos map in (SAM). An earthquake catastrophe in Akjala, the plain between Aiyion (Aigion, Aeghion) and Korinthos devastated, the highest damage at Valymitika and Trypia, Aiyion ruined, Kalamaki injured, at Korinthos many houses injured (PAT), 15 km^2 large lump along the coast of Akhaia, 13 km long crack, tsunami waves 2 m high in the Gulf of Korinthos (ANS), fissures, sand craters, Casualties (CG, GGE, LC).
1862, May.24,	36.8^oN, 28.3^oE, R.26c, I_{max}-VII? (ONE, MJD), epic.in the sea? Rodhos (Rhodes), some old walls ruined, felt at Marmaris and other localities along the Anatolian coast, in the islands Nisiron and Khalki (PAT).

TABLE I - A
(continued)

1862, June 21,	$36\frac{1}{2}^{o}$N, 25^{o}E, h-i, R.26b, I_{max}-VII-VIII (GGK), I_{max}-VIII, r-390 km, (MGG), M-6.8 (GGF), I_{max}-IX (MF), epi. in the sea. Damage in Milos, Antimelos, Sifnus, Folegaziros and Thira (Santorin), felt in Ieioponnisos, Zakinthos (Zante) and Kriti (Crete), allegedly felt also in Malta (LAM), fissures in the houses (LC).
1863, April 22,	$20^{h}30^{m}$, $36\frac{1}{2}^{o}$N, 3.2^{o}W, R.26c, h-i, I_o-IX-XI (GGK), I_o-XI, r-1380 km (GG), M-8.5 (GGF), 36.3^{o}N, 28.0 E, I_o-IX, M-6.7, H-$10^{h}20^{m}$ (ONB), I_o IX-X5MJD), I_o-X (CAM). An earthquake catastrophe, thirteen villages in the Rodhos (Rhodes) were destroyed (Trianda, Bastida, Maritsa, Demetria, Salakos, Dimilia, Lardos, Katavia, Laerma, Pilona, Lachania, Istridos, Monotilos, Massari), casulties, other villages were partly destroyed, in tital 2050 houses were thrown down, strongly felt at Izmir (Smyrna), felt at Aydın, Nazilli, Beirut (Beyrouth), Gelibolu (Gallipopi) Iraklion (Candia), Suez, Mersine, Cairo V, Jerusalem, Malta, Tripopi(?), several houses in the island Kos destroyed some others and the cathedral seriously injured, some houses destroyed in Makri, Marmara and Khalkı, no damage in the island Symi (PAP, SAM).
1864, Jan.10-11,	Rodhos (Rhodes) IX (CAM), Makri VIII (MJD), epicenter? R.26c, not mentioned by (ONB, GG, PAT), questionable.
1864, Oct. 2,	36.1^{o}N 29.5^{o}E, R.26c, I_o-?, I_o-VII, M-6.1 (ONB,EGU). Cracks in the island of Meis, felt at Fethiye (PL).

TABLE I - A
(continued)

1866, Jan. 31,	36.4°N, 25.3°E, h-n?, F.26b, I_{max}-VII, r-230 km (GG), I_o-IX (MF), volcanic, M-6.1 (GCE). A heavy shock in Thira (Santorin) followed on Febr. 1, by an eruption of the volcano Thira (GG, PAT). 50 houses and two churches were damaged at Nea Kaimeni, the continuing subsidence (without shocks) splitted the houses (SAM).
1866, Febr.6,	13^h45^m, 36°N, 24°E, h-n, F.26a, I_{max}-VIII (GG), I_o-VII - IX (GGK), M-$6\frac{1}{4}$ (GGE). At Patrai two houses collapsed and some others injured, at Tripolis houses fissured, felt in the country as far as Argos (but not felt there) and Kithira (PAT). 8 m high tsunami at Avlemon (ANS), epicenter probably in Kithira (GGK).
1867, Sept.20,	03^h15^m, $36\frac{1}{2}$°N, $22\frac{1}{4}$°E, h-i, F.26a, I_{max}-VIII - X (GGK), I_o-VIII (MJD), I_{max} -IX, r-700 km (GG, CAM), I_{max}-X (MF), 36°N, 23°E, (SAM, LC), A dissastrous shock in the province of Mani, Laconia, tsunami along the south coast of Peloponnisos (ANS), felt in Kerkira (Corfu), Zakinthos, at Fillatra, Avia, Kalamai (Calamata), Navplijpn (severe), Khalki, Patrai (slight), Tripolis, Athinai (slight), Sparti, Kithira (Cerigo) Khania (Canea). Gythion destroyed by tsunami. Damage at Oesylos, at Kythnos tiles fell from roofs, Areopolis suffered much, violent shaking at the cape Drosos where houses collapsed and some persons perished, at Izetzino thirty houses thrown down, at Petrina walls of a church fissured, the belfy of the monastory of Zarbitza fell, new springs originated, felt also in Sicily, Kriti, Malta, tsunami observed at Catania (PAT, FC, GGT, LC), felt at Brindisi (MCA). (FC) gives a damaging foreshock on Sept.19, 17-18^h with a very large shaken area.

TAPLE I - A
(continued)

1868, May 3, $36\frac{3}{4}^{o}$N, 27^{o}E, h-n, R.26c, I_o-VII (GG), I_o-VI-VII (GGK), A heavy shock in the Samos, heavily felt at Pagondhas, (Pagonda) where 100 houses were, damaged, some poor ones collapsed (GGK), I_o-VI-VIII, I_o-VII (MJD).

1869, April 18, 04^h, $36\frac{1}{2}^{o}$N, $27\frac{1}{2}^{o}$E, h-i, R.26c, I_o-VIII (GG, MJD), I_o-VII-X (GGK), r-400 km (GG), 05^h45^m, 36.3^{o}N, 28.0^{o}E, I_o VIII (ONB), I_o-X M-6.9 (GGE). A disastrous shock in the island Syme, 75 houses thrown down, most of the houses seriously damaged, all houses damaged, several victims, rockslides, the villages in the islands Niseros, Radhos and Kalimnos suffered also much, felt over Sporades and on the coast at Izmir and Bursa (SAM, PAT, FC), a strong aftershock on April 22 (SAM, GG).

1869, Dec.1, 18^h, 36.8^{o}N, 28.3^{o}E, h-n, R.26c, I_o-VIII, r-220 km, M-6.1 (ONB, EGU), 37^{o}N, 28^{o}E, I_o-X (GG, CAM), I_o-IX, X (GGK, MJD), M-$7\frac{1}{2}$ (GGE). A damaging shock with the focus near Mentece (Menteche), changes in springs, Izmir was violently shaken, the small town Ula completely destroyed, at Marmaris cracks in the ground and walls fissured, felt also in Rhodes and Makri (FC, PAF), Bodrum, Simi, Mitilimi (LC), smaller damage at Ula and Mugla (GGK).

1870, Febr. 22, (36.6^{o}N, 29.1^{o}E), R.26c, I_{max} IV III?, I_o-VII, M-5.1(ONB), I_o-IX (CAM), At Fethiye strong, uplift of the shoreline (PL), at Makri several houses collapsed, felt in Rhodos, at Amfissa and in the Gulf of Korinthos (SAM, FC, GGK).

1871, Jan.22, 36^{o}N, 24^{o}E, R.26b, I_o-?, I_o-VII - VIII (GGK), M-6.4 (GGE). A sequence of shocks in Milos, the strongest effects (no damage) observed in Pyinnos, Kimolos and Serifos, near Kastro the ground fissured (GGK).

TABLE I - A
(continued)

1871, June 7,	36.8°N, 23.3°', R.26c, I_o-VII, M-5.5 (ONB, EGU), M-$6\frac{1}{4}$ (GGE). A damaging shock in the Sporades, little damage also at Marmaris (SAM, PAT, FC, GGK, LC), epicenter in the Sporades, felt over the nearby coast of Anatolia (PL).
1872, Apr.2,	07^h45^m, 36.2°N, 36.1°E, R.35, I_o-X, M-7.3 (ONB, PL, EGU), Apr.3 (CAM, PL, MJD). A disastrous earthquake at Antakya (Antiochia) one third of which was totally ruined, 500-1800 victims, the other houses were seriously damaged except the 150 wooden ones, also one half of the town Samandag (Süveydiye) destroyed Altınözü was damaged, damage at Fatikli, felt at Haleb (Aleppo) Beirut, Esh Sham (Damascus), Diyarbakır, Iskenderun (Alexandretta) and Tripolis (FC, LC, İK), Tel-Aviv-Jaffa? (KAD). Aftershock of the same intencity I-X? on April 10 (ONB),, (FC), gives only "an earthquake at Antiochia". Another aftershock with I_o-VII in the night on May 15 (ONB).
1873, Jan.31,	23^h15^m, $37\frac{3}{4}$°N, 27°E, h-n, R.26c, I_o-VIII - IX (GGK), I_o-IX, r-320 km (GG, CAM), M-6.6 (GGE), 38.4°N, 27.2°E, I_o-VII (ONB), I_o-VIII (MJD). A very severe shock in Samos, particularly its eastern part suffered very much, at Wathy and Chora many houses became uninhabitable, felt in the Mikale peninsula and at Izmir, Afyonkarahisar (SAM, FC), Thessaloniki, (LC), a strong aftershock on Febr. 29 (GG).
1874, June, 28,	37.8°N, 26.8°E, R.26c, I_o-VII (EGU).

TABLE I - A
(continued)

1874, Nov.16,	36^{O}N, 28^{O}E, r.26c, I_{o}-VII - IX? (GGK). M-7.35.5 (GGE). A heavy shock in Rodhos, felt as far as Istanbul (GGK), this report might correspond to Nov. 18.
1875, July 7,	$37\frac{3}{4}^{O}$N, 27^{O}E, h-n, R.26c, I_{o}-VII-IX? (GGK), I_{o}-IX M-$6\frac{3}{4}$ (GGE). An earthquake destroyed 150 houses in Samos (SAM, LC).
1865, Aug.21,	36.2^{O}N, 36.3^{O}E, R.35, I_{o}-VII?, M-5.5 (ONE, Not mentioned in (FC, PK, EGU).
1887, July 17,	$07^{h}45^{m}$, 36.1^{O}N, 26^{O}E, h-i, R.26b, I_{max}-VII (GGC,MJD), I_{max}-VI-VII (GGC), I_{max}-VI (GG), P-250,000 km^{2}, M-7.7 (GGE). Houses fissured at Iraklion and in Rodhos, largly at El Iskandariya (Alexandria), Izmir, Khios, Mikonos, Neapolis, Zakinthos, Kalamai, Tripolis, Mesolongion, Methana, Patrai (GGC), felt in Sicily (BI).
1891, May 11,	18^{h} $37\frac{1}{2}^{O}$E, h-n, R.26a, I_{o}-VII?, I_{o}-VI, r-250 km, swarm (GG), I_{o}-V-VI (GGK), I_{o}X (CAM) M-6.1 (GGE). Many houses, especially the old ones, were fissured at Kythnos during the strongest shock of a swarm, felt at Syra, Tinos, Andros, Khios, Çeşme, Athinai, Aiyion (GGC).
1892, Dec.27,	$18^{h}30^{m}$, $37\frac{3}{4}^{O}$N, 26^{O}E, h-n, R.26c, I_{o}-VII (GG), I_{o} VI-VII (GGK), M-$5\frac{1}{2}$ (GGE). A swarm in Samos (GG), several poor houses collapsed in the eastern part of Samos (GGK).
1896, June 26,	36.9^{O}N, 28.1^{O}E, R.26c, I_{o}-VII? Marmaris, Kerme Bay (EGU).

TABLE I - A
(continued)

1896, Oct. 27,	$36\frac{1}{2}^{o}$N, 28^{o}E, h-n, R.26c, I_o-VII - VIII (GGK), I_o-VI (EGU), I_o-VIII, r-240 km (GG), M-6.2 (GGE). Partly destructive effects in Rodhos; Bodrum and Marmaris in Asia Minor were slightly damaged, strongly felt at Kenydieghiz, Mugla and Elmali, slight at Aydın and Izmir (SAM).
1898, Dec.3,	$05^{h}50^{m}$, $37\frac{3}{4}^{o}$N, 21^{o}E, h-n, R.26a, I_o-VII - VIII, I_o-VII, r-90 km (GG), I_o-VI-VII (GGK). At Zakinthos some poor houses and a part of the theater collapsed, small fissures at Amilias (GGK), rock-slides also in the island Voidi, changes in wells, tsunami (GG), light tsunami (ANS).
1899, Jan.22,	$07^{h}49^{m}$, $37\frac{1}{4}^{o}$N, $21\frac{3}{4}$ E, h-n, R.26a, I_o-VIII - IX (GGK), I_o - IX, r_5-100 km, r-200 km (GG), M-6.7 (GGE), I_o - X (CAM, MJD, MD), isos, map in (MCA). Serious damage at Kyparissia and surroundings, main shock, casualties (GG), Gjirokaster IV (MD), serious damage also in Messinia, in total 245 houses destroyed, more than 275 houses uninhabitable, more details in (GCM), tsunami at Messini, Kyparrissia, Marathos (ANS).

REFERENCES TO THE CATALOGUE OF SHOCKS

Note: Capital letter abreviations written in paranthesis for each event indicates the source of the information. A list of these sources arranged according to alphabetical order can be seen below. Definatio of symbols used in this table can be found in V.Karnik (1971).

ANC N.N, Ambraseys: The seismic history of Cyprus. Revue de l'Union Int.de Secours, Mars 1965, No.3, 25-48.

ANS N.N. Ambraseys: Data for the investigations of the seismic sea-waves in the Eastern Mediterranean. Bull.Seism.Soc.Am.52, (1962), 895-913.

BI M.Baratta: I terremoti d'Italia. Torino 1901, 950 pp.

CAM A. Cavasino: Note sur catalogo dei terremiti destruttui dal 1501 al 1929 nel bacino del Mediterraneo, 29-36.
A. Cavasino: Catalogo dei terremoti avertiti nel bacino del Mediterraneo del 1501 al 1929, 37-60.
R.Ac.Nat.del Lincei, Publ.della Com.It,perlo studio delle grand calamita, Vol.II, Mem.Sc.e Techn., Roma 1931.

EGU K.Ergin, U.Güçlü, Z.Uz: Catalog of earthquakes for Turkey and surrounding area, Tech.Univ.Istanbul, 1967.

FC C.W.C.Fuchs: Statistik der Erdbeben von 1895-1885. Sitzungsber-unte d.M.Mathem.naturw.Ges.,XC II.Bd.I,Abt.215-625, Wien 1886.

GG A.G.Galanopoulos: A catalogue of shocks with I_o - VI or M-i for the years 1801-1958. Seism.Lab., Athens Univ., Athens 1960,119 pp

GGE A.G.Galanopoulos: Evidence for the seat of the strait-producing forces. Ann.di Geof. XVIII (1965), No.4, 399 - 409.

(Ref.to Catalogue of Shocks cont).

GGK A.G.Galanopoulos: Earthquake catalogue of Greece. Manuscript 1966, 181.
A.G. Galanopoulos: Die Seismizitat der Insel Chios.Gerl.Beitr. z.Geophys. 63 (1954), Heft 4,253-264).

KAD D.H. Kallner-Amiran: A riveed earthquake-catalogue of Palestine. Israel Exploration Journal, 1950-51, No.4, 223-236.

LC Lersch: Erdbeban-Chronik fur die Zeit von 2362 v. Cnorlios 1897. Manuscript, archives of the Zentralinstut für Physik der Erde, Jena.

MCA C.Morrelli: Carta seismica del Albania. Reale Academia d'Italia, Commissione Italiana de Studio per i problemi del soccorso alle poponzioni, Vol.X, Firenze 1942, 121 pp.

MF F.Montandon: Les tremblements de terre destructeurs au Europe. Geneve 1953, 195 pp.
F.Montandon: Les seismes de forte intensite en Suisse. Revue pour l'etude des calmaties, Bull.de l'union Internat. de Secours, Fasc.18-21 (1942) 20-21 (1943), 105 pp.

MJD J.Milne: Catalogue de destructive earthquakes. A.D. 7 to 1899. Partsmouth 1911, 92 pp.

MMC R.Mallet and J.W. Mallet: The earthquake catalogue of the British Association with the discussion, curves and maps etc. Trans. of the British Assoc. for the Advanc. of Sc., 1852 to 1858. London 1858, 362 pp.

(Ref.to Catalogue of Shocks cont.)

ONB N.Öcal: Kurze Liste der Erdbeben in der Türkei bis 1800 (I_o - IX). Manuscript, 1961, 2.

PAP A. Perrey: Menoire sur les tremblements de terre ressentis dans la Peninsule Turco-Hellenique et en Syrei, Presente a la séance de l'Juillet 1848. Mem.Ac.R.de Belgique, T.XXIII, 75 pp.

PAT A.Perrey: Notes sur les tramblements de terre en 1854-1871, avec suppiments pour les années anterieurs. Bulletin de l'Ac. Royale des Sciences, des Letres et des Beaux-Arts de Belgique, 1855-1872.

PK J.Plessard, B.Kogoj: Catalogue des seismes rugentis au Liban, Annate,Memiores de l'Observatoire de Ksara, Tome IV, Cather 1,12.

PL N.Pınar, E.Lahn: Türkiye depremleri izahlı kataloğu. T.C. Bayındırlık Bakanlığı, Yapı ve İmar İşleri Reisliği Yayınlarından, Seri:6, Sayı:36, Ankara 1952, 53 pp.

SAE A.Sreberg: Erdbebengeographei Handbuch der Geophysik, 1932, Brand IV, Abschnitt IV, 688-1006.

(Ref.to Catalogue of Shocks cont.)

SAM A.Sieberg: Untersuchungen über Erdbeben und Bruchschollenbau im Östl. Mittelmeergebiet. Denkschriften der med.-nature.Ges zu Jena, 18. Band, 2.Lief., Jena 1932, 161-273.

SF J.F. Schmitt: Studien der Erdbeben, Leipzig 1875, 324 pp.

SNP N.Shalem: Seismicity in Palestine and neighbouring areas (macroseismical investigation). 15 tables, manuscript, 79, 1960.

TABLE II - A

CATALOGUE OF SHOCKS IN THE EASTERN MEDITERRANEAN
AND IN THE NEAR VICINITY
OF THE TURKISH COAST
(11 A.D. - 1900)

NO	DATE	LAT(N)	LONG(E)	I	M	REF.CATALOGUE
1	110	36.2	36.0	VIII	6.37	K.E.
2	115	36.20	36.10	VI	5.18	K.E.
3	334	36.23	36.1	VI	5.18	K.E.
4	341	36.23	36.1	VI	5.18	K.E.
5	396	36.23	36.1	VI	5.18	K.E.
6	457	36.23	36.1	VI	5.18	K.E.
7	500	36.12	35.9	VI	5.18	K.E.
8	518	36.88	36.6	VI	5.18	K.E.
9	525	36.23	36.1	VI	5.18	K.E.
10	526	36.12	35.9	VI	5.18	K.E.
11	527/528	36.23	36.1	X	7.55	K.E.
12	528	36.40	29.2	VI	5.18	K.E.
13	553	36.23	36.1	VI	5.18	K.E.
14	579 and 589	36.23	36.1	VI	5.18	K.E.
15	713	36.23	36.1	VI	5.18	K.E.
16	859	36.23	36.1	VI	5.18	K.E.
17	1091	36.23	36.1	VI	5.18	K.E.
18	1481	36.30	28.0	VI	5.18	K.E.
19	1493	36.80	27.2	VII	5.77	K.E.
20	1635	36.30	28.0	VI	5.18	K.E.
21	1660	36.20	28.0	VI	5.18	K.E.
22	1726	36.23	36.1	VI	5.18	K.E.
23	1759	36.88	30.6	VI	5.18	K.E.
24	1922	36.40	36.2	VI	5.18	K.E.
25	17-10-1843	36.20	28.0	V	4.59	K.E.
26	1847	36.62	36.1	VI	5.18	K.E.
27	1849	36.60	29.4	VI	5.18	K.E.
28	28-2/3-4-1851	36.40	28.6	VI	5.18	K.E.
29	19-10-1852	36.4	28.6	VII	5.77	SAT. K.E.
30	1854	36.12	35.9	VI	5.18	K.E.

TABLE II - A
(continued)

NO	DATE	LAT(N)	LONG(E)	I	M	REF.CATALOGUE
31	1855	36.62	29.1	VI	5.18	K.E.
32	12-10-1856	36.5	27.5	VI	5.18	K.E.
33	1857	36.85	28.3	VI	5.18	K.E.
34	1858	36.88	30.6	V	4.59	K.E.
35	1859	36.2	28.0	VI	5.18	K.E.
36	1862	36.85	28.3	VI	5.18	K.E.
37	1863	36.1	29.1	VI	5.18	K.E.
38	2-10-1864	36.2	29.6	VIII	6.37	SAT. K.E.
39	1-12-1865	36.20	28.0	VI	5.18	K.E.
40	11/16-1-1866	36.2	28.0	VI	5.18	K.E.
41	22/24-9-1866	36.4	29.2	VI	5.18	K.E.
42	1-12-1869	36.8	27.9	VIII	6.37	SAT. K.E.
43	22-2-1870	36.5	28.7	VI	5.18	K.E.
44	7-6-1871	36.85	28.3	VII	5.77	SAT. K.E.
45	3-4-1872	36.2	36.2	X	7.55	SAT. K.E.
46	1873	36.12	35.9	VI	5.18	K.E.
47	21-8-1875	36.20	36.10	VII	5.77	K.E.
48	1885	36.0	28.0	V	4.59	K.E.
49	23/25-5-1891	36.5	26.0	VI	5.18	K.E.
50	1894	36.23	36.1	V	4.59	K.E.
51	26-6-1896	36.9	28.1	VI	5.77	SAT. K.E.
52	22-10-1896	36.2	28.0	VI	5.18	K.E.
53	1-1896	36.9	35.0	VI	5.18	K.E.
54	5-1897	36.7	28.6	VII	5.77	SAT. K.E.
55	6-1900	36.95	28.7	V	4.59	K.E.

LIST OF ABBREVIATIONS USED IN TABLE II.

K.E. : Türkiye ve Civarının Deprem Kataloğu, Kâzım Ergin Uğur Güçlü, Zeki Uz. İ.T.Ü. Maden Fakültesi Arz Fiziği Enstitüsü Yayınları, No:24, 1967.

SAT. : Türkiye Deprem Şiddetleri Kataloğu, S.Okamoto, A.Tabban, T.Tanuma, Deprem Araştırma Enstitüsü, Ankara, 1970.

TABLE III - A

CATALOGUE OF EARTHQUAKES FOR THE
EASTERN MEDITERRANEAN AREA
M 5
(1900 - 1974)

NO	TARİH	SAAT	ENLEM	BOYLAM	H(km)	MAG	KAYNAK	
NO	DATE	TIME Hr.Min.Sec.	LAT(N)	LONG(E)	H(km)	MAG	REF. SOURCE	REMARKS
1	3-29-1903	223000	32.2	35.4	10	5.6	4	
2	7-19-1903	180790	35.00	30.00	n	5.7	(4)	
3	5-17-1908	123054	35.00	24.00	100	6.75	1,3,4	
4	2-18-1910	050918	36.00	24.50	150	7.00	1,3,4	
5	8-21-1910	161130	34.00	27.00	170	6.50	1,3,4	xx
6	4- 4-1911	154354	36.50	25.50	140	7.00	1,3,4	
7	4-30-1911	204230	36.00	30.00	180	6.25	1,3,4	
8	9-30-1913	073348	35.00	24.00	60	6.25	1,3,4	
9	6-24-1915	061730	35.00	24.00	60	5.75	1,3,4	
10	7-27-1916	0307-	36.0	25.50	n	5.0	4	
11	3-17-1918	134505	36.0	28.0	n	5.5	2,4	
12	7- 1-1918	110200	34.5	25.0	n	5.0	4	
13	7-16-1918	200346	35.50	25.50	150	6.5	1,2,3,4	xx
14	9-23-1918	021320	36.0	28.0	n	5.1	4	
15	9-30-1918	072805	36.7	24.1	n	5.0	4	
16	7-18-1919	070120	36.00	28.00	n	5.2	2,4	
17	8-24-1919	181618	36.0	28.0	n	5.4	4	
18	10-25-1919	170959	36.47	27.01	10	5.8	2,4	
19	10-26-1919	062-	37.0	26.0	n	5.0	4	
20	4- 2-1920	153425	36.75	26.64	10	5.5	2	
21	5- 1-1920	06304	37.0	28.7	n	5.0	2,4	
22	9- 6-1920	062910	35.0	24.0	n	5.0	4	
23	11- 6-1920	092043	36.25	25.50	n	5.5	4	
24	1-25-1921	097	36.25	25.50	n	5.2	4	
25	1-27-1921	113009	36.0	28.0	n	5.4	2.4	
26	4-20-1921	160420	34.0	33.0	n	5.2	1,3,4	
27	5-22-1921	212316	37.0	28.7	n	5.2	2,4	
28	10- 4-1921	052300	34.5	25.0	n	5.2	4	
29	3- 8-1922	173345	34.5	25.0	n	5.2	4	
30	8-11-1922	081946	35.36	27.70	10	6.5	2,4	xxx
31	8-13-1922	000953	36.0	28.0	40	6.75	1,2,3,4	x,xx
32	8-17-1922	150336	36.0	28.0	-	5.0	2	
33	3-10-1923	194840	34.5	27.5	n	5.6	4	
34	6- 4-1923	203300	35.5	25.5	n	5.1	4	
35	8- 1-1923	081638	35.0	25.0	150	6.60	1,3,4	
36	12-31-1923	194842	34.5	25.0	n	5.2	4	
37	2-27-1924	202420	33.0	36.0	n	5.8	4	
38	1-27-1925	081700	33.5	27.0	n	5.2	4	
39	4- 4-1925	233436	35.5	29.0	n	5.0	4	
40	4- 5-1925	030425	36.22	29.02	100	5.7	2,4	
41	4-12-1925	192535	35.50	29.00	n	5.0	2	

TABLE III - A
(continued)

NO	TARİH	SAAT	ENLEM	BOYLAM	H(km)	MAG	KAYNAK	
NO	DATE	TIME Hr.Min.Sec.	LAT(N)	LONG(E)	H(km)	MAG	REF. SOURCE	REMARKS
42	4-16-1925	061430	35.5	29.0		5.2	2,4	
43	3- 1-1926	200142	36.8	30.0	n	5.8	4	
44	3-18-1926	140609	35.0	29.5	n	6.9	1,2,3,4	xx
45	3-21-1926	220412	35.5	29.0	n	5.0	4	
46	3-23-1926	015835	35.5	29.0	n	5.3	4	
47	3-24-1926	070430	35.5	29.0	n	5.5	4	
48	4- 1-1926	0504-	35.5	29.0	n	5.0	4	
49	4-22-1926	071154	35.99	29.23	140	5.2	2,4	xxx
50	6-26-1926	194634	36.50	27.50	100	7.9	1,2,3,4	
51	6-27-1926	021312	36.0	28.0		5.3	4	
52	7- 5-1926	092154	36.5	27.0	150	7.0	2,3,4	xx
53	3-24-1927	144635	35.0	26.0	n	5.4	4	
54	7-11-1927	130407	32.0	35.50		6.50	1,3,4	
55	3-22-1928	175055	32.1	35.5	n	5.2	4	
56	3-27-1929	074146	36.75	26.50	120	5.75	1,3,4	
57	4-17-1929	114827	35.8	25.0		5.3	4	
58	5- 1-1929	193644	34.0	28.0	n	5.2	4	
59	11-11-1929	073615	36.8	26.5	i	5.0	4	
60	1-29-1930	105350	35.0	27.5	n	5.3	4	
61	2-14-1930	183820	35.75	24.75	130	6.75	1,3,4	
62	3- 6-1930	082142	34.50	26.00	130	5.75	1,3,4	
63	3- 6-1930	091832	35.00	24.50	130	6.00	1,3,4	
64	8-22-1930	004454	35.0	27.5	n	5.0	4	
65	4-20-1930	203340	34.0	27.0	n	5.1	4	
66	5-14-1932	034454	36.00	28.50	-	5.60	1,2,3	xx
67	6-29-1932	023001	35.5	27.5	-	5.60	1,2,3,4	
68	8- 9-1932	074422	34.5	27.5	n	5.2	4	
69	10-23-1932	133635	35.25	27.50	-	5.6	2,3,4	xx
70	4-23-1933	055735	36.75	27.25	50	6.75	1,2,3,4	
71	4-28-1933	222841	35.25	27.00	-	5.60	1,3,4	
72	5-15-1933	200137	36.35	26.8	10	5.2	2	
73	3- 8-1934	025647	33.25	26.00	-	5.6	1,3,4	xx
74	11- 9-1934	137056	36.75	25.75	140	6.25	1,2,3,4	xx
75	11-21-1934	222613	34.0	26.0	-	5.60	1,3,4	
76	2-25-1935	025137	35.75	25.00	80	6.75	1,3,4	
77	3-18-1935	084041	35.50	27.00	130	6.25	1,2,3,4	xx
78	4-28-1936	231526	36.75	26.75	130	6.25	1,2,3,4	xx
79	8- 8-1936	041243	34.00	26.00	60	5.60	1,3,4	
80	1- 2-1937	140402	35.00	25.00	-	5.60	1,3,4	
81	1-16-1938	133715	36.50	28.0	200	5.25	3,4	
82	2-10-1938	203753	34.8	26.2	n	5.5	4	
83	6- 3-1938	163803	34.50	27.50	120	5.75	1,3,4	
84	3-13-1939	033645	36.0	29.0	n	5.0	4	
85	1- 6-1940	190440	35.65	25.97	50	5.5	2,4	
86	2-29-1940	160742	35.50	25.50	-	6.00	1,3,4	xx
87	8-21-1941		34.00	27.00	-	6.50	1	
88	12-13-1941	061605	37.00	28.00	100	6.00	3	
89	5- 9-1942	043707	35.5	26.0	100	5.75	1,3,4	xx
90	6-16-1942	042730	33.8	26.5	n	5.6	4	

TABLE III-A
(continued)

NO	TARİH	SAAT	ENLEM	BOYLAM	H(km)	MAG	KAYNAK	
NO	DATE	TIME Hr.Min.Sec.	LAT(N)	LONG(E)	H(km)	MAG	REF. SOURCE	REMAR
91	6-21-1942	043843	36.50	27.50	130	6.25	1,3,4	xx
92	9- 1-1942	084215	36.4	27.4	n	5.7	2,4	xxx
93	11- 1-1943	115616	36.27	27.15	10	5.3	2,4	xxx
94	6-27-1943	100537	35.00	26.00	100	5.75	1,3,4	xx
95	10-16-1943	130853	36.50	27.50	110	6.25	1,2,3,4	xx
96	11-15-1943	114308	36.58	29.07	140	5.5	2,4	xxx
97	11-20-1943	100157	36.44	28.44	40	5.5	2,4	xxx
98	1- 5-1944	050503	36.4	27.4	-	5.0	2,4	x
99	5-27-1944	235230	36.00	27.50	100	6.25	2,3,4	xx
100	7-20-1944	103729	35.87	27.11	80	5.3	2,4	xxx
101	8- 9-1944	173627	36.5	27.5	100	5.5	2,3,4	xx
102	8-17-1944	132809	35.37	26.40	50	5.3	2,4	xxx
103	9- 2-1945	115357	33.75	28.50	80	6.50	3,4	
104	5-12-1946	073643	35.5	26.5	n	5.0	4	
105	7-16-1946	052626	33.8	25.3	n	5.7	4	
106	10-13-1946	212431	33.8	26.5	n	5.3	4	
107	10-18-1946	043344	33.8	26.5	n	5.0	4	
108	3-28-1947	034032	33.8	25.4	n	5.0	4	
109	2- 9-1948	25815	35.50	27.50	-	7.11	1,2,3,4	xx
110	2-10-1948	155859	35.35	27.56	70	5.2	2,4	xxx
111	2-12-1948	222720	35.77	27.45	100	5.4	2,4	xxx
112	2-15-1948	175506	35.72	27.22	80	5.4	2,4	xxx
113	3- 6-1948	201248	34.8	25.6	n	5.2	4	
114	3-29-1948	023253	35.64	27.28	80	5.4	2,4	xxx
115	7-24-1948	060305	35.2	24.4	100	7.0	2,4	x,xxx
116	10-18-1948	090000	35.64	27.18	40	5.6	2,4	xxx
117	10-19-1948	030437	35.63	27.65	80	5.0	2	
118	7- 7-1949	122114	35.92	27.34	60	5.2	2	
119	9-12-1949	134837	34.8	26.2	n	5.1	4	
120	2-12-1950	094347	34.7	24.1	n	5.0	4	
121	9-23-1950	062340	34.8	25.6	n	5.3	1,4	
122	12-28-1950	223132	35.51	27.26	70	5.2	4	
123	1-33-1951	230723	32.4	33.4	n	5.7	4	
124	10- 1-1951	012633	34.6	26.7	n	5.0	2	
125	11- 5-1951	134355	36.0	29.0		5.2	2,3,4	
126	10-22-1952	041452	36.70	27.90		5.50	1,3,4	x,xx
127	12-17-1952	230355	34.75	24.75		6.75	1,2,3,4	xx
128	12-31-1952	144836	35.50	25.75		6.00	4	
129	1- 1-1953	101717	35.7	25.8	n	5.0	4	
130	2- 7-1953	223105	35.00	24.50		5.50	3,4	
131	2-14-1953	084313	35.5	26.50	100	6.25	1,2,3,4	xx
132	3-13-1953	141554	34.0	25.0	i	5.6	4	
133	6-23-1953	015312	36.0	25.0	100	5.5	3,4	
134	9- 5-1953	010818	35.80	27.30		5.5	2,3,4	x,xx
135	12-20-1953	175620	35.99	27.27	40	5.1	2	
136	1- 2-1954	011321	36.50	27.50		5.63	1,2,3,4	xx

TABLE III-A
(continued)

NO	TARİH	SAAT	ENLEM	BOYLAM	H(km)	MAG	KAYNAK	
NO	DATE	TIME Hr.Min.Sec.	LAT(N)	LONG(E)	H(km)	MAG	REF. SOURCE	REMARK
137	2-22-1954	180918	35.0	27.5	-	5.34	1,3	
138	5- 3-1954	132941	35.5	27.5		5.63	1,3,4	
139	8- 5-1954	203908	35.80	27.50		5.50	3	
140	11-23-1954	232254	35.89	27.6	40	5.0	2	
141	8-28-1955	133917	37.0	27.0		5.25	3,4	
142	9-12-1955	060924	32.90	29.80	50	6.75	1,3,4	x,xx
143	3-16-1956	193238	33.567	35.517	-	6.50	1,3	x
144	6-11-1956	011125	34.50	26.50		5.40	3	
145	7- 8-1956	130522	36.90	26.00		5.00	3	
146	7- 9-1956	031139	37.00	26.00		7.80	1,2,3	x,xx
147	7-10-1956	030125	37.00	26.00		5.50	1,2,3	xx
148	7-22-1956	030125	37.00	26.30		5.50	3	
149	7-30-1956	091457	35.75	25.75		5.75	1,2,3	x,xx
150	9- 6-1956	114641	35.62	25.9	40	5.8	2,3	xx
151	9-16-1956	180743	35.91	25.97	40	5.0	2	
152	10-29-1956	073456	35.50	26.00		5.25	2,3	x,xx
153	12- 2-1956	194113	36.80	25.70		5.25	3	
154	12-18-1956	175302	31.50	35.25		5.38	1,3	xx
155	2-5 -1957	172033	36.37	28.88	60	5.2	2	
156	2-9 -1957	013933	36.75	26.25		5.25	2,3	
157	4-24-1957	191005	36.00	28.50		6.87	1,2,3	xx
158	4-25-1957	022536	36.50	28.90		7.13	1,2,3	xx
159	4-25-1957	075208	36.12	28.6	10	5.0	2	
160	4-26-1957	063343	36.30	29.10		6.38	1,2,3	xx
161	10-30-1957	014301	35.30	27.20		5.50	1,3	x,xx
162	12-5 -1957	135531	35.47	27.74	40	5.2	2	
163	3-4- 1958	113218	36.34	27.85	120	5.2	2	
164	4-3- 1958	071837	35.25	27.25		6.40	1,3	x
165	5-9- 1958	024037	36.50	27.50		5.27	2,3	x,xx
166	5-27-1958	182746	36.8	26.76	160	5.1	2	
167	6-30-1958	084241	36.50	27.40	100	6.25	1,2,3	x,xx
168	7-15-1958	075917	33.50	23.50		5.17	3	
169	9-4 -1958	000250	35.80	26.40		5.40	1,3	
170	9-4 -1958	000300	36.56	26.72	40	5.0	2	
171	1-26-1959	113844	36.83	29.23	70	5.4	2	
172	4-25-1959	002641	37.00	28.50		6.06	2,3	x,xx
173	5-14-1959	063655	35.10	24.90		6.50	3	xx
174	5-20-1959	163052	36.90	26.30		5.50	3	
175	6-10-1959	041403	37.75	24.25		5.50	3,1	
176	7-12-1959	165231	36.03	26.28	80	5.3	2	
177	9-28-1959	093518	35.74	30.08	100	5.1	2	
178	11-19-1959	140024	36.00	27.00		5.54	3	
179	12- 8-1959	093518	36.91	29.07	70	5.0	2	
180	1-26-1960	130538	36.75	29.25		5.50	2,3	xx
181	9-16-1960	012803	35.58	28.49	40	5.2	2	
182	1- 7-1961	103055	35.42	26.14	80	5.5	2	
183	2-23-1961	214550	36.90	27.30	25	5.75	1,2,3	xx
184	2-27-1961	214007	36.57	27.00	70	5.0	2	
185	3-14-1961	191717	34.50	26.60	25	5.25	3	
186	5-23-1961	024518	36.80	28.70	70	6.25	1,2,3	xx

TABLE III-A
(continued)

NO	TARİH	SAAT	ENLEM	BOYLAM	H(km)	MAG	KAYNAK	
NO	DATE	TIME Hr.Min.Sec.	LAT(N)	LONG(E)	H(km)	MAG	REF. SOURCE	REMARK
187	5-25-1961	131142	37.00	26.90		5.0	3	
188	4-4 -1962	205932	34.00	24.50		5.0	3	
189	4-16-1962	071906	36.15	27.23	140	5.4	2	
190	4-28-1962	111853	36.10	27.0		5.9	2,3	
191	9-10-1962	093628	35.60	27.50		5.60	3	x
192	3-4 -1963	151015	35.00	27.80		5.00	3	x
193	3-11-1963	072714	37.00	28.50		5.90	3	
194	5-23-1963	101449	36.40	29.40		5.60	3	
195	7-26-1963	194639	36.84	28.76	80	5.10	2	x
196	4-8 -1964	141228	35.04	24.29	64	5.10	3	
197	7-18-1964	034019	36.13	26.01	99	5.0	2,3	
198	8-25-1964	111152	35.75	28.84	51.1	5.3	2	
199	8-25-1964	143733	35.55	28.82	35	5.6	2	
200	8-27-1964	193159	35.56	28.84	38	5.4	2	
201	9-18-1964	000847	35.69	29.07	40	5.3	2	
202	12-31-1964	161802	35.76	25.51	89	5.00	2,3	
203	1-7 -1965	102217	36.50	26.85	35	5.00	3	
204	4-9 -1965	235702	35.06	24.31	39	5.90	3	
205	4-27-1965	140905	35.65	23.53	37	5.50	3	
206	11-28-1965	052605	36.12	27.43	73	5.70	2,3	
207	3-29-1966	184141	37	29.6		5.0	2	
208	4-21-1966	064526	34.49	25.69	51	5.0	3	
209	5-9 -1966	004253	34.43	26.44	13	5.30	3	
210	6-1 -1967	103923	36.81	29.26	43	5.00	3	
211	12-5 -1967	052005	36.53	26.85	137	5.9	2	
212	2-7 -1968	222219	36.65	26.74	153	5.7	2,3	
213	2-20-1968	165045	36.15	27.39	64	5.0	2	
214	3-28-1968	074101	36.80	24.80		5.10	3	
215	5-30-1968	174026	35.45	27.88	27	5.9	2,3	
216	7-8 -1968	174106	34.47	25.08	38	5.30	3	
217	7-27-1968	024551	35.43	27.82	29	5.0	3	
218	8-15-1968	022943	35.18	26.70	48	5.0	3	
219	10-31-1968	032214	36.63	27.01	2	5.4	2,3	
220	11-10-1968	125037	34.44	23.77	1	5.0	3	
221	11-11-1968	233422	36.61	27.15	23	5.0	2	
222	11-12-1968	033739	36.74	27.11	26	5.0	2	
223	12-15-1968	075211	36.60	26.92	31	5.40	2,3	
224	1-14-1969	231206	36.11	29.19	22	6.30	2,3	
225	4-16-1969	232106	35.23	27.72	58	5.10	3	x
226	5-1 -1969	180216	35.41	27.68	51	5.10	3	
227	5-14-1969	100517	35.33	27.72	43	5.10	3	
228	6-13-1969	151330	34.43	25.04	22	5.80	3	
229	9-6 -1969	203040	36.73	28.35	72	5.0	2,3	
230	9-28-1969	225408	34.30	25.15	29	5.30	3	
231	12-1 -1969	201803	34.85	24.22	35	5.10	3	
232	12-31-1969	053705	34.44	26.11	54	5.00	3	
233	2-22-1970	154831	35.21	25.24	43	5.10	3	
234	11-11-1970	205812	35.99	28.24	35	5.2	2	
235	1-3 -1971	231843	34.63	26.32	47	5.20	3	
236	8-11-1971	053727	36.807	23.957	109	5.0	3	

TABLE III-A
(continued)

NO	TARİH	SAAT	ENLEM	BOYLAM	H(km)	MAG	KAYNAK	
NO	DATE	TIME Hr.Min.Sec.	LAT(N)	LONG(E)	H(km)	MAG	REF. SOURCE	REMARKS
237	10-13-1971	032626	34.23	26.06	17	5.0	3	
238	11-12-1971	123050	36.615	27.084	23	5.10	3	
239	4-29-1972	182938	34.80	24.65	48	5.10	3	
240	9-26-1972	121659	34.24	26.16	23	5.0	3	
241	11-5 -1972	192542	35.03	24.76	32	5.10	3	
242	12-2- 1972	132822	35.285	27.056	36	5.10	3	
243	4-6- 1973	141357	34.41	25.17	37	5.10	3	
244	11-12-1973	001149	35.395	27.653	0	5.10	3	
245	11-29-1973	105744	35.18	23.81	37	5.60	3	
246	12-5 -1973	035050	35.36	26.41	70	5.0	3	

SOURCES UTILIZED IN THE PREPARATION OF THIS CATALOGUE :

1) Türkiye Deprem Şiddetleri Kataloğu
S.Okomato, A.Tabban and T. Tanuma.
Deprem Araştırma Enstitüsü, Ankara 1970 -

2) An Earthquake Catalogue for Turkey for the Interval (1913-1970)
E.Alsan, Levent Tezuçan and Markus Bath
Kandilli Observatory Seismological Dept., Istanbul 1975.

3) International Seismological Center (Computer output data for the Period (1900-1973), England.

4) Seismicity for the European Area.
V.Karnik
D. Reidel Rublishing Company, Holland, 1969.

REMARKS:

x Maximum magnitude recorded data is selected among the listed earthquakes which occur in a short period of time (minutes).

xx This data exists in several indicated sources with minor differences either in time or in latitude longitude coordinates. The catalogued event is the one given in source 3.

xxx This event is not listed in source 3 but appears in the other sources.

n Indicates h-5-50 km normal depth focus in the earth's crust.

i Indicates h-60-300 km, intermediate depth focus below the crust in the transitional zone of the upper mantle.

This catalogue excludes the events occurred in the region defined by 300 km radius circle with center at Akkuyu.

APPENDIX B

TSUNAMI MODIFICATION ON THE CONTINENTAL SHELF

In order to study the topographical effects on tsunami propagation of Turkish and Cyprus coasts and their adjoining shelf regions,consider a channel region with transverse depth variations only. Negliecting earth's rotation (due to scaling arguments), the corresponding wave equation

$$(h\eta_x)_x + h\eta_{yy} - \frac{1}{g}\eta_{tt} = 0 \qquad (B.1)$$

models the propogation, where η is the surface displacement, $h = h(x)$ the depth, g the gravitational acceleration and the y axis is ligned along the channel. Assuming the propogation along y-axis to be of the form $y \sim e^{i(ky-\omega t)}$ with a single harmonic component in time, (B.1) becomes

$$(h\eta_x)_x + (\frac{\omega^2}{g} - k^2 h)\,\eta = 0 \qquad (B.2)$$

The effects of wave modification due to the presence of a shelf region, and possible coupling between the shelf and the deeper channel can be studied by solving Eq.(B.2) for given side conditions.

Guided wave propagation in a canal is to a great extent determined by the rapid changes of bottom topography in the transverse direction. For a first examination consider a linear variation in depth over the shelf:

$$h = H_1\, x / l_1 \;, \qquad 0 \le x \le l_1 \qquad (B.3)$$

and let the depth be increasing rapidly after the shelf break at $x = l_1$. In such a system, strong coupling of the shelf region to the deeper section is expected. The assumption to be made here is that when the volume of the shelf area is small w.r.t. the volume of the deeper and wider channel section, the motion on the shelf is driven by the pressure forces of the motion in the larger channel, namely η is prescribed at $x = l_1$.

For typical numerical model runs, the sustined oscillations near Akkuyu have periods of T = 1000 sec. and wave lengths of L = 100 km. The depth at the shelf break is H_1 = 400 m. Therefore, in Eq.(B.2) the ratio of the last two terms are at most

$$\frac{k^2 \sqrt{gH_1}}{\omega^2} = \frac{T^2 \sqrt{gH_1}}{L^2} = 0.4 \qquad \text{(B.4)}$$

and consequently the equation can be simplified by neglecting longitudinal wave propagation along the shelf for large time (i.e. by setting $k = 0$).

B.1 Simple Harmonic Oscillations:

For the linear depth variation in Eq.(B.3) and simple harmonic motions $\eta \sim e^{-\ t}$, the pure transverse oscillations ($k = 0$) on the shelf region are obtained by solving

$$(x\eta_x)_x + \frac{\omega^2 l_1}{g H_1} \eta = 0 \qquad \text{(B.5)}$$

The solution that is finite at $x = 0$ is in terms of the zeroth order Bessel function J_o :

$$\eta = \eta_o e^{-i\omega t} \frac{J_o \ (\Omega \sqrt{x/l_1})}{J_o \ (\Omega \ )} \qquad \text{(B.6)}$$

where η_o is the amplitude specified at $x = l_1$ and $\Omega = 2\ wl_1/\ g\ H_1$. The amplification factor at $x = 0$ is $1/|J_o(\Omega)|$, plotted in Fig.B.1. Resonant amplification occurs at the frequencies $\omega_n = j_n = \sqrt{g}\ H_1/2l_1$, corresponding to the roots of $J_o(j_n) = 0$.

B.2. Transient Oscillations:

Transient oscillations set up on the shelf by a tsunami incidence can be modeled by using the same assumptions utilized above, i.e. by neglecting longitudinal wave propagation and by specifying the water surface displacement at the shelf break. For example, consider the time dependence

$$\eta\ (t, l_1) = f\ (t) = \begin{cases} 0 , & t < 0 \\ \eta_0 \sin \omega_0 t , & t \geq 0 \end{cases} \qquad (B.7)$$

for the boundary condition specified at the shelf break. Then, the shelf oscillations are obtained by solving Eq. (B.1) as an initial value problem. In order to simpli the s olution, let

$$\eta = f(t) + \hat{\eta}\ (x, t) \qquad (B.8)$$

(B.8)

and assume a linear depth variation $h = H_1\ x/l_1$ in $0 \leq x \leq l_1$, then it is required to solve:

$$(x\hat{\eta}_x)_x - \frac{l_1}{gH_1}\hat{\eta}_{tt} = \frac{l_1}{gH_1} f_{tt} \qquad (B.9a)$$

$$\hat{\eta}(t, l_1) = 0 \qquad (B.9b)$$

$$\hat{\eta}_t\ (0, l_1) = 0 \qquad (B.9c)$$

By comparing with Eq.5 (B.5) and (B.6) a solution of the form

$$\hat{\eta} = \sum_{n=1}^{\infty} \psi_n\ (t)\ J_0\ (\Omega_n \sqrt{x/l_1}) \qquad (B.10)$$

is assumed, such that the x-dependent part satisfies Eq.(B.5). Substitution into Eq.(B.9a) yields,

$$(\psi_n)_{tt} + \omega_n^2 \Psi_n = - \frac{2}{\Omega_n J_1(\Omega_n)} f_{tt} \qquad \text{(B.11)}$$

where $\Omega_n = \omega_n l_1/\sqrt{gH_1}$ and J_1 is the Bessel's function of the first order. Here, Ω_n are obtained by requiring Eq.(B.9.a.) to be valid, i.e. from $J_o(\Omega_n) = 0$ or $\Omega_n = j_n$. The general solution for the surface displacement is given by

$$\eta = \sum_{n=1}^{\infty} \frac{2\eta_o \omega_n^2}{j_n (\omega_o^2 - \omega_n^2) J_1(j_n)} \left(\frac{\omega_o}{\omega_n} \sin \omega_n t - \sin \omega_o t\right) J_o(j_n \sqrt{x/l_1})$$

(B.12)

If the excitation frequency ω_o is close to one of the natural frequencies; i.e. if $\omega_o = \omega_m + \varepsilon$, then

$$\omega_o^2 - \omega_m^2 = (\omega_o - \omega_m) \quad (\omega + \omega_m) = 2\varepsilon\omega_m$$

and only one term will dominate in the series Solution (B.12). The solution in this case can be simplified as:

$$\eta \simeq - \frac{\sqrt{g H_1}}{2 l_1 (\omega_o - \omega_m) J_1(j_m)} \sin \frac{\omega_o - \omega_m}{2} t \cos \omega_m t \; J_o(j_m \sqrt{x/l_1})$$

(B.13)

This oscillation is composed of a carrier wave with frequency ω_m modulated by an envelope term with frequency $(\omega_o - \omega_m)/2$. As the forcing and natural frequencies become closer, the beating amplitude and period increases.

The values of j_n and $J_1(j_n)$ for the first few modes are listed in Table B.1.

TABLE B.1.

n	j_n	$J_1(j_n)$
1	2.40	0.52
2	5.52	-0.34
3	8.65	0.27
4	11.79	-0.23

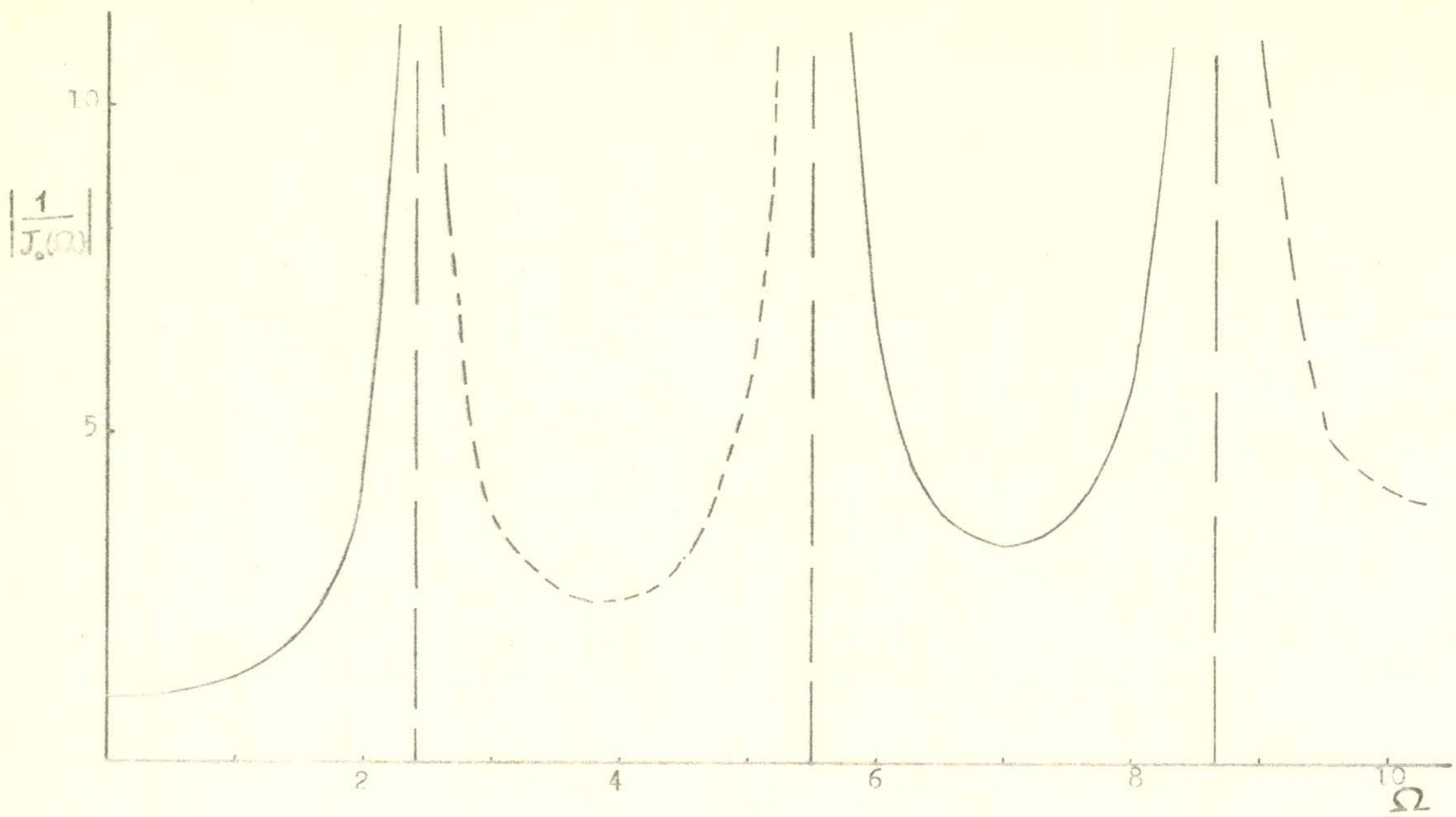

Figure B.1 Amplification Factor At x=0